Development of a New Class of Necroptosis Inhibitors That Bind Allosterically to Human and Mouse MLKL

Inaugural-Dissertation

zur

Erlangung des Doktorgrades

der Mathematisch-Naturwissenschaftlichen Fakultät

der Universität zu Köln

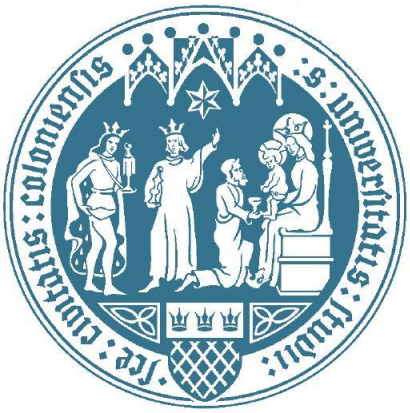

vorgelegt von

Yasmin Abdelwahab

aus

Ägypten

2023

Berichterstatter: (Gutachter) Prof. Dr. Ana J. García-Saéz

Prof. Dr. Hamid Kashkar

Tag der mündlichen Prüfung: 26.02.2024

Summary

Necroptosis is a form of regulated cell death that results in the release of inflammatory cellular contents after plasma membrane permeabilization, thus triggering the immune response. Mixed Lineage Kinase domain-like pseudokinase (MLKL) is the protein that mediates plasma membrane disruption in necroptosis. This type of cell death has been linked to a broad range of inflammatory diseases. Therefore, targeting MLKL to inhibit necroptosis represents an attractive strategy, as this protein is the only one solely associated with this pathway. However, the development of MLKL inhibitors is still in its infancy, and the existing ones are limited to lab research. In Prof. Dr. Ana Garcia Saez's lab, a new druggable hydrophobic pocket in MLKL was discovered. Based on this knowledge, a new strategy was developed to specifically regulate necroptosis by allosterically targeting MLKL with small molecules that interact with this site. Two proof of principle compounds (MBA-h1 and MBA-m1) were identified by *in-silico* analysis. In this thesis, we characterized these two compounds using cell-based assays aimed to determine their inhibitory effect in necroptosis, the mechanism of how they modulate MLKL activation, and their binding to MLKL. We also assessed their capability to interact with recombinant MLKL. Both MBAs were able to bind to MLKL and inhibit the kinetics of cell death in a dose-dependent manner. The MBAs paved the way for the investigation of new compounds that have the same mechanism of action. Based on this, an extended *in-silico* screening was performed, and potential hits were identified and characterized in terms of their inhibition and binding to MLKL *in-vitro*. This screening was followed by two further rounds of characterization of analogs of initially identified hits. The top compounds outperform already existing MLKL inhibitors as they block necroptosis in mouse and human cells. Therefore, in this work, we offer a new concept for inhibiting necroptosis that is based on targeting a newly identified intramolecular interaction in MLKL, that is essential for its activation.

Zusammenfassung

Nekroptose ist eine Form des regulierten Zelltods, die zum Platzen der Plasmamembran, und somit zur Freisetzung von Zellbestandteilen und zur Immunantwort führt. Mixed Lineage Kinase domain-like pseudokinase (MLKL) ist das Effektorprotein, das für die Permeabilisierung der Plasmamembran bei der Nekroptose verantwortlich ist. Nekroptose ist mit einer Vielzahl entzündlicher Erkrankungen assoziiert. Aus diesem Grund ist die Inhibierung von MLKL eine attraktive Therapiemöglichkeit, da es das einzige Protein in der Signalkette ist, das ausschließlich mit Nekroptose assoziiert wird. Die Entwicklung neuer MLKL-Inhibitoren steckt jedoch noch in den Anfangsstadien und die existierenden Inhibitoren weisen viele Einschränkungen auf. Im Labor von Prof. Dr. Ana Garcia-Saez wurde eine hydrophobe Tasche in MLKL identifiziert, die als Angriffspunkt für Inhibitoren dienen könnte. Auf dieser Grundlage wurde eine neue Strategie entwickelt, um die Nekroptose gezielt zu regulieren, indem MLKL durch kleine Moleküle, die mit dieser Stelle interagieren, allosterisch gehemmt wird. Zwei Proof-of-Principle Verbindungen (MBA-h1 und MBA-m1) wurden durch in silico Analysen identifiziert. In dieser Arbeit wurden diese beiden Verbindungen in zellbasierten Assays charakterisiert: ihre inhibitorische Wirkung auf die Nekroptose, der Mechanismus, mit dem sie die Aktivierung von MLKL modulieren, und ihre Bindung an MLKL wurden bestimmt. Zusätzlich wurde ihre Wechselwirkung mit rekombinantem MLKL untersucht. Beide MBAs waren in der Lage, MLKL zu binden und die Zelltodkinetik dosisabhängig zu hemmen. Die aus den MBAs gewonnenen Erkenntnisse ermöglichten die Suche nach neuen Verbindungen mit ähnlichem Wirkmechanismus. Darauf aufbauend wurde ein erweitertes In-silico-Screening durchgeführt, bei dem potenzielle Treffer identifiziert und in vitro hinsichtlich ihrer Bindung an MLKL und Inhibierung charakterisiert wurden. Diesem Screening folgten zwei weitere Runden zur Charakterisierung von Analoga der identifizierten Treffer .Die besten Verbindungen übertrafen die bereits existierenden MLKL-Inhibitoren, da sie in der Lage waren, die Nekroptose sowohl in menschlichen als auch in Mauszellen zu hemmen. Zusammenfassend wird in dieser Arbeit ein neuer Ansatz zur Hemmung der Nekroptose vorgeschlagen. Die Hemmung basiert auf einer neu identifizierten intramolekularen Interaktion in MLKL, die für seine Aktivierung essentiell ist.

Erklärung zur Dissertation

gemäß der Promotionsordnung vom 12. März 2020

„Hiermit versichere ich an Eides statt, dass ich die vorliegende Dissertation selbstständig und ohne die Benutzung anderer als der angegebenen Hilfsmittel und Literatur angefertigt habe. Alle Stellen, die wörtlich oder sinngemäß aus veröffentlichten und nicht veröffentlichten Werken dem Wortlaut oder dem Sinn nach entnommen wurden, sind als solche kenntlich gemacht. Ich versichere an Eides statt, dass diese Dissertation noch keiner anderen Fakultät oder Universität zur Prüfung vorgelegen hat; dass sie - abgesehen von unten angegebenen Teilpublikationen und eingebundenen Artikeln und Manuskripten - noch nicht veröffentlicht worden ist sowie, dass ich eine Veröffentlichung der Dissertation vor Abschluss der Promotion nicht ohne Genehmigung des Promotionsausschusses vornehmen werde. Die Bestimmungen dieser Ordnung sind mir bekannt. Darüber hinaus erkläre ich hiermit, dass ich die Ordnung zur Sicherung guter wissenschaftlicher Praxis und zum Umgang mit wissenschaftlichem Fehlverhalten der Universität zu Köln gelesen und sie bei der Durchführung der Dissertation zugrundeliegenden Arbeiten und der schriftlich verfassten Dissertation beachtet habe und verpflichte mich hiermit, die dort genannten Vorgaben bei allen wissenschaftlichen Tätigkeiten zu beachten und umzusetzen. Ich versichere, dass die eingereichte elektronische Fassung der eingereichten Druckfassung vollständig entspricht."

Datum, Name und Unterschrift

17.12.2023, Yasmin Abdelwahab

Acknowledgments

First of all, I would like to thank and express my gratitude to my supervisor, Prof. Dr. Ana Garcia, for giving me the chance to participate in this amazing project. Her continuous support, guidance, and help have always been of great value to me. Her ability to encourage me and give me more positive energy to continue through the most challenging times helped me throughout these previous 4 years. I would also like to thank Dr. Uris Ros for always guiding, supporting, and teaching me everything; her presence at the beginning of my PhD was invaluable; even when she was on maternity leave, she continued supporting me, and I can never forget all the moments she invested in me, I am very grateful to her. I can never forget the invaluable help from Raed Shalaby. He has always been there for me as a college and as a brother since I first met him in Tübingen during my master's thesis. I would also like to extend my thanks to Lisa and Veronica for always being there for me and the continuous scientific and non-scientific discussions; their presence made me continue what I have achieved now. Also, I must thank all the lab members for making the work environment this amazing.

Furthermore, I would like to thank my family, my dad, my mom, and my brother Abdullah for always believing in me when no one else believed in me. The love and support they showed me were unconditional, regardless of how far they were from me; they have been so close to my heart and were always the first ones I called whenever I faced any problem. Thank you, Dad, for paving this fantastic path for me. I will always make you proud of me. Furthermore, I would like to thank Faried, my husband, for always being there for me regardless of how busy he is and for showing me the meaning of fighting for someone you love. I want to express my deep gratitude to my friends for always supporting me in my decisions. Thank you, Sarah, Ebrahim, and Salma. I want to mention that regardless of how hard life gets, it is just to prepare you for more incredible adventures and challenges.

Table of Contents

Author contributions

Certain figures within this thesis have been produced in collaboration with others:

In chapter 3:

- Figure 3.5: Blots of MLKL phosphorylation and membrane translocation in HT-29 were performed by Bastian Marx.
- Figure 3.17: MST experiment and data analysis were performed by Raed Shalaby.

List of Figures

List of Tables

Abbreviations

4HB	4-Helical Bundle
ACD	Accidental Dell Death
AD	Alzheimer's Disease
ALK	Anaplastic Lymphoma Kinase
BMDMs	Bone marrow-derived macrophage
CETSA	Cellular Thermal Shift Assay
cIAP1/2	cellular Inhibitors of Apoptosis
CLP	Cecum Ligation and Puncture-induced sepsis
CM5	Carboxymethyl dextran-coated sensor chip
c-MET	Mesenchymal-Epithelial Transition
COPD	Coronary Obstructive Pulmonary Disease
CRBN	Cereblon
DAI	DNA sensor
DFG	Asp-Phe-Gly
DISC	Death-Inducing Signaling Complex
DMSO	Dimethyl sulfoxide
DR	Cell Death Receptor
EDC/NHS	1-Ethyl-3-(3-dimethylaminopropyl)carbodiimide /N-hydroxysuccinimide
FADD	Fas-Associated protein with Death Domain
FBS	Fetal bovine serum albumin
GFE	Gly-Phe-Glu
GSDMD	Gasdermin D
HRD	His-Arg-Asp
HRP	Horseradish peroxidase
ICD	Immunogenic Cell Death
IKK	The IkB Kinase
IPF	Idiopathic Pulmonary Fibrosis
IRI	Ischemic Reperfusion Injury
IVA	Influenza Virus A
Kd	Knockdown
Ko	Knockout

LPS	Lipopolysaccharide
LUBAC	Linear ubiquitin chain Assembly Complex
MAPK	Mitogen-Activated Protein Kinase
MBAs	MLKL Binding Agents
MD	Molecular dynamics
MDF	Mouse Dermal Fibroblasts
MLKL	Mixed Lineage Kinase domain-Like pseudokinase
MRSA	Methicillin-resistant *Staphylococcus aureus*
MS	Multiple Sclerosis
MST	Microscale thermophoresis
Nec-1s	Necrostatin 2
NEMO	NF-κB Essential Modulator
NF-κB	Nuclear Factor 'kappa-light-chain-enhancer' of activated B-cells
NSA	Necrosulfonamide
NTC	Non-Toxic concentration
NTD	N-terminal Domain
PCD	Programmed Cell Death
PCR	Polymerase chain reaction
PD	Parkinson's Disease
pMLKL	Phosphorylated MLKL
Poly(I:C)	Polyinosine-polycytidylic acid
PROTACs	PROteolysis Targeting Chimeras
PRRs	Pattern Recognition Receptors
psK	pseudokinase
RCD	Regulated Cell Death
RHIM	RIP Homotypic Interaction Motifs
RIPK1	Receptor-Interacting Protein Kinase 1
RIPK3	Receptor-Interacting Protein Kinase 3
SC	Soluble concentration
shRNA	Small hairpin RNA
siRNA	Small interfering RNA
SIRS	Systemic Inflammatory Response Syndrome
SPR	Surface Plasmon Resonance
TAB	(TAK)1-Binding proteins

TAB2/3	TAK1-Binding protein 2/3
TAK	Transforming growth factor-β-Activated Kinase
TAK1	TGF-Activated Kinase 1
TBS-T	Tris-buffered saline with 0.1% Tween
TG	Triglycerides
TIR	Toll/IL1 Receptor
TLR	Toll-Like Receptor
TNF	Tumor Necrosis Factor
TNFR1	TNF Receptor 1
TRADD	TNFR1-Associated Death Domain
TRAF2	TNF-Receptor-Associated Factor 2
TRIF	Toll/IL-1 Receptor domain-containing adaptor inducing IFN-β
VAIK	Val-Ala-Ile-Lys
VEGFR2	Vascular Endothelial Growth Factor Receptor 2
WB	Western blotting
ZBP1	Z DNA Binding Protein 1

1. Introduction

1.1 Regulated Cell Death

Cell death is not only considered a consequence of cellular life, but it also participates in the targeted elimination of less fit cells, as well as potentially harmful cells (Galluzzi et al., 2018). It serves significant purposes in development, maintaining tissue homeostasis, and host defense (Galluzzi et al., 2016; Nagata & Tanaka, 2017). For instance, it was estimated that the cellular turnover rate in adult humans is about 330 billion cells per day (Sender & Milo, 2021).

Cell death is classified into two significant categories: accidental cell death (ACD) and regulated cell death (RCD) (Galluzzi et al., 2015) (Figure 1.1). ACD occurs in response to non-physiological triggers, such as chemical, physical, or mechanical stress (Vanden Berghe et al., 2014). Necrosis has been long defined as a form of unregulated and accidental way of cell death in response to different stimuli (Weinlich et al., 2017). Cells undergoing necrosis display specific morphological characteristics, which include swelling and enlargement, membrane rupture, and the release of cellular contents, triggering the immune response.

RCD can occur in two dramatically opposite scenarios. The first scenario is when RCD occurs in the absence of any external environmental turbulence. It is referred to as Programmed Cell Death (PCD) and is considered to be a built-in mechanism within the cells (Jorgensen et al., 2017). On the other hand, the second scenario occurs when the cells are exposed to intrinsic or extrinsic turbulence as an adaptive response to the occurring stress (Galluzzi et al., 2015). Currently, the most well-studied and identified forms of RCD are apoptosis, ferroptosis, necroptosis, pyroptosis, and autophagy (J. Cui et al., 2021). Apoptosis is considered the best-understood form of RCD that accounts for almost half of the cellular turnover in the human body (Sender & Milo, 2021).

Apoptosis is a highly regulated process of cell death and has an essential role in various physiological and pathophysiological conditions (Wong, 2011). Apoptosis is recognized by its unique morphology, which includes DNA fragmentation, blebbing of the plasma membrane, cell shrinkage, and the formation of apoptotic bodies (Figure 1.1) (Taylor et al., 2008). This process is super-efficient and considered as a clean way of cell death. However, in some recent studies, it was reported that there is an emerging type of apoptosis that is immunogenic (Montico et al., 2018), where crucial interactions between apoptotic cells and the immune system take place. Necroptosis, which is another form of RCD, occurs in response to disturbances in the intracellular or extracellular cellular microenvironment. It generally

manifests morphological changes similar to those that occur in necrosis, which is also considered, together with pyroptosis and ferroptosis, as a form of regulated necrosis (Figure 1.1) (Galluzzi et al., 2018). However, it does not occur accidentally but is tightly regulated by genetically encoded signaling molecular mechanisms and under conditions of caspase inactivation (de Almagro & Vucic, 2015).

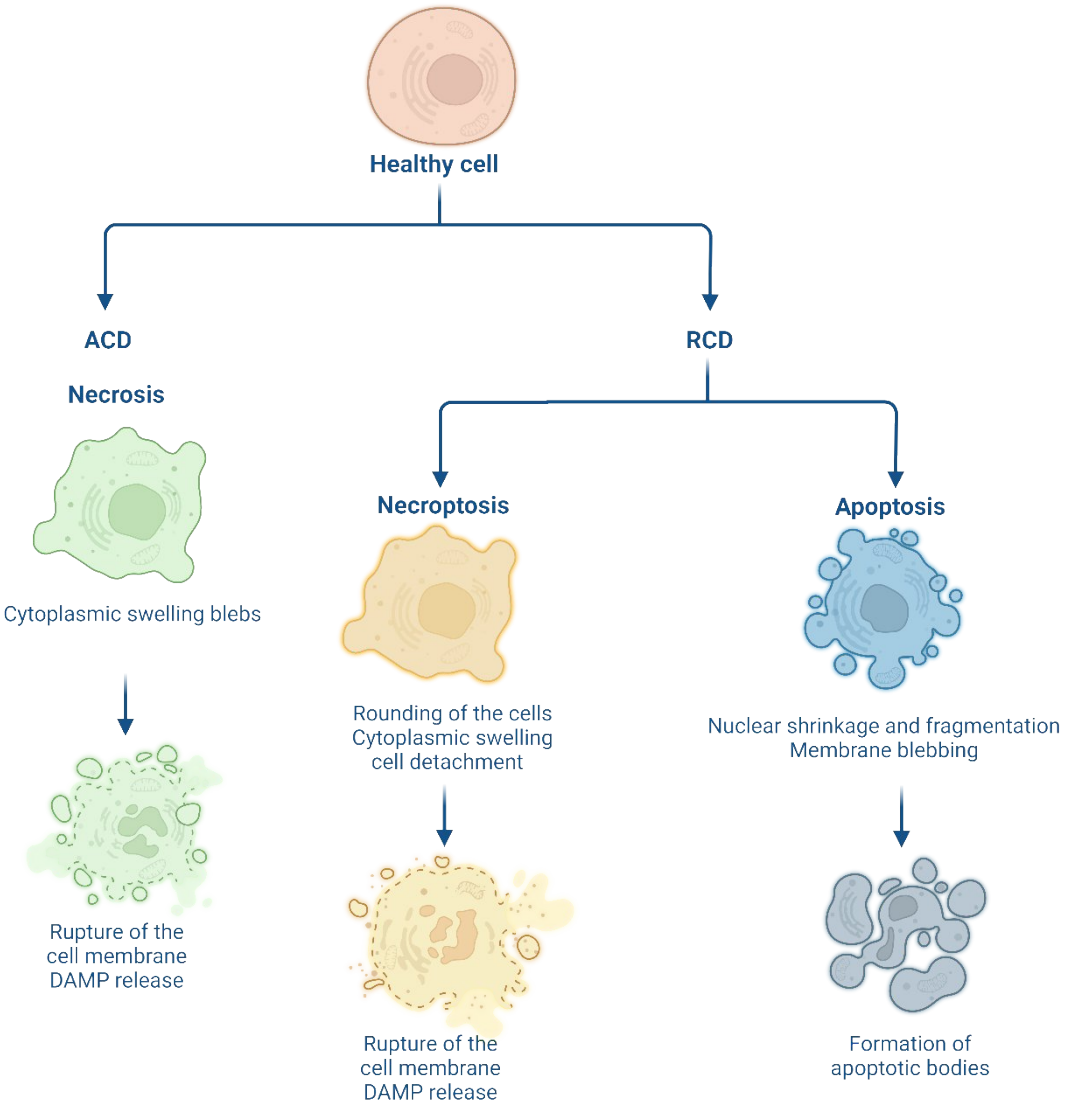

Figure 1. 1 Schematic representation of changes in cell morphology during different forms of cell death.

This diagram illustrates the morphological hallmarks of apoptosis, necrosis, and necroptosis. Apoptosis is marked by distinct features that include cell and nuclei shrinkage, fragmentation followed by membrane blebbing, and the formation of apoptotic bodies. In contrast, necrosis and necroptosis exhibit some similar morphological changes including cell membrane rupture. This rupture results in the release of intracellular contents into the extracellular matrix. Figure prepared by using BioRender.com.

1.2 The Necroptotic Pathway

Necroptosis is one of the most thoroughly understood type of regulated necrosis. It is activated by different cell death receptors (Taraborrelli et al., 2018), Pattern Recognition Receptors (PRRs) (S. He et al., 2011), and intracellular RNA and DNA (Cho et al., 2009b). Tumor Necrosis Factor (TNF) induced necroptosis is the most extensively studied signaling pathway among the various triggers of necroptosis (Figure 1.2). In this pathway, TNF triggers an inflammatory reaction by initiating the activation of proinflammatory genes through the Nuclear Factor 'kappa-light-chain-enhancer' of activated B-cells (NF-κB) signaling pathway (Z. Zhou et al., 2012b). Upon TNF binding to its receptor, TNF Receptor 1 (TNFR1), it leads to the formation of complex I, which is a membrane-associated signaling platform composed of different adaptor proteins. This complex includes several key components, such as the TNFR1-Associated Death Domain (TRADD), TNF-Receptor-Associated Factor 2 (TRAF2), Receptor-Interacting Protein Kinase 1 (RIPK1), cellular Inhibitors of Apoptosis (cIAP1 or cIAP2), and the Linear Ubiquitin chain Assembly Complex (LUBAC) (J. Chen & Chen, 2013). In complex I, RIPK1 is ubiquitinylated by cIAPs and LUBAC with k63-linked and linear ubiquitin chains, which allows the recruitment of downstream proteins such as TGF-Activated Kinase 1 (TAK1), TAK1-Binding protein 2/3 (TAB2/3), and the IkB Kinase (IKK) complex that is assembled from IKK-α, IKK-β, and NF-κB Essential Modulator (NEMO) (Figure 1.2). When the downstream complexes are recruited, the NF-κB and the Mitogen-Activated Protein Kinase (MAPK) pathways are activated, subsequently increasing the expression of pro-survival and proinflammatory genes (Annibaldi & Meier, 2018; Seo et al., 2021).

Apart from activating necroptosis via TNF, various triggers can cause necroptosis initiation. Death receptors such as Fas (known as CD95 or Apo-1), Death Receptor 3 (DR3) (known as Apo-3), Death Receptor 4 (DR4) (known as Apo-2 or TRAILR1), Death Receptor 5 (DR5) (known as TRAIL-R2), and Death Receptor 6 (DR6) primarily engage the death receptor complex. This complex is composed of FADD and caspase-8, which is known as a Death-Inducing Signaling Complex (DISC) when they bind to their respective ligands. When cIAPs and caspase-8 are inhibited, death receptors facilitate the initiation of the necrosome, subsequently leading to necroptosis execution (Bittner et al., 2017; Feoktistova et al., 2011; Geserick et al., 2009; Strilic et al., 2016).

The formation of the necrosome is triggered by the RIP Homotypic Interaction Motifs (RHIM)-containing protein activation. In the mammalian proteome, there are mainly four proteins with the RHIM domain, including RIPK1 and Receptor-Interacting Protein Kinase 3 (RIPK3). The

Toll-Like Receptor (TLR), adapter Toll/IL-1 receptor domain-containing adaptor inducing IFN-β (TRIF), and the potential DNA sensor Z-DNA binding protein 1 (ZBP1) (also known as DAI) also encode the RHIM domain (Sun et al., 2012). Upon the activation of these proteins, the assembly of the necrosome takes place. In the necrosome, RIPK3 autophosphorylation leads to the recruitment and phosphorylation of Mixed Lineage Kinase domain-Like (MLKL), the final executor of necroptosis. MLKL phosphorylation promotes a conformational change in its structure, revealing the 4-Helical Bundle (4HB) domain that acts as a trigger for oligomerization and plasma membrane translocation (Davies et al., 2018; Murphy et al., 2013; Petrie et al., 2018). MLKL oligomers at the plasma membrane are responsible for cell death execution (Galluzzi et al., 2014) (Figure 1.2).

Canonical necrosome

In the canonical necrosome, RIPK3 is activated via interactions with RIPK1. This interaction can happen when complex I becomes unstable, or the ubiquitination of RIPK1 is inhibited. In this situation, TNF has the potential to induce the assembly of cytosolic apoptotic complex (referred to as complex IIa or ripoptosome) (S. He & Wang, 2018; Tenev et al., 2011). This complex is composed of Fas-Associated Protein with Death Domain (FADD) and caspase-8, which is essential for carrying out the process of apoptosis. When the balance between caspase-8 and RIPK3 activity is disrupted due to caspase-8 inhibition or RIPK3 overexpression, complex IIa can be converted into the necrosome (Cho et al., 2009b; S. He et al., 2009; D.-W. Zhang et al., 2009), followed by the assembly of a large amyloid-like structure. In this context, when RIPK1 is phosphorylated, RIPK3 is auto-phosphorylated, and the RHIM-dependent RIPK3 oligomers recruit MLKL to the necrosome. This interaction results in the phosphorylation of MLKL, which promotes a conformational change in its structure, revealing the 4-helical bundle (4HB) domain that acts as a trigger for oligomerization and plasma membrane translocation (Davies et al., 2018; Murphy et al., 2013; Petrie et al., 2018). These MLKL oligomers at the plasma membrane are responsible for cell death execution (Galluzzi et al., 2014) (Figure 1.2).

Non-canonical necrosome

Moreover, Toll-Like Receptors 3/4 (TLR3 and TLR4), which are known as PPRs, can trigger the initiation of necroptosis by the formation of a non-canonical necrosome through TIRF-RIPK3 interactions via their RHIM domains (S. He et al., 2011; Kaiser et al., 2013). In the presence of polylysine-polycytidylic acid (poly(I:C)), lipopolysaccharide (LPS), and in

response to some bacterial or viral infections (Kircheis & Planz, 2023), both TLR3 and TLR4 are activated. In conditions of caspase-8 inhibition, activated TLRs facilitate the assembly of the necrosome mediated by TRIF, which includes TRIF, RIPK3, and MLKL. As a result, necroptosis is executed (Figure 1.2).

As a response to viral infection, another RHIM motif-containing protein ZBP1 can trigger and initiate necroptosis (Maelfait et al., 2017; Thapa et al., 2016; Upton et al., 2012). When ZBP1 detects viral RNA or endogenous cellular RNA, it engages RIPK3 also via RHIM homotypic interaction, generating another type of non-canonical necrosome. In this context, RIPK1 has an antagonizing role, where it inhibits necroptosis (X.-Y. Chen et al., 2022). Furthermore, ZBP1 has been associated with cell death induced by LPS, and it is capable of inducing caspase-8 activation and inflammasome activation through its interaction with RIPK1 via their RHIM domains (Muendlein et al., 2022) (Figure 1.2).

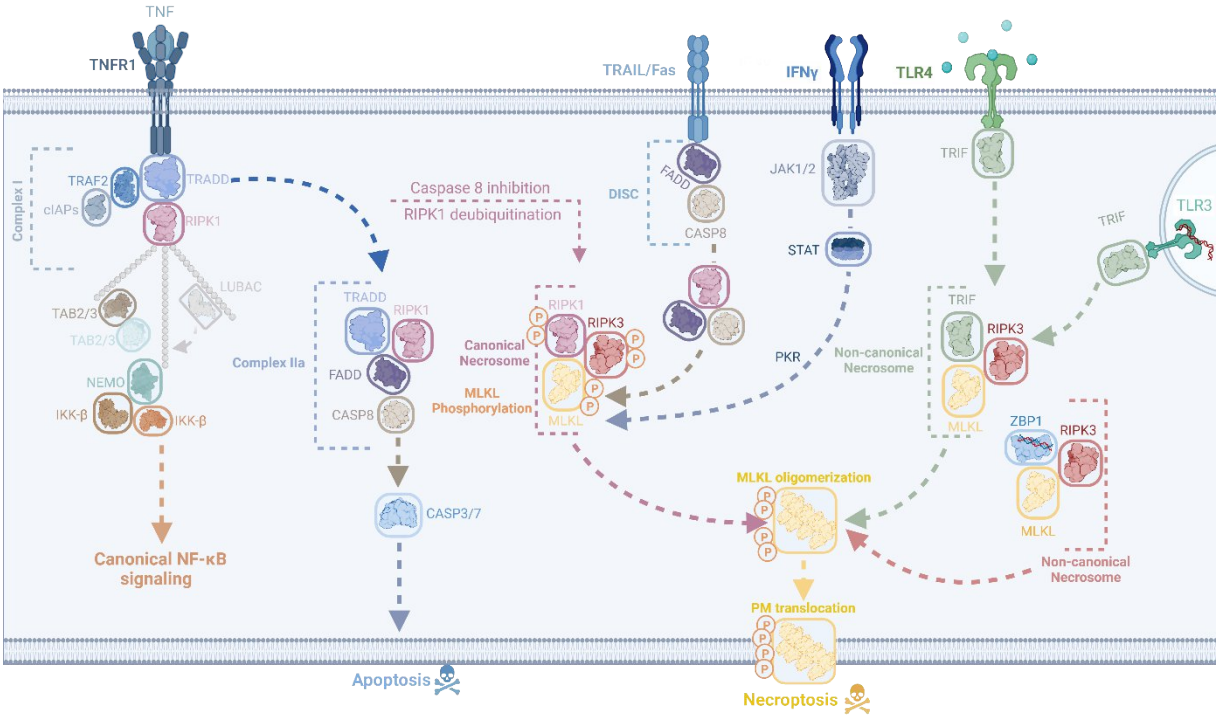

Figure 1. 2 Molecular mechanisms of necroptosis.

TNF binding to TNFR1 induces the formation of complex I, which is composed of TRADD, TRAF2, cIAPs, RIPK1, TAK1, LUBAC, and the IKK complex. cIAP1/2 generates Lys63 linked chains on RIPK1, forming a scaffold for binding LUBAC and TAK-TAB complex. Nemo-IKK complex is recruited upon linear ubiquitination of RIPK1 induced by LUBAC, which leads to the activation of the survival pathway mediated by NF-κB. When cIAPs or NF-κB targeted protein synthesis are inhibited, complex IIa is formed. This complex is composed of TRADD, FADD, and caspase-8. Activated caspase-8 induces apoptosis by induction of downstream caspases such as caspase-3/7.

In conditions of caspase-8 inhibition and RIPK1 deubiquitination, the canonical necrosome is assembled via RIPK1 and RIPK3 homotypic interactions through their RHIM domain, resulting in the activation

of MLKL through a phosphorylation cascade. The activated MLKL undergoes oligomerization and then is translocated to the plasma membrane to execute necroptosis.

TLR activation and nucleotide sensing proteins can initiate necroptosis via the formation of non-canonical necrosome. LPS, Poly I:C, double-stranded RNA can induce the formation of the non-canonical necrosome that is TRIF dependent. Viral-RNA or endogenous RNA binds to ZBP1, resulting in RIPK1-independent necroptosis through the formation of another non-canonical necrosome that is composed of RIPK3-ZBP1 and MLKL. The figure was prepared by using BioRender.com.

1.2.1 MLKL Structure and Activation

MLKL represents the final protein in the kinase cascade responsible for the execution of necroptosis. The structure of both mouse and human MLKL comprises two functional regions: an initial 4HB domain at the N-terminus and a pseudokinase (psK) domain at the C-terminus (Figure 1.3A, B). These two domains are connected by a two-helical linker, which is often referred to as the brace helices.

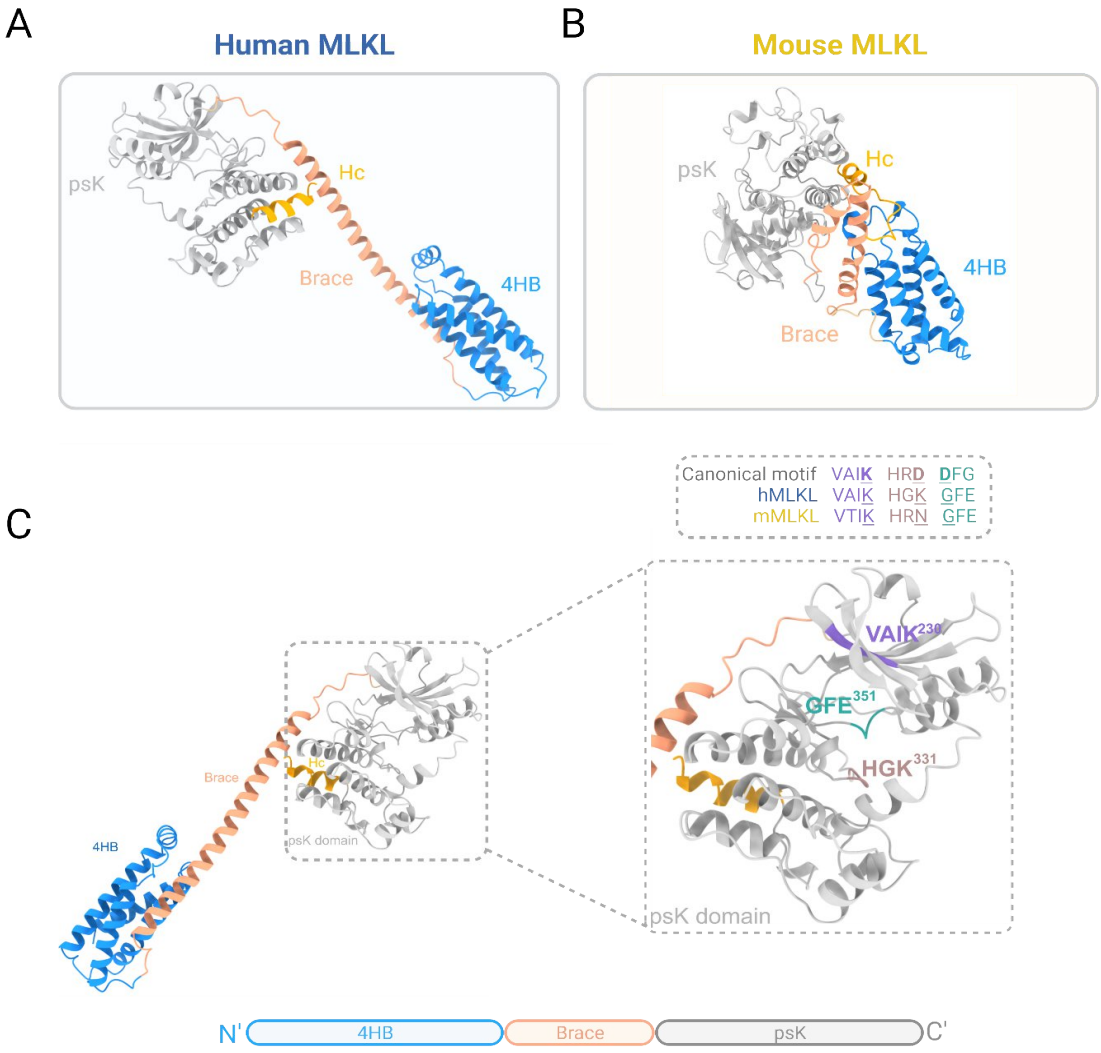

Figure 1. 3 Structure of MLKL: the deadly psK.

(A, B) Structure human MLKL isoform 1 (hMLKL1) (AlphaFold prediction Q8NB16) (A) and of mouse MLKL isoform 2 (mMLKL2) (PDB 4BTF) (B) showing different domains of MLKL. Sequence divergences at key kinase catalytic motifs that convert mouse or human MLKL into a catalytically dead kinase. (C). The 4HB is highlighted in dodger blue, the braces in light salmon, the psK in silver, and the Hc in orange. The figure was created by using ChimeraX and BioRender.com.

Despite the similarities between mouse and human MLKL in terms of their activation, mouse and human MLKL are not interchangeable and cannot be substituted for one another (Davies et al., 2018; Petrie et al., 2018; Tanzer et al., 2016). This means that human MLKL cannot complement mouse MLKL in mouse necroptotic environments and *vice versa*. This was validated by the fact that mouse and human MLKL can only interact and be phosphorylated with its correspondent RIPK3, suggesting a divergent co-evolution of MLKL and RIPK3 across different species (Tanzer et al., 2016). The core of MLKL activation is its RIPK3-mediated phosphorylation of the activation loop of the MLKL psK domain at T357/S358 in human MLKL and S345 in mouse MLKL, which is considered the key hallmark of MLKL activation (Murphy et al., 2013; Sun et al., 2012; Tanzer et al., 2016).

MLKL N-terminal domain (NTD): lethal in a league of its own

The N-terminal 4HB domain, comprising the residues 1-125 in mouse MLKL and 1-124 in human MLKL, serves as the 'lethal' component (Tanzer et al., 2016). In both human and mouse, it has been shown that the 4HB is of absolute necessity for necroptosis execution (Liccardi & Annibaldi, 2023). However, recent studies suggest that the ability of the 4HB to exert necroptosis is distinct between the two species (Alvarez-Diaz et al., 2016; Davies et al., 2018; Petrie et al., 2019). For instance, it is sufficient to kill the cells upon the expression of the amino-terminal 4HB of the mouse MLKL (Hildebrand et al., 2014). Furthermore, the recombinant 4HB domain of mouse MLKL permeabilizes lipid bilayers *in vitro* (Tanzer et al., 2016). On the other hand, the 4HB of the human MLKL shows less potency in the ability to execute cell death alone, and it has been shown that it could depend on some conditions, such as forced oligomerization (Tanzer et al., 2016). The basis behind these differences is still elusive and is a matter of investigation (Murphy, 2020).

The deduction of how the 4HB domain disrupts membranes through structural and functional analysis is still challenging due to the lack of substantial similarity between this domain when compared to other protein families (Petrie et al., 2017a). However, it is believed that its killing activity is attributed to its direct action on the plasma membrane, where the amphipathic α-helices of the MLKL 4HB are arranged into a coiled-coil arrangement, and the hydrophobic faces are hidden in the core of the structure (Flores-Romero et al., 2020; Murphy et al., 2013;

Su et al., 2014). Such arrangement is also observed in the ancient 4HB domain characterized in yeast and called the HeLo domain (Daskalov et al., 2016). The HeLo domain-containing proteins are abundant in yeast and have some similar domains in plants, and MLKL is the sole example in animals (Jubic et al., 2019; Mahdi et al., 2019).

The psK domain: a dead kinase

The psK domain is considered to act as a molecular swap that shifts between the active and inactive states of MLKL, as it attaches to and restrains the 4HB domain in a dormant state, non-activated state (Davies et al., 2018; Quarato et al., 2016; Su et al., 2014). Additionally, the psK domain serves as a signal transducer, where the phosphorylation of the activation loop at T357/S358 residues in human MLKL and S345 in mouse MLKL acts as a signal for MLKL activation (Murphy et al., 2013; Sun et al., 2012; Tanzer et al., 2016). This occurrence is believed to induce conformational changes within the psK, leading to the exposure of the 4HB domain. This exposure facilitates the formation of MLKL oligomers, plasma membrane translocation, and subsequently, membrane permeabilization and cell death (Petrie et al., 2019).

The psK domain has a similar structure to protein kinase domains in terms of their topology. Nonetheless, they are considered catalytically defective or non-functional because they are missing the essential residues that are required for phosphoryl transfer. Eventually, even when available in elevated concentrations, they do not show any measurable autophosphorylation or the capability to phosphorylate other proteins (Murphy et al., 2013; Sun et al., 2012).

In a typical active protein kinase, three essential patterns are conserved (Hanks et al., 1988). These motifs are (Figure 1.3C):

i. Val-Ala.-Ile-Lys (VAIK), which plays an essential role in positioning ATP during the catalytic process, specifically, the Lys residue side chain that is responsible for placing the α and β-phosphates during the transfer to phosphate groups.
ii. His-Arg-Asp (HRD), which is located in the catalytic loop, where the Asp side chain has a role in the catalytic activity that works in conjunction with the Asp of the third motif.
iii. Asp-Phe-Gly (DFG), which is located in the activation loop. Here, both the second and third motifs work on binding to the Mg^{2+} ion, which in turn coordinates the β and γ phosphates of the ATP.

In the majority of species, the VAIK motif is conserved in MLKL. However, it's noteworthy that the second motif, HRD, is substituted into different sequences, and in almost all species,

the DFG motif is altered to Gly-Phe-Glu (GFE). What is puzzling is that even without the presence of Mg^{2+} and Mn^{2+} ions, MLKL can still interact with ATP, ADP, and the analog of ATP called AMP-PNP despite lacking any hydrolytic activity (Kearney et al., 2014; Murphy et al., 2013).

The brace helices: not just a mere connection

The brace helices, which link the 4HB with the psK domain, have a more significant role in MLKL function than merely connecting these two domains. The two brace helices have a dual function. They not only transmit the structural changes caused by the psK phosphorylation mediated by RIPK3 to the 4HB domain but also serve as a platform for MLKL oligomerization (Davies et al., 2018; Meng et al., 2023; Quarato et al., 2016; Su et al., 2014). In addition, they also play a role in the regulation of activity, as they inhibit the intrinsic activity of the 4HB domain (Davies et al., 2018). Interestingly, there is a nine-amino-acid length difference in the brace region of the mouse MLKL compared to the human MLKL due to an insertion in the first brace helix of the human MLKL. This minor insertion could be the cause of notable structural differences in the overall folding of human and mouse MLKL, as predicted by AlphaFold (Figure 1.3A, B), and could also provide some explanations about their divergent mechanism of activation (Davies et al., 2018; Meng et al., 2023).

The impact of post-translational modifications to MLKL activation

Phosphorylation of the necroptosis mediators is the better-understood signal for propagation of the necroptotic cascade. Phosphorylation of both RIPK1 and RIPK3 is required for the formation of the necrosome, while MLKL phosphorylation serves as a signal for oligomerization and membrane translocation (Hildebrand et al., 2014; Murphy et al., 2013; Petrie et al., 2018; Quarato et al., 2016; Su et al., 2014; Wang et al., 2014b). RIPK1 is believed to be phosphorylated by either underlying autophosphorylation within its activation loop (Cho et al., 2009a) or by RIPK3-mediated phosphorylation (Petrie et al., 2017b). On the contrary, there is currently no concrete evidence that RIPK1 can phosphorylate RIPK3, although it has been observed that RIPK3 phosphorylation has been decreased in cells treated with necrostatin-1 (RIPK1 inhibitor) (Cho et al., 2009a). In both human and mouse MLKL, RIPK3 has been shown to phosphorylate specific Thr/Ser residues (specifically, T357/S358 in human MLKL and S347, S345, T349, and S352 in mouse MLKL) (Sun et al., 2012; Xie et al., 2013). When the T357 and S358 phospho-sites in human MLKL were mutated to Ala, necroptosis was blocked but did not hinder the binding to RIPK3 (Sun et al., 2012). This confirms that MLKL

phosphorylation is not only crucial for its activity but also for its ability to interact with RIPK3 (Meng et al., 2022). Furthermore, additional phosphorylation sites have been discovered in the mouse MLKL, which are S158, S228, and S248 (Tanzer et al., 2015). Mutating S158 or S248 to Ala, which eliminates phosphorylation but not to Asp or Glu to mimic the phosphorylated version of the protein, resulted in enhanced necroptosis even in the absence of external stimuli (Günther et al., 2016; Tanzer et al., 2015). This suggested that MLKL phosphorylation may affect the potential to regulate necroptosis either positively or negatively.

Within the necroptotic pathway, not only phosphorylation but also ubiquitination is a post-translational modification that is crucial in facilitating the regulation of MLKL (Z. Liu et al., 2021; Miyata et al., 2021; Yoon et al., 2022). Still, this is a matter of current debate, with many controversial opinions on how MLKL ubiquitination affects necroptosis signaling. One study suggests that MLKL ubiquitination of K219 is crucial for its activation (Garcia et al., 2021), and this sensitizes the cells to die by necroptosis, while another one claims that MLKL ubiquitination initiates its downregulation by promoting its degradation (Z. Liu et al., 2021).

More powerful when united- the oligomeric state of MLKL

One characteristic feature of cells undergoing necroptosis is the presence of phosphorylated MLKL oligomers in the plasma membrane (Samson et al., 2020). The exact structure of MLKL oligomers formation is still a subject of debate in the scientific community. Several studies have reported the formation of MLKL trimers (Davies et al., 2018; Hildebrand et al., 2014), tetramers (Petrie et al., 2018), hexamers (Wang et al., 2014a), octamers (Huang et al., 2017), and even polymers (S. Liu et al., 2017). Additionally, biophysical analyses of recombinant MLKL, such as small-angle X-ray scattering, analytical ultracentrifugation, and native mass spectrometry, have revealed that trimers of mouse MLKL are formed while the human MLKL assembles into tetramers (Davies et al., 2018; Hildebrand et al., 2014). Nevertheless, it is important to note that the ability of mouse MLKL to form higher-order oligomers within the cells is still under investigation and cannot be excluded. It was found that MLKL migrates in a non-reducing SDS polyacrylamide gel electrophoresis as a high-molecular-weight structure due to the possible presence of intramolecular disulfide bonds (S. Liu et al., 2017). However, whether these disulfide bonds are formed after the cell lysis or within the cells is still unclear.

Intriguingly, the sole formation of MLKL oligomers does not, by itself, trigger necroptosis. Recent evidence has shown that mutations in the 4HB domain's α-helix of human MLKL (D107A/E110A) have completely abolished the ability of necroptotic cell death induction,

despite the continuous ability to form MLKL oligomers was still intact (Petrie et al., 2018). In line with this, similar observations were found in the mouse MLKL orthologs (R105A/D106A and E109A/E110A) that resulted in a similar loss of necroptotic cell death but retained the ability to form higher-order oligomers (Hildebrand et al., 2014; Tanzer et al., 2016). Together, this data suggests cofactors play a crucial role in necroptosis via engagement with the 4HB domain.

MLKL in the plasma membrane: the omen of a disaster

Phosphorylated MLKL oligomers in the cells's plasma membrane are a typical feature of necroptosis (Y.-N. Gong et al., 2019). The translocation of MLKL oligomers to the plasma membrane is mainly mediated by several interactions between the cluster of positively charged residues in the 4HB domain of MLKL and the phosphatidylinositol phospholipids in the plasma membrane (Dondelinger et al., 2014). These interactions were further confirmed by a study that shows that the binding of specific monobody to specific residues in the α4-helix of the 4HB (D107, E111, L114) domain blocks the translocation of human MLKL oligomers to the plasma membrane, and their mutation hinders the membrane translocation (Petrie et al., 2020). MLKL translocation to the plasma membrane is considered the ultimate step required for its activation. However, the exact molecular mechanism of how MLKL mediates cell death is still unclear (Flores-Romero et al., 2020; Martinez-Osorio et al., 2023). Current models include:

i. Partial insertion of the 4HB domain, which is facilitated by specific interactions between the positively charged residues and the negatively charged phospholipids (Dondelinger et al., 2014; Quarato et al., 2016).

ii. Pore or channel formation, which involves the assembly of stable structures and the complete incorporation of MLKL oligomers in the plasma membrane (Wang et al., 2014b).

iii. Association with auxiliary transporters to facilitate ion imbalance and osmolysis (Cai et al., 2014; X. Chen et al., 2014).

1.2.2 Hc-Helix Accommodation into a Hydrophobic Groove of MLKL is Essential for Necroptosis

In the Lab of Prof. Dr. Ana Garcia Saez, different isoforms of MLKL have been extensively investigated (Ros et al., unpublished). Alternative splicing for the MLKL gene encodes for different isoforms in both human and mouse MLKL (Figure 1.4). In the human MLKL, three different variants are identified, known as hMLKL0, hMLKL1 (Q8NB16-1), and hMLKL2 (Q8NB16-2). Similarly, in the mouse MLKL, there are three different variants generated by alternative slicing. They are known as mMLKL1 (Q9D2Y4-1), mMLKL2 (Q9D2Y4-2), and mMLKL3 (Q9D2Y4-2).

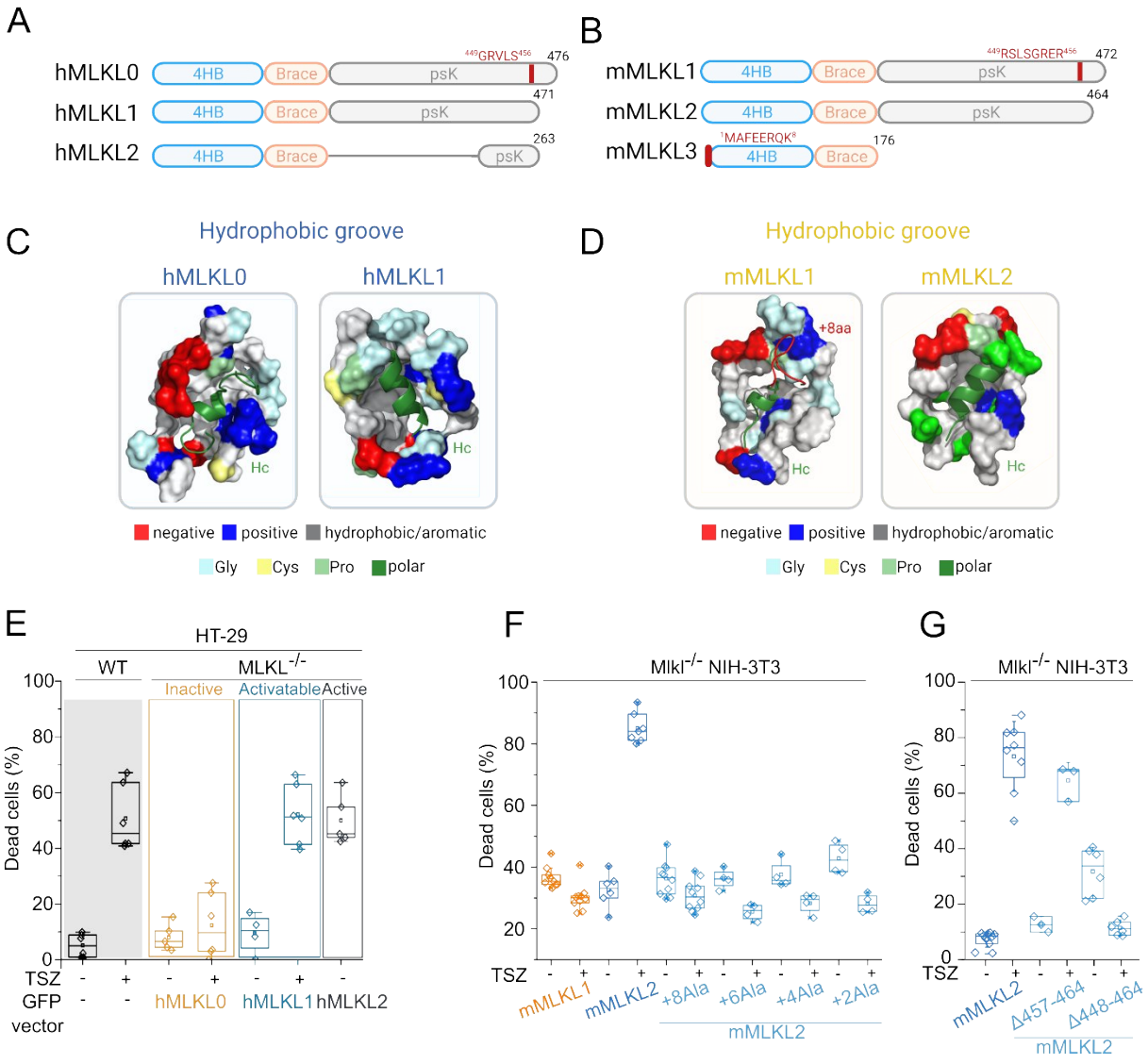

Figure 1. 4 Analysis of different isoforms of mouse and human MLKL disclosed a new mode of regulation.

(A, B) Domain structure of human (A) and mouse (B) MLKL isoforms. (C, D) Structural representation of the hydrophobic groove of hMLKL0, hMLKL1 (C), mMLKL1, and mMLKL2 (D). (E) Necroptotic activity of different isoforms of hMLKL in MLKL ko HT-29 cells transfected with GFP-tagged MLKL versions. (F, G) Necroptotic activity of different isoforms of mMLKL in MLKL ko NIH-3T3 cells transfected with GFP-tagged mMLKL isoforms and mutants in which Ala segments of different length were inserted before the Hc of mMLKL2 (F) or C-terminal deletion mutants (G) (Ros et al, unpublished).

Upon the structural and functional analysis of the different mouse MLKL isoforms, it was observed that mMLKL1 only differs from the mMLKL2 by the presence of eight extra amino acids at the C-terminal end of the psK domain (Figure 1.4A, B). This insertion causes the unfolding of the most terminal α-helix (Hc) in mMLKL1. In addition, hMLKL0 was also identified in humans. This isoform contains an additional five amino acids sequence at the Hc of hMLKL, being equivalent to mMLKL1 in mouse. The Hc α-helix was found to insert into a hydrophobic groove in hMLKL1 and mMLKL2 but was disrupted in structural models of hMLKL0 and mMLKL1 (Figure 1C, D). Interestingly, hMLKL0 and mMLKL1 are inactive variants, while hMLKL1 and mMLKL2 can be activated upon necroptotic stimuli (Figure 1.4E). This observation led to the hypothesis that accommodation of the Hc into a hydrophobic groove of MLKL is essential for its activation. This was further validated with the use of mutants that alter Hc-groove interactions, including Ala insertion mutants and C-terminal deletion mutants at the Hc of mMLKL2, as well as point mutations in residues of the putative groove (Figure 1.4F).

1.3 Exploring MLKL as a Prospective Therapeutic Target to Treat Diseases

Necroptosis has been implicated in the pathophysiology of a wide range of different diseases spanning broad disease categories. This includes inflammatory diseases (Weinlich et al., 2017), infectious diseases (Cho et al., 2009c; Xia et al., 2020), diseases of the Central Nervous System (CNS) (Faergeman et al., 2020; Ofengeim et al., 2015; Y. Zhou et al., 2017), Cardiovascular Diseases (CVD) (Zhe-Wei et al., 2018), and other diseases that affect vital organs such as kidney (Belavgeni et al., 2020), liver (Dara et al., 2016b, 2016a; Ni et al., 2019), and pancreas (Hildebrand et al., 2021).

Numerous studies have employed different experimental approaches to establish the connection between necroptotic effector proteins (RIPK1, RIPK3, and MLKL) and the pathogenesis of these diseases. These approaches can be broadly grouped into three major categories. Firstly, the employment of different experiments that include the generation of knockdown (kd) or knockout (ko) mice of RIPK1, RIPK3, and MLKL by using techniques such as short hairpin RNA (shRNA), small interfering RNA (siRNA), as well as CRISPR/Cas9, enabling the study of their effect in the *in-vivo* animal disease models. Secondly, the comprehensive analysis of

protein/gene expression in patient tissue samples has provided invaluable evidence of the involvement of necroptosis with these pathological conditions. Lastly, the pharmacological inhibition of these necroptotic effector proteins by using different available inhibitors (Gardner et al., 2022).

1.3.1 Understanding the Effect of MLKL Knockout in the Etiology of Different Diseases

Following the discovery of the potential role of MLKL in executing necroptosis, strains of MLKL ko mice have been generated to investigate the impact of this protein on various diseases (Murphy et al., 2013). The success of these mice strains has been evident, as the genetic deletion of MLKL did not lead to any developmental consequences in the absence of challenges such as the potentiation of different diseases. Indeed, MLKL ko mice are born according to the expected Mendelian ratios and show indistinguishable characteristics compared to wild-type (wt) littermates at birth and throughout adulthood (Crutchfield et al., 2021; J. Wu et al., 2013). The examination of MLKL's role in mouse models has revealed that, in the majority of instances, MLKL ko provides protection regardless of the initiated disease type (Figure 1.5). However, some evidence suggests that enhancement of MLK-induced necroptosis can be advantageous in the context of different malignancies (Meng et al., 2021).

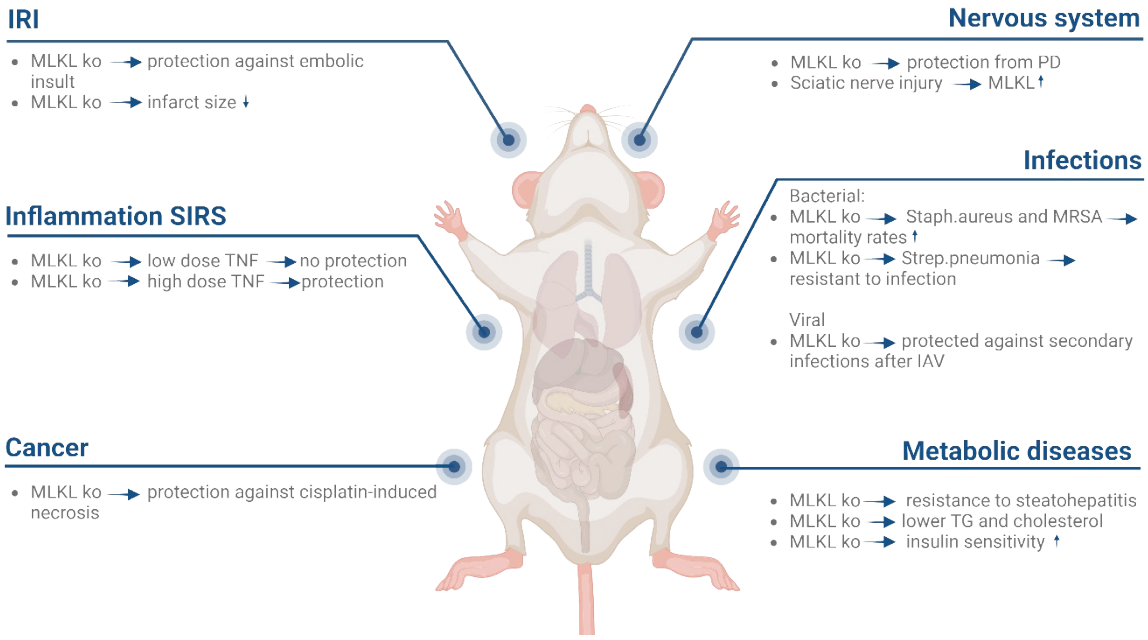

Figure 1. 5 Evidence linking the involvement of MLKL ko with protection in mice models.

Evidence obtained in mouse models pointing the crucial role of MLKL in the pathogenesis of different diseases. MLKL ko shown to have protective effects against certain infections and diseases in the nervous system and metabolic diseases, IRI, and cancer treatment-induced toxicity. Arrows indicate an

increase (↑) or decrease (↓) of disease-associated symptoms. The figure was created by using BioRender.com.

Neurological diseases

Recent findings have increasingly emphasized the role of MLKL in neurological diseases within mouse models. There is controversial evidence indicating variations in the tolerance of MLKL ko among different mouse models. For instance, in a chemically induced Parkinson's Disease (PD) mouse model, MLKL ko mice exhibited protection against neurotoxic inflammatory responses due to elevated dopamine levels (Lin et al., 2020). However, in other models, such as Sciatic Nerve Injury (SNI), the examination of MLKL levels in myelin sheath was shown to be elevated, promoting the breakdown and subsequent nerve regeneration. Furthermore, nerve generation was accelerated with the overexpression of MLKL in this model (Ying et al., 2018).

Ischemia and Reperfusion Injury (IRI)

MLKL, along with cell death mechanisms in general, plays a significant role in the etiology of IRI within the context of an infarction. MLKL, in particular, can directly impact blood vessel occlusion and end-organ damage in response to the deprivation of oxygen and ATP (Luedde et al., 2014). Data derived from MLKL ko mice indicates partial protection against the initial embolic insult, accompanied by a reduction in infarct size and improved locomotive recovery after stroke (Shi et al., 2020; J. Yang et al., 2018). These findings suggest that the modulation of MLKL activity may hold promise in mitigating the consequences of IRI associated with the infarction.

Infection

The role of MLKL deficiency in response to infection is controversial and depends on the nature of the infecting agent, whether it is bacterial or viral infection. In bacterial infections, MLKL-dependent necroptosis serves as a protective mechanism to eliminate pathogens and reduce their side effects. For instance, in chronic infection with *Staphylococcus aureus* and methicillin-resistant *S. aureus* (MRSA), MLKL ko exacerbates bacterial burden and elevates mortality rates (D'Cruz et al., 2018; Kitur et al., 2016). However, in particular bacterial infections, such as *Streptococcus pneumonia* and *Serratia marcescens*, MLKL ko were resistant to infections in comparison to wt mice (Gonzalez-Juarbe et al., 2020; González-Juarbe et al., 2015). Furthermore, MLKL ko mice were protected from the polymicrobial shock induced by Cecum Ligation and Puncture-induced sepsis (CLP) pathogens (H. Chen et al., 2020).

In the context of viral infections, MLKL ko mice exhibited protection against various viral strains. When exposed to a lethal dose of Influenza Virus A (IVA), these mice demonstrate resistance to lung damage caused by the virus (T. Zhang et al., 2020). Furthermore, MLKL deficiency extends protection from inflammation associated with the infection, particularly in later stages secondary to IVA exposure. Notably, MLKL ko mice also show protection from cardiac remodeling followed by IAV infection (Gonzalez-Juarbe et al., 2020). Altogether, these findings showed the different responses of MLKL-deficient mice to bacterial and viral infections, emphasizing the infection as a crucial determinant in the observed outcome.

Inflammation

The impact of MLKL on mouse models of inflammation is versatile and depends on various factors, particularly on the stimuli that initiate the inflammation, its severity, and the location of the inflammation. For instance, in the Systemic Inflammatory Response Syndrome (SIRS), the response of MLKL ko mice differs based on the mode of inflammation induction. When induced by low doses of TNFα, MLKL ko mice did not exhibit protection from the side effects (Newton et al., 2016). However, when induced by high doses of TNFα, MLKL ko mice showed a protective response in this model of inflammation (Moerke et al., 2019; Newton et al., 2016; Pierotti et al., 2020). This variability illustrates the role of MLKL in different inflammatory contexts, highlighting the sensitivity of its effects to the specific conditions of inflammation.

Metabolic diseases

The deficiency of MLKL achieved either through its ko or pharmacological inhibition, has proven to have beneficial effects on a wide range of liver disease side effects. MLKL ko mice exhibited resistance to steatohepatitis by the reduction of both the fats *de-novo* synthesis and expression of chemokine ligands (Saeed et al., 2019). In line with this notion, the pharmacological inhibition of MLKL by using RIPA-56, which downregulates the expression of MLKL, showed protection against high-fat diet steatosis (Majdi et al., 2020).

Additionally, the advantageous role of MLKL ko extends to various metabolic syndromes. MLKL ko results in lower serum triglycerides and cholesterol levels, protecting against dyslipidemia (Saeed et al., 2019). Furthermore, MLKL ko mice were protected against insulin resistance and showed improved insulin sensitivity and reduced fasting blood glucose of mice on a high-fat diet (H. Xu et al., 2019). Finally, MLKL inhibition was shown to be beneficial in atherogenesis, where it reduces the size of the necrotic core (Rasheed et al., 2020).

Cancer and cancer treatment

Cisplatin stands out as one of the most known chemotherapeutic agents for solid cancer treatment; nevertheless, its consumption is usually associated with nephrotoxic side effects. Interestingly, MLKL ko mice have demonstrated protection against cisplatin-induced tubular necrosis in contrast to their wt counterparts (Y. Xu et al., 2015). This fact suggests the potential for enhancing the use of cisplatin in combination with MLKL inhibitory agents to eliminate the possible side effects.

1.3.2 MLKL: A Promising Therapeutic Target for Addressing Human Diseases

Based on observations obtained from mouse models, MLKL and necroptosis exhibit dual roles. On one hand, necroptosis can act as a defense mechanism against various insults to cells and tissues in response to infections and diseases. On the other hand, necroptosis can be responsible for the development of the disease. However, evolutionary insights from modern-day carnivores, such as metatherians and aves, where MLKL and/or RIPK3 are genetically deleted, have offered valuable perspectives on how complex vertebrates can survive without necroptosis (Dondelinger et al., 2016). This observation supports the idea of the intricate interplay and cooperation between different PCD mechanisms (Doerflinger et al., 2020). Moreover, insights from this evolutionary perspective suggest that pharmacological inhibition of MLKL and necroptosis in humans may not compromise pathogenic defense. Recent studies even indicate that inhibiting necroptosis could potentially reduce inflammatory responses, which, in many cases, cause a more significant threat than the infection itself (T. Zhang et al., 2020).

In any case, extrapolation from the data obtained from mouse models of MLKL ko or mutants must be carefully adapted to the knowledge of key differences between the human and mouse MLKL structures and regulation, especially in the context of clinical trials (Davies et al., 2020; Petrie et al., 2018; Tanzer et al., 2016). For instance, the withdrawal of some RIPK1 inhibitors from phase I and II clinical trials for pancreatic cancer and chronic inflammatory diseases due to lack of efficacy highlights the importance of adapting the insights from mouse models to the unique aspects of human biology (Martens et al., 2020; Weisel et al., 2021).

After the comprehensive exploration of MLKL's potential roles in various mouse models, the attention now turns to its impact on diverse human diseases. The intriguing observation that the deletion of MLKL can provide protection against some diseases holds promise for its substantial application in human health. Indeed, the examination of human samples using antibodies targeting both MLKL and phosphorylated MLKL reveals its potential for

involvement in a broad spectrum of human health-related conditions (Figure 1.6). Delving deeper into the association of MLKL with various human diseases not only enhances our understanding of the molecular mechanisms underlying these conditions but also the investigation of its potential as a novel therapeutic target (Martinez-Osorio et al., 2023).

Nervous system diseases

Exploring their role in neurodegenerative diseases, both MLKL and its activated form the phosphorylated MLKL levels were found to be elevated in derived postmortem tissues of patients with PD (Iannielli et al., 2018), a disorder characterized by motor dysfunction and cognitive impairment. In addition, similar findings were observed in samples from the brains of patients with Alzheimer's Disease (AD) (Caccamo et al., 2017), which is a progressive condition marked by memory loss and a decline in cognitive abilities. Furthermore, MLKL has been detected in pathological samples from the critical lesions of patients with multiple sclerosis, an autoimmune disease that affects the central nervous system and leads to several neurological symptoms (Picon et al., 2021).

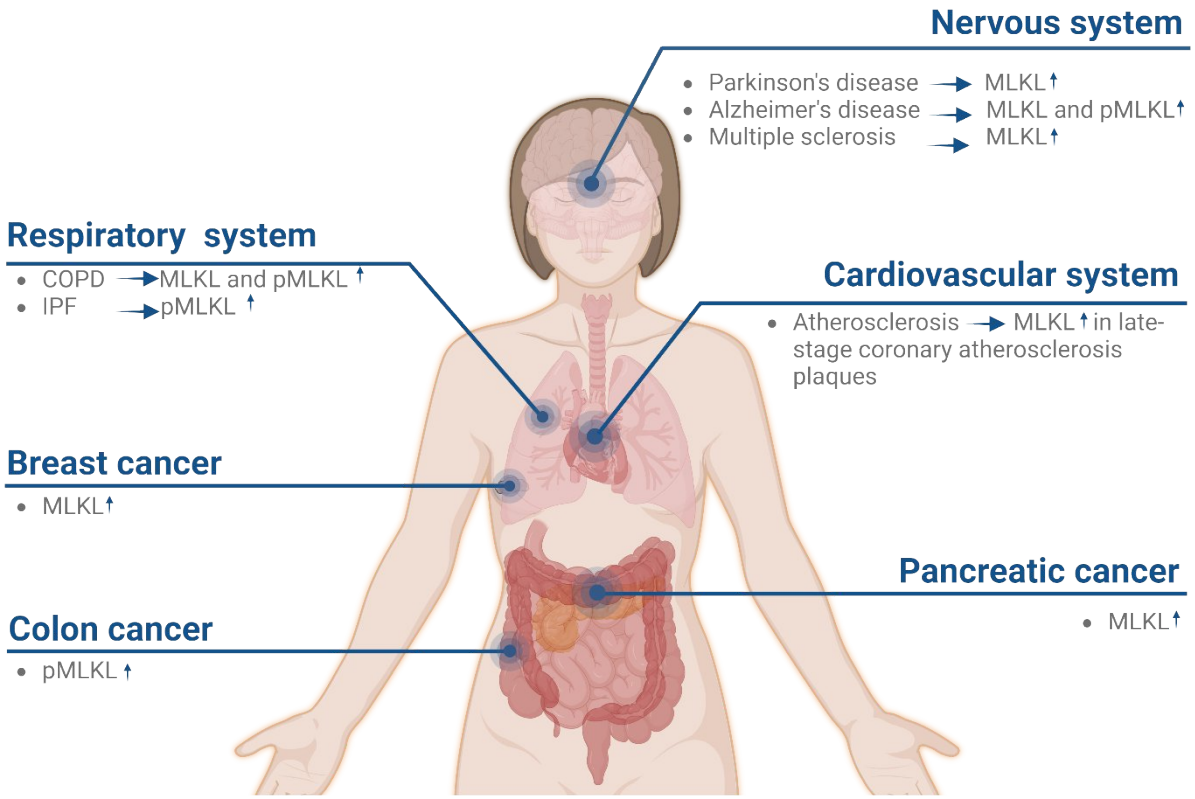

Figure 1. 6 Evidence linking the involvement of MLKL upregulation with different human diseases.

MLKL has a crucial role in the pathogenesis of different diseases related to the central nervous system, the cardiovascular system, and the respiratory system. Upregulation or activation of MLKL contributes to different types of cancer, such as pancreatic cancer, breast cancer, and colon cancer. Arrows indicate an increase (↑) in MLKL or phosphorylated MLKL. The figure was created by using BioRender.com. Adapted from (Martinez-Osorio et al., 2023).

Cardiovascular system diseases

Within the domain of CVD, MLKL has emerged as a crucial player linked to the pathophysiology of atherosclerosis (Kamal et al., 2021; Karunakaran et al., 2016). Atherosclerosis is characterized by the persistent inflammatory impact on arterial walls, and it poses a significant threat by potentially triggering abrupt blood clots, thereby precipitating conditions such as heart attacks or strokes (Badimon et al., 2012). Notably, patients with unstable carotid atherosclerosis have been found to exhibit elevated levels of MLKL within samples extracted from atherosclerotic plaques (Karunakaran et al., 2016). Moreover, it has been identified that the low-density lipoprotein is a factor that promotes the transcription of MLKL and facilitates its phosphorylation (Karunakaran et al., 2016). This finding manifests the potential role of MLKL in the development and progression of disease complications.

Respiratory system diseases

Compelling evidence points towards the involvement of MLKL in the pathogenesis of two significant pulmonary diseases: Coronary Obstructive Pulmonary Disease (COPD) and Idiopathic Pulmonary Fibrosis (IPF). These conditions are marked by chronic respiratory issues, and investigations have revealed the close involvement of MLKL. In particular, elevated levels of MLKL have been observed in the lung tissues of individuals affected with COPD (Lu et al., 2021) and IPF (Lee et al., 2018). This finding highlights the potential contribution of MLKL to the progression of these diseases, and current investigations aim to ameliorate the impact of COPD and IPF on respiratory health.

MLKL and cancer

The role of MLKL in cancer remains controversial, given that necroptosis appears to have a dual effect, potentially acting both against and in favor of cancer development and progression. Indeed, the levels of necroptosis can vary, being either diminished or increased in different types of cancer cells (Y. Gong et al., 2019). On one side, the reduced expression of RIPK3 and MLKL is associated with unfavorable prognosis in a range of cancer types, including breast cancer (Won et al., 2021), colorectal cancer (Conev et al., 2019), acute myeloid leukemia (Nugues et al., 2014), head and neck squamous cell carcinoma (McCormick et al., 2016), melanoma, cervical squamous cell carcinoma (Ruan et al., 2015), gastric cancer (Ertao et al.,

2016), and ovarian cancer (L. He et al., 2013). On the other hand, research conducted on pancreatic cancer patients revealed that aside from RIPK1 and RIPK3, higher MLKL levels were identified in the aggressive form of human pancreatic cancer tissue cells (Martens et al., 2021). Furthermore, activated MLKL has been elevated in patients with colon cancer and tumor tissues of esophageal cancer and neck squamous cell carcinoma (X. Liu et al., 2021).

1.4 Ending the Life of the Assassin: Therapeutic Targeting of MLKL

Several studies reinforce the fact that necroptosis is involved in the pathophysiology of numerous diseases (W. Zhou & Yuan, 2014). This makes the core proteins RIPK1, RIPK3, and MLKL, compelling targets or drug development in the treatment of necroptosis-related diseases. In fact, more than 20 classes of RIPK1 inhibitors have been developed as drugs to treat several diseases, and some of them are already in clinical trials (Harris et al., 2017; Z. Li et al., 2022; Ren et al., 2017). Furthermore, RIPK3 inhibitors were also reported to be efficient in different mouse models of necroptosis-related diseases (S. Wu et al., 2021; H. Zhang et al., 2019).

Despite the fact that targeting MLKL to inhibit necroptosis would represent a very attractive option, the development of MLKL inhibitors is still limited. Targeting MLKL represents a highly promising therapeutic avenue with the potential to tackle a broad spectrum of necroptosis-related diseases and can potentially add several advantages over the currently available necroptosis inhibitors. First, MLKL is the final executor for necroptosis known so far, and in contrast to RIPK1 and RIPK3, MLKL is not connected to other cellular pathways, and it can overcome the limitations observed upon targeting RIPK1 and RIPK3 because their inhibition can affect apoptosis or facilitate the induction of aberrant apoptosis, respectively (Newton, 2015; Patton et al., 2023). Second, MLKL is a pseudokinase, and its mechanism of action differs from the known kinases, such as RIPK1 and RIPK3, which will reduce the possibility of potential off-targets. Moreover, targeting MLKL can be achieved not only by targeting the psK domain but also by targeting other domains in the protein, such as the 4HB domain and the brace region (Martinez-Osorio et al., 2023).

Despite the central role of MLKL in necroptosis, the exact mechanism of how in executes cell death is not fully elucidated yet. Therefore, developing inhibitors for MLKL will not only hold promise for treating various diseases but also will contribute to a deeper understanding of the complexity of its function. In recent years, significant efforts have been directed toward

developing small molecules targeting different regions of MLKL, including the psK and the 4HB domains. Furthermore, innovative studies have proven that targeting MLKL can also be achieved by developing new techniques that manage to inhibit MLKL successfully; this includes monobodies (Petrie et al., 2020) and PROteolysis Targeting Chimeras (PROTACs) (Rathje et al., 2023a).

The subsequent section will summarize the main properties of the MLKL inhibitors (Figure 1.7) that have been discovered or are still under development. Existing small molecules targeting MLKL can be categorized into two primary groups: inhibitors that interact with the psK domain or inhibitors and binders that interact with the 4HB domain.

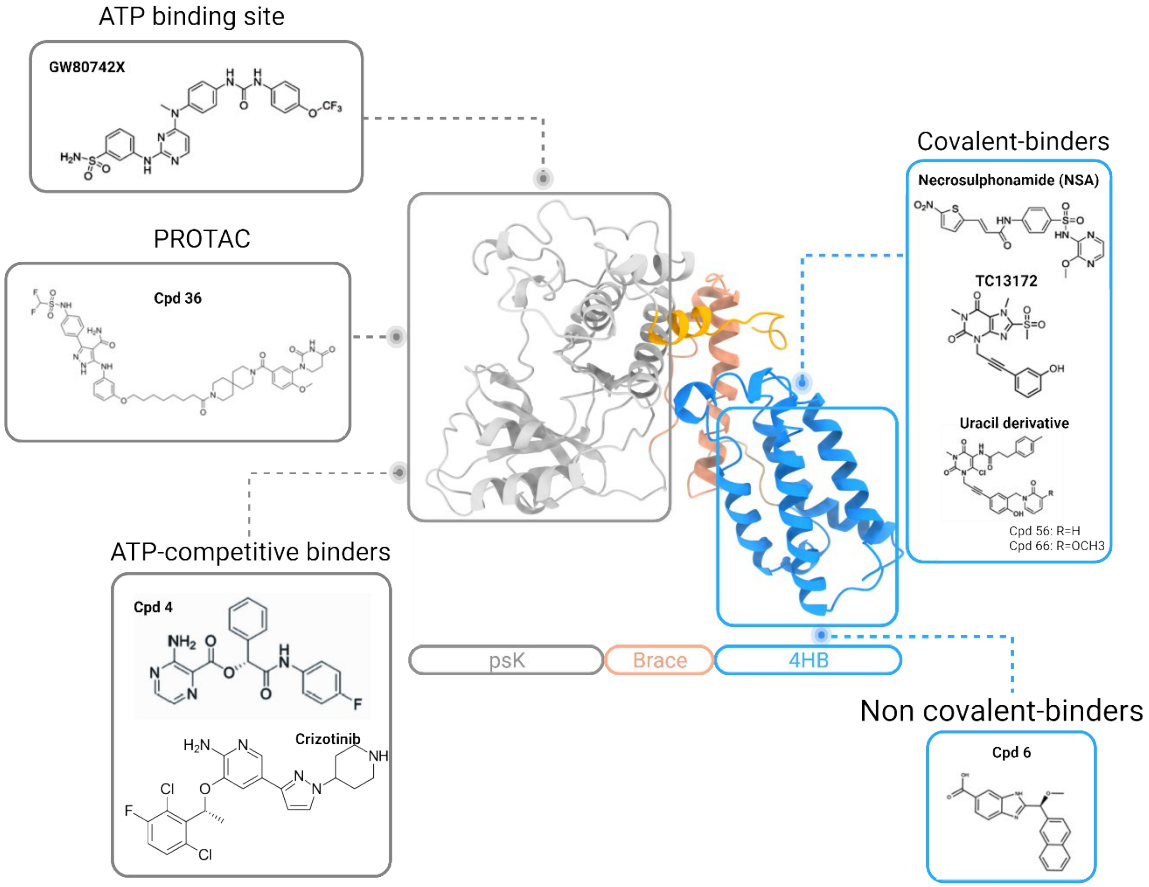

Figure 1. 7 Current existing inhibitors or binders targeting MLKL.

The scheme shows the structure of the different domains of MLKL with currently available small molecules that target them. Targeting the Hc (in yellow) represents a new strategy for selective inhibition of MLKL.

1.4.1 Targeting the psK Domain

Due to the pivotal role of the psK domain in the function of MLKL, developing small molecules that target it was from the early approaches to discover necroptosis inhibitors. The first MLKL inhibitor that targeted this site was GW806742X (also known as compound 1 (Cpd1) or aminopyridine 42), which was discovered after screening against the recombinant mouse MLKL using thermal shift assays (Hildebrand et al., 2014). It inhibits necroptosis in mouse dermal fibroblasts (MDF) with a concentration required to achieve 50% inhibition (IC50) of less than 50 nM. When the compound was tested in human cell lines, it showed moderate potency in TNF-stimulated FADD-deficient Jurkat cells with an IC50 of 1.85 μM and high toxicity profiles with approximately 2 μM (Ma et al., 2016; Pierotti et al., 2020). Furthermore, Cpd1 did not affect MLKL phosphorylation, suggesting that it did not affect the RIPK3 binding; however, it blocked MLKL membrane translocation (Gardner et al., 2022; Murphy et al., 2014). In contrast with this evidence, this compound was found to suffer from poor kinome selectivity, as it was able to inhibit 56 out of 403 kinases at 1 μM. RIPK1 and RIPK3 were from these kinases, and this might imply that its inhibitory activity might be due to its effect on the RIPK kinases and not only on MLKL (Hildebrand et al., 2014).

In another study by (Ma et al., 2016), Cpd4 and crizotinib were identified as binders to the psK of MLKL. The screening for these inhibitors was done against the active site of MLKL from a library of 5000 compounds by using an ATP-competitive probe displacement assay. Both compounds were found to be more specific as they have a higher affinity towards MLKL in comparison to RIPK1 and RIPK3. Indeed, Cpd 4 is only bound to MLKL out of 403 other kinases at 1 μM. Despite their sub-μM affinity towards MLKL, these compounds failed to inhibit necroptosis. In a complementary study, Cpd2 was identified as a derivative of Cpd1 with a more potent effect that can bind to either the psK domain or the full-length human and mouse MLKL (Pierotti et al., 2020).

From a mechanistic point of view, kinase inhibitors can be classified into two categories, depending on their mechanism of binding and whether they bind to the active or inactive conformation of the kinase (Dar & Shokat, 2011). Type I kinase inhibitors bind to the kinase domain by forming hydrogen bonds with the kinase hinge and occupy the adenosine binding pocket. Type II kinase inhibitors also bind to the adenosine binding pocket but form a GFD-out configuration. Cpd1 was classified as a type II inhibitor, while Cpd4 and crizotinib were classified as type I inhibitors (Ma et al., 2016). Furthermore, it was found that Cpd1 competes with the ATP or ADP at the ATP binding site of MLKL, and this was further confirmed by its

failure to interact with the MLKL K219M mutant that has a defective ATP binding site (Pierotti et al., 2020). Additionally, Cpd2 was found to bind to the nucleotide-binding site by hydrogen bonding with E250, G349, and C286 MLKL residues (Pierotti et al., 2020).

Additional screening was conducted to find MLKL inhibitors that bind to the psK domain. In a patent submitted by Garner, J. D. 2020, a series of pyrazole carboxamide-based MLKL binders were reported to bind to MLKL within the nanomolar range (less than 10 nM). These compounds have a 1000-fold selectivity over the typical RIPK kinases RIPK1 and RIPK3. This patent was the starting point of another study conducted by (Rathje et al., 2023b) on PROTACs development as a novel approach to down-regulate MLKL and subsequently inhibit necroptosis. This method is based on proteolytic targeting chimeras that can be used to target protein of interest (POI), which results in its downregulation and often allows for greater effect than with the use of the POI ligand alone. These molecules are composed of three main components: the ligand that binds to the POI, the E3 ligase, and a linker that links the two binding motifs. The PROTAC known as Cpd36 was synthesized by using an MLKL binder with no inhibitory activity and a cereblon (CRBN) ligand, both connected by a linker (Rathje et al., 2023b). This molecule managed to achieve 90% of MLKL degradation at µM concentrations and protected from necroptosis in cells. Mechanistically, it was shown that Cpd36 recruits MLKL to the E3 ligase CRBN and facilitates its proteasomal degradation.

Altogether, while offering a promising category for necroptosis inhibitors, these studies highlight the challenges and drawbacks faced in developing inhibitors targeting the psK domain of MLKL. These challenges are mainly due to the lack of selectivity towards MLKL and the presence of potential off-targets. In fact, Cpd1 was initially designed as a Vascular Endothelial Growth Factor Receptor 2 (VEGFR2) inhibitor (Sammond et al., 2005), and crizotinib was developed as an inhibitor for Mesenchymal-Epithelial Transition (c-MET) and Anaplastic Lymphoma Kinase (ALK) (J. J. Cui et al., 2011), which exemplifies the lack of selectivity for MLKL. This underscores the need for enhanced specificity in the design and development of MLKL inhibitors.

1.4.2 Targeting the Executioner of the Assassin: The 4HB domain

In a study where they made a screening campaign of 200 000 compounds against HT-29 cells stimulated by TSZ to induce necroptosis, one hit (14) inhibited necroptosis with an IC50 of less than 1 µM (Sun et al., 2012). This compound was further optimized, and a 3-methoxypyrazin-2-yl derivative known as necrosulfamide (NSA) was developed. NSA was then tested against different cell lines (human or mouse), including HT-29, L929, and NIH-3T3. Notably, NSA

only inhibited necroptosis in the human cell line (HT-29) with completely no effect on the mouse cell lines. This discovery pinpointed MLKL as the primary target of NSA and established it as the central executor for necroptosis (Liao et al., 2014; Sun et al., 2012).

Consequently, NSA has become a widely employed tool in experimental research for investigating necroptosis in cellular contexts. In addition, a xanthine-based hit with strong necroptosis inhibition properties was also identified from the same screening (Yan et al., 2017). After rounds of optimization, TC13172 was identified and emerged as a potent MLKL inhibitor with remarkable potency in the low nanomolar range. TC13172 was also tested using a similar approach to detect its inhibitory effects in different cell lines. Strikingly, it also inhibited necroptosis only in human HT-29 cells, and no effect was observed in mouse L929 or NIH-3T3 cells. This high species specificity is attributed to their mechanism of action, where it was found that both bind covalently to the C86 within the α-4 helix of the 4HB domain, which is exclusive to human MLKL (Yan et al., 2017). Consequently, these inhibitors are unsuitable for fundamental research or pre-clinical investigations involving mice or murine cells.

While NSA and TC13172 are known for their significant potency, they also suffer from some drawbacks. In particular, both NSA and TC13172 exhibited cytotoxicity at concentrations more than 10 μM (B. Cui et al., 2022). Furthermore, NSA exhibits moderate potency and restricted Structure Activity Relationship (SAR), as well as its ability to target other surface Cys residues rather than a specific binding pocket. In fact, in a more recent study, it was found that NSA displayed cross-reactivity with gasdermin D (GSDMD) directly or upstream via caspase-1, and pyroptosis was inhibited as a consequence (Rashidi et al., 2019; Rathkey et al., 2018). This limits the further development of NSA and restricts its usage only *in-vitro* primate cell research. The presence of methyl sulfone in TC13172, as its functional group is activated by hydrogen boning with C86 in human MLKL, makes it susceptible to reacting with nucleophilic agents, which will generate a by-product with substantial toxicity in cells and reduced metabolic stability (B. Cui et al., 2022). In more recent studies attempting to develop new covalent MLKL binders with enhanced properties that overcome the drawbacks observed with the previous inhibitors, a novel family of compounds was developed based on TC13172. In the updated generation of inhibitors, the xanthine core found in TC13172 was substituted with a uracil core (B. Cui et al., 2022). This alteration resulted in improved drug-like characteristics, including enhanced stability and reduced risk of off-target (Cui et al., 2022).

Furthermore, uracil compounds did not inhibit necroptosis in mouse embryonic fibroblasts (MEF) cells, which suggests that they also have the same mechanism of action by binding to

the C86 and also exhibit species selectivity towards the human MLKL (B. Cui et al., 2022). Although NSA, TC13172, and the uracil derivatives all target C86 in human MLKL, they appear to employ distinct inhibition mechanisms. In addition to the interaction with C86, NSA creates a π-cation interaction with L157 found in the second brace helix. Conversely, TC13172 functions by stabilizing the pack of α-6 helix from the brace region against the 4HB domain by forming π-π stacking interactions with F148 (Rübbelke et al., 2020). In the case of the uracil-derived compound 56, covalent binding to C86 takes place through the replacement of the 6-Cl group, resulting in the establishment of π-π interactions between its core and F148 of MLKL (B. Cui et al., 2022).

Despite employing similar covalent binding mechanisms to interact with MLKL, NSA, TC13172, and uracil-derived compounds influence the hallmarks of MLKL activation in slightly varying ways. None of them interfere with the activation of the upstream kinases RIPK1 and RIPK3 or affect MLKL phosphorylation that RIPK3 mediates. Precisely, NSA results in partial inhibition of MLKL oligomerization, a more potent effect compared to that observed with uracil derivatives. In contrast, TC13172 completely inhibits the oligomerization of MLKL. Importantly, all inhibitors within this category entirely prevent the translocation to cellular membranes (B. Cui et al., 2022; Gardner et al., 2022).

In a recent study with the aim of developing novel inhibitors that target the 4HB of MLKL, the compound P28 was identified as a potent inhibitor of necroptosis and showed antifibrotic effects (Oh et al., 2023). P28 acted by blocking the phosphorylation of MLKL and its oligomerization after the cells; furthermore, it inhibited the translocation of MLKL to the plasma membrane. Mechanistically, P28 was able to covalently modify the C86 residues in the FSNRSNI**C**RFLTASQDK peptide at the N-terminal region of MLKL. In comparison to the previously mentioned covalently binding inhibitors, treatment with P28 successfully reduced the activation level of hepatic stellate cells and hepatic fibrosis markers expression that was induced by necroptosis.

Recently, a series of fragments that bind noncovalently to the MLKL was reported after a screening of a fragment library against the recombinant 4HB domain of human MLKL. A starting molecule, Cpd1, which has an indole moiety, was selected for further optimization. From this optimization, Cpd5 and 7 emerged as the enhanced derivatives with improved binding affinity but were still within the μM concentration range (more than 50 μM) (Rübbelke et al., 2021a). These compounds bind to a hydrophobic pocket at the end of the 4HB domain, opposite to C86, which is the target residue for irreversible MLKL inhibitors. Interestingly, it was

observed that the detergent nonyl-maltoside, in conjunction with phytic acid, functions as an activator of the 4HB domain and can compete with Cpd5 for binding to MLKL. This finding raised the possibility that these compounds might be capable of inhibiting MLKL in cell-based assays (Rübbelke et al., 2021b). The rationale behind this lies in the structural similarity of these detergents to inositol phosphates, which are essential for MLKL oligomerization and translocation to the membrane. Regrettably, the activity of Cpd5 could not be assessed in cells due to its limited membrane permeability, and it did not exhibit activity in an in vitro liposome leakage assay. Therefore, further optimization is still necessary to establish their effectiveness as MLKL inhibitors.

1.5 Aims

Necroptosis is a form of RCD that results in the release of inflammatory cellular contents after plasma membrane permeabilization, thus triggering the immune response. Necroptosis seems to be implicated in a wide range of pathophysiological conditions that include infectious diseases, liver disorders, kidney injuries, neurodegenerative diseases, cardiovascular disorders, autoimmune diseases, and cancer. MLKL is the necroptosis executor of plasma membrane permeabilization and, therefore can potentially be also connected to these diseases. Despite the fact that targeting MLKL to inhibit necroptosis represents a very attractive strategy, the development of MLKL inhibitors is still limited. The currently available inhibitors of MLKL have some drawbacks, such as being unspecific towards MLKL and having low stability and selectivity. Furthermore, no inhibitor has been reported for the mouse MLKL so far.

These facts motivated us to investigate new potential inhibitors that target MLKL. Research in the lab of Prof. Dr. Ana Garcia Saez identified a previously undiscovered hydrophobic pocket within MLKL, which, remarkably, has a potential role in regulating the process of necroptosis. An *in-silico* screening against either a model of phosphomimetic human MLKL or phosphomimetic mouse MLKL was performed, and two compounds were identified. These compounds, referred to as MLKL Binding Agents (MBAs), should allosterically bind to human MLKL (MBA-h1) and mouse MLKL (MBA-m1) and disrupt the interaction between the Hc and the hydrophobic groove. An extended *in-silico* screening was further performed to identify additional compounds with optimized properties.

Therefore, the main aims of this thesis were to:

I. Characterize and validate the proof-of-principle compounds (MBA-h1 and MBA-m1) by:
    - Evaluating their inhibitory effect on necroptotic cell death.
    - Assessing their effect on the hallmarks of MLKL activation.
    - Determining their ability to bind to MLKL *in-vitro* and cells.

II. Characterize the new compounds identified in the extended *in-silico* screening by:
    - Evaluating their inhibitory effect in a cell-based necroptotic assay.
    - Evaluating their binding to the recombinant MLKL *in-vitro*.

2. Materials and Methods

2.1 Materials

Table 2. 1 Reagents

Reagent	Company
DMEM medium	Sigma-Aldrich
DRAQ7	Invitrogen
Fetal Bovine Serum (FBS)	Thermofisher
GSK-872	Biozol
Human TNFα	Peprotech
Murine TNFα	Peprotech
Necrostatin-1s (Nec-1s)	Cayman
NSA	Sigma-Aldrich
Penicillin/Streptomycin (P/S)	Thermofisher
Phosphatase inhibitor	Roche
Protease inhibitor	Roche
Recombinant human TRAIL	Merk
RIPA	Thermofisher
Smac mimetic LCL-161	Active Biochem
SuperSignal™ West Pico PLUS Chemiluminescent Substrate	ThermoScientific
Trypsin-EDTA solution 10X	Sigma
Xanthine-TC	Boehringer Ingelheim
zVAD	APEXBIO

Small Molecules: The small molecules were purchased from MolPort and were first dissolved in dimethylsulphoxide (DMSO) to have 10 mM stock solutions and further diluted with DMEM to reach the desired concentrations for cell-based assay.

Table 2. 2 Buffers and solutions

Buffer/Solution	Composition
5x SDS sample buffer	50 % glycerol (w/v), 10% SDS, 10% β-mercaptoethanol, 300 mM Tris-HCl, 0.025% bromophenol blue, pH 6
Blocking buffer	5% non-fat milk in TBS-T or 2.5% bovine serum albumin in TBS-T
Dulbecco's Modified Eagle Medium (DMEM)	With 1000 mg/L glucose, L-glutamine, and sodium bicarbonate, liquid, sterile-filtered, suitable for cell culture
Freezing medium	90% FBS/10% Dimethylsulfoxide (DMSO)
IP buffer	20 mM Tris-HCl, 120 mM NaCl, 0.5% NP-40, pH 8
Isolation buffer	250 nM sucrose, 5 mM Tris, 2 mM EDTA, pH 7.4
Lysis buffer	10 mM Tris/Cl, 150 mM NaCl, 0.5 mM EDTA, 0.5% nonidet NP-40, pH 7.5
MST buffer	PBS with 0.05% tween
PBS (10x)	18 mM KH_2PO_4,100 mM Na_2HPO_4, 27 mM KCl, 1.4 M NaCl, pH 7.4
Ponceau	0.1 % Ponceau S in 5% acetic acid
RIPA	50 mM Tris HCl, 150 mM NaCl, 1.0% (v/v) NP-40, 0.5% (w/v)

	Sodium Deoxycholate, 1.0 mM EDTA, 0.1% (w/v) SDS and 0.01% (w/v) sodium azide at a pH of 7.4.
SPR buffer	50 mM HEPES, 300 mM NaCl, pH 7.5
SPR immobilization buffer	10 mM MES, pH 6
Trypsin-EDTA solution 10X	0.5% Trypsin (1:250) Gamma irradiated and 0.2% EDTA in 0.85% normal saline w/o Phenol red Sterile filtered

Table 2. 3 Antibodies

Antibody	Company
Anti-human S358 MLKL (EPR9514)	Abcam
Anti-mouse RIPK3 (D4G2A)	Cell Signaling
Primary anti-mouse MLKL clone 3H1	EMD Millipore Corp
Primary anti-mouse S345 (EPR9515(2))	Abcam
Primary anti-RIP (D94C12)	Cell Signaling
Primary GAPDH (D4C6R	Cell Signaling
Primary VDAC2 (11663)	Proteintech
β-Actin (C4)	Cruz Biotechnology

2.2 Methods and Protocols

Cell lines and maintenance

All cells were cultured in low-glucose DMEM media supplemented with 10% FBS and 1% P/S. Cells were cultured in a humidified incubator at 37 °C with 5% CO_2. When sub-culturing cells, the growth medium was removed, and cells were washed with PBS before adding trypsin-EDTA. Cells were left to incubate at 37 °C until all had detached. Detached cells were diluted in full growth medium and centrifuged at 200 *g* for 5 minutes to pellet. Pelleted cells were resuspended in an appropriate volume of full-growth medium and plated as required. The cells were frequently passaged at sub-confluence and seeded at a density of 1–5 x 10^4 cells/mL.

Table 2. 4 Cell lines

Cell line	Obtained from
HT-29	Provided by Prof. Klaus Schulze-Osthoff and Dr. Frank Essmann, IFIB, University of Tübingen
wt NIH-3T3	Provided by Dr. Stefan Krautwald, Department of Nephrology and Hypertension, University Hospital Schleswig-Holstein
MLKL ko NIH-3T3 CRISPR/Cas9	Provided by Dr. Stefan Krautwald, Department of Nephrology and Hypertension, University Hospital Schleswig-Holstein
HeLa-hRIPK3	Provided by Dr. Stefan Krautwald, Department of Nephrology and Hypertension, University Hospital Schleswig-Holstein, and Prof. Dr. Henning Walczak

Freezing and thawing cells

Cells were grown to approximately 70-80% confluency before being trypsinized and centrifuged as previously described. Pelleted cells were resuspended in the appropriate volume of the freezing medium. Cells were then aliquoted into cryotubes and slowly frozen to -80 °C at -1 °C/min in a Mr. Frosty Freezing Container (ThermoFisher Scientific). For thawing, cells were quickly thawed in a 37 °C water bath and diluted in a complete growth medium before centrifuging at 200 *g* for 5 minutes. Cells were then resuspended in a fresh growth medium.

Treatments to induce cell death

Cells were treated with any of the following:

1- A mixture of the mouse or human TNF (T) (30 ng/mL), Smac mimetic LCL-161 (S) (20 µM), and the pan-caspase inhibitor zVAD (Z) (20 µM), or only TZ to induce necroptosis in mouse and human cell lines.

2- A mixture of the human TRAIL (100 ng/mL), Smac mimetic LCL-161 (S) (20 µM), and the pan-caspase inhibitor zVAD (Z) (20 µM) to induce necroptosis in human cell lines.

3- A mixture of the mouse or human TNF (T) (30 ng/mL) and Smac mimetic LCL-161 (S) (20 µM) to induce apoptosis in mouse cell lines.

IncuCyte experiments

Kinetics of cell death were followed using the IncuCyte bioimaging platform (Essen, UK). One day before treatment, cells were seeded in 96-well plates ($1x10^4$ cells per well for wt NIH, MLKL ko NIH-3T3, and HeLa-hRIP3) and ($3x10^4$ cells per well for HT-29). Then, cells were treated to induce necroptosis, as mentioned in the previous section, in the absence or the presence of the inhibitors. In the experiment, four images per well were captured, analyzed, and averaged. Cell death was measured by the incorporation of 0.1 µM DRAQ7. Data was collected as a count of DRAQ7 positive cells and normalized, taking as 100% the maximum count of cell death in the experiment or using cell-by-cell analysis.

Western blotting (WB)

Cells were seeded to the desired confluence and were treated the following day according to the desired outcome of each experiment. After treatment, cells were washed with PBS to remove any remaining media and serum and detached using a cell scraper. Then, cells were collected and centrifuged at 500 *g* for 5 minutes. Cell pellets were resuspended in lysis buffer or RIPA buffer, depending on the protein of interest. Protease and phosphatase inhibitors were added to the lysis buffer to prevent protein degradation. Lysed cells were incubated on ice for

30 minutes to allow efficient cell lysis. The lysate was centrifuged at 500 *g* for 30 minutes, and the supernatant (the lysate) was collected. Protein concentration was measured in the lysate using a Bradford assay (BioRad, Germany), and then, samples were mixed with 5x SDS sample buffer with or without BME and heated at 95 °C for 10 minutes.

Proteins were separated using SDS-PAGE Gel Electrophoresis with either 12% polyacrylamide or 4 to 15% gradient gels. Equal amounts of protein samples were loaded onto the gels, which were resolved at constant voltage (180 V) for 90 minutes. Then, proteins were transferred from the gel to a Polyvinylidene difluoride (PVDF) membrane using wet transfer (BioRad, Germany). Successful transfers were validated by staining the membrane with Ponceau S. After that. Membranes were incubated with a blocking solution (5% BSA in TBS-T), followed by primary antibody incubation overnight at 4 °C. The day after, membranes were washed three times with TBS-T for 10 minutes and incubated with secondary antibodies conjugated to the horseradish peroxidase (HRP) enzyme for signal detection. Bands were visualized in a dark room, with a developer machine or BioRad ChemiDoc Imaging System, and using the SuperSignal™ West Pico PLUS Chemiluminescent Substrate (ThermoScientific, Germany). Shown blots are representative of at least two independent experiments.

Subcellular fractionation

After treatment, cells were resuspended in isolation buffer (250 nM sucrose, 5 mM Tris, 2 mM EDTA, pH 7.4) and then mechanically lysed using a 25G 0.5 x 25 mm syringe, passing the sample through the syringe 40 times. The cell lysate was then centrifuged for 10 minutes at 14 000 *g*, and the supernatant was further centrifuged for 1 hour at 100 000 *g* and 4 °C. From this last centrifugation, the supernatant was collected as a cytosolic fraction, and the pellet was washed, centrifuged 1 h at 100 000 *g* and 4 °C and finally collected as the membrane fraction. Both cytosolic and membrane fractions were mixed with SDS-PAGE sample buffer with or without reducing agents, heated, and loaded into a 12% or a 4 to 15% gradient gel. Protein separation, transfer, and detection were carried out as described before.

Cellular thermal shift assay (CETSA)

NIH-3T3 or HT-29 cells were seeded to obtain $3x10^5$ cells per temperature point. Cells were treated for 1 hour with DMSO or 10 µM MBA-m1 and 100 µM MBA-h1 either in the presence or the absence of TSZ. Cells were pelleted, washed with PBS, resuspended in 100 µL PBS, and loaded into Polymerase Chain Reaction (PCR) tubes. An additional centrifugation step was done to remove the supernatant. Then, cells were heated at a given temperature (52 – 60 °C) for 3 minutes and cooled at room temperature for 1 minute using a Thermal Cycler (Bio-Rad,

Germany). Cells were resuspended in lysis buffer with protease inhibitors and subjected to 3 cycles of freezing and thawing for lysis. The soluble and precipitated fractions of proteins were separated by centrifugation for 30 minutes at 13 000 *g* and 4 °C. Soluble protein fractions were resolved by SDS-PAGE and analyzed by WB.

Surface Plasmon Resonance (SPR)

SPR experiments were performed using the Biacore™ T200 device and analyzed by using Biacore T200 evaluation software. Recombinant MLKL variants (hMLKL2 and mMLKL2) were first immobilized (using an amine coupling reaction) on a CM5 sensor chip (Cytiva, Germany). The CM5 chip was first activated by flowing EDC/NHS with a 10 µL/min rate. Followed by MLKL (10 µM) injection in SPR buffer, excess reactive groups were deactivated by passing ethanolamine through the chip. The typical immobilization protocol can be implemented as the default predefined methods and wizard templates in all Biacore™ systems. To perform the SPR experiments, small molecules were prepared in a concentration range of 12.5 µM to 200 µM diluted in DMSO. Solvent correction and running buffer were prepared according to Tables 2.5 and 2.6, respectively. Data were fitted to a 1:1 binding kinetic interaction model to calculate the binding affinity Kd.

Table 2. 5 Solutions for solvent correction and 2% DMSO running buffer

	1.5% DMSO	2.8% DMSO	2% DMSO
SPR buffer	9.8 mL	9.8 mL	450 mL
100% DMSO	0.15 mL	0.28 mL	9 mL
Final volume	10 mL	10 mL	459 mL

Table 2. 6 Solvent correction preparation

Buffer	1	2	3	4	5	6	7	8
1.5% DMSO	0	200	400	600	800	1000	1200	1400
2.5% DMSO	1400	1200	1000	800	600	400	200	0

Microscale thermophoresis (MST)

Recombinant MLKL variants (hMLKL1, mMLKL2) were labeled with Atto-655 NHS ester dye using the standard protocol (ATTO-TEC GmbH-Siegen, Germany). MST experiments were performed on a Nanotemper Monolith NT.115 (info) and analyzed using OriginPro software (Microsoft, USA). The inhibitors were incubated (in a concentration range of 7.6 nM – 125 µM) with 100 nM Atto-655-MLKL for 15 minutes in PBS with 0.05% Tween. Afterward, samples were loaded on glass capillaries, and MST was performed using 80% excitation power

and 40% MST power. Dissociation constants (Kd) were derived from the mass action equation using NanoTemper analysis software. Data were fitted in OriginPro software following a 1:1 binding model.

3. Results

The structural analysis done in a patent by Prof. Ana García Sáez in 2021 (García Sáez et al., 2021) about the Hc/groove interaction in different MLKL isoforms and mutants supported a hypothesis that MLKL can be targeted by small molecule compounds that eventually can inhibit necroptosis. In this thesis, our primary objective was to prove this hypothesis. To this end, we characterized two previously identified proof-of-principle compounds that were screened against phosphomimetic human (phMLKL) or phosphomimetic mouse MLKL (pmMLKL). These compounds, referred to as MBA-h1 and MBA-m1, were subjected to a comprehensive characterization process to validate this conceptual framework. To characterize these compounds, we started by evaluating their inhibitory effects on necroptotic cell death, along with the assessment of their toxicity and binding to MLKL *in-vitro* and in cells. Subsequent analyses included an examination of their impact on MLKL activation hallmarks and an investigation into their potential off-target effects (Figure 3.1).

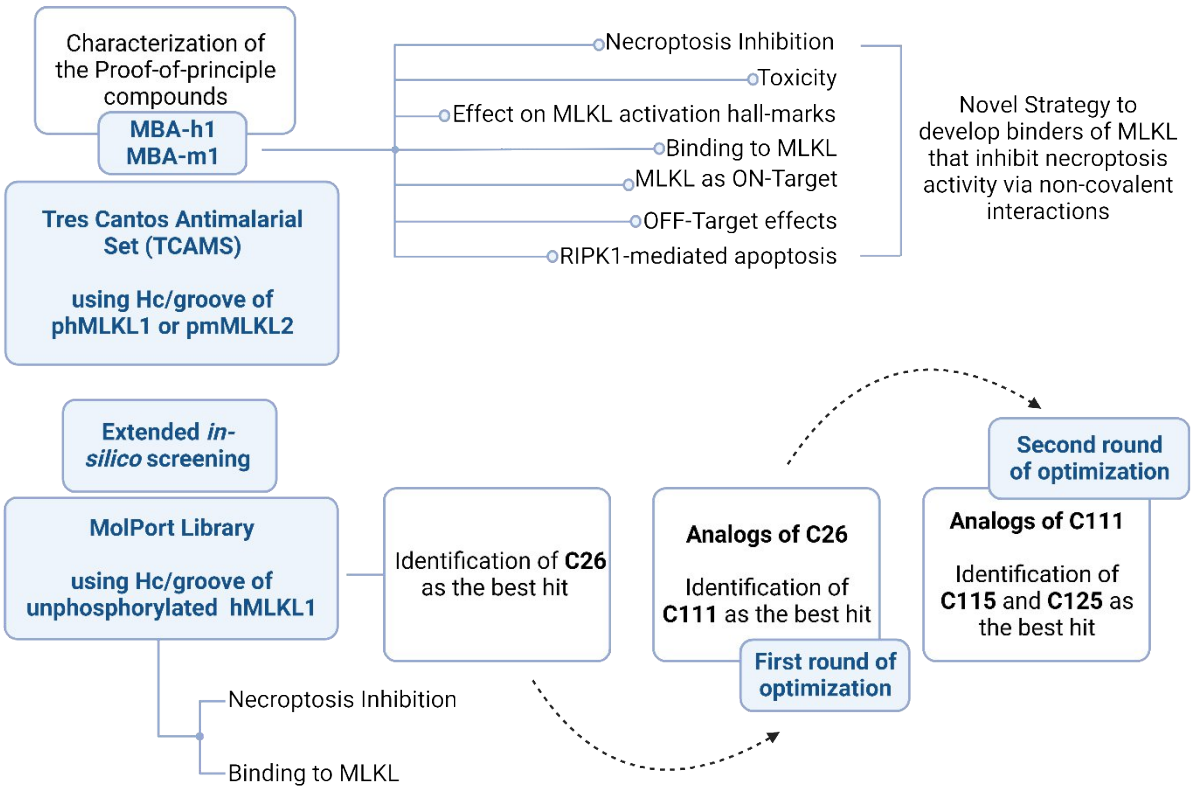

Figure 3. 1. Schematic representation of the PhD thesis pipeline.

Schematic representation illustrates the workflow and the methodology employed throughout the thesis, starting with the identification and characterization of the proof-of-principle compounds and extending to the characterization of compounds identified throughout additional *in-silico* screening rounds.

Following the characterization of these compounds, we explored the possibility of identifying additional compounds that act by the same mechanism. An additional extensive *in-silico*

screening was conducted, resulting in the identification of compounds that were further characterized. A systematic methodology was employed that began with the assessment of their binding affinity with the recombinant human and mouse MLKL, followed by evaluating their inhibitory effects on necroptotic cell death in human and mouse cell lines. Upon the identification of the most promising compound with optimal binding affinity and inhibitory effects, we initiated a subsequent *in-silico* screening to identify analogs with optimized properties. These analogs underwent further characterization using the initially employed methodology. This iterative process resulted in two optimization rounds, which will be described in detail throughout the thesis (Figure 3.1).

It is noteworthy to mention that Dr. Pedro A. Valiente conducted the *in-silico* screening of the proof-of-principle compounds, while Dr. Ekaterina Shevchenko carried out the extended *in-silico* screening and the optimization rounds in the research group of Prof. Dr. Antti Poso.

3.1 MLKL Binding Agents (MBAs) can Selectively Inhibit Necroptosis

To prove our hypothesis, our collaborator, Dr. Pedro A. Valiente, conducted a comprehensive *in-silico* screening by using the ‘‘Tres Cantos Antimalarial Set’’ (TCAMS) database that is publicly available at the Chembl-NTD database (http://www.ebi.ac.uk/chemblntd) with the Autodock Vina software against the phMLKL or pmMLKL. This screening led to the identification of two commercially available compounds, namely MBA-h1 and MBA-m1, that target either human MLKL or mouse MLKL, respectively (Figure 3.1A, B). These small molecules were selected as proof-of-principle compounds to validate the feasibility of inhibiting MLKL by targeting the interaction between the Hc/groove of MLKL. Then, we implemented a series of assays, including the assessment and characterization of the impact of these compounds on inhibiting necroptosis in cellular-based assays. Additionally, we investigated their toxicity and examined their influence on the hallmarks of MLKL activation. Furthermore, we assessed the binding between these compounds and the recombinant MLKL in *in-vitro* and cellular-based assays. We further characterized MLKL as a target and excluded potential OFF-target effects, namely their possible interaction with RIPK1 and 3.

We found that MBA-h1 delayed the kinetics of necroptotic cell death in both HeLa-hRIPK3 and HT-29 cells (Figure 3.2C, D), while MBA-m1 delayed the kinetics of necroptotic cell death in NIH-3T3 cells (Figure 3.2E). The effect of the inhibitors was dose-dependent, and the concentration needed to achieve their effect fell within the μM range for both compounds, approximately 50 μM for MBA-h1 and 10 μM for MBA-m1, respectively (Figure 3.2F, G). It is worth mentioning that the inhibitory effects of the MBAs were lost over time in both human

and mouse cell lines, and we speculate that this kinetic effect is a consequence of the inhibitors targeting MLKL via non-covalent interactions, therefore acting as reversible inhibitors.

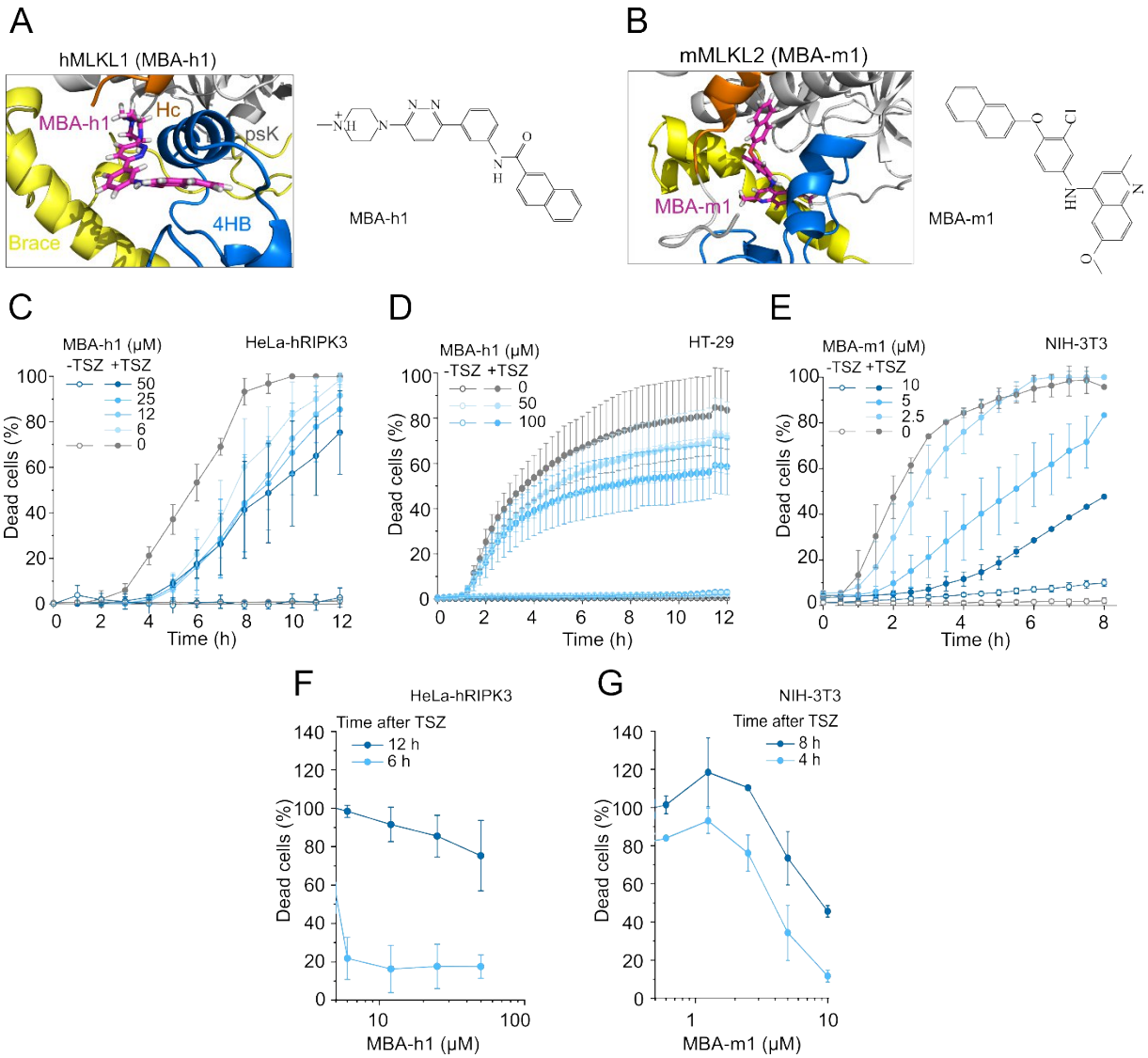

Figure 3. 2 Inhibitory effect of MBA-h1 and MBA-m1 on necroptotic cell death.

(A, B) 3D structure models of hMLKL1-MBA-h1 and mMLKL2-MBA-m1 complexes with the chemical structure of MBA-h1 (A) and MBA-m1 (B). The 4HB is highlighted in blue, the brace is yellow, the psK in silver, the Hc in orange, and the MBAs are in pink.

(C-E) Effect of MBA-h1 on necroptosis induced in HeLa-hRIPK3 (C) and in HT-29 (D) or MBA-m1 in NIH-3T3 (E).

(F, G) Dose-response of the inhibitory effect of MBA-h1 (F) and MBA-m1 (G) at the indicated time points in HeLa-hRIPK3 and NIH-3T3, respectively.

Necroptosis was induced by using a mixture of TNF (30 ng/mL), Smac mimetic (20 μM), and zVAD (20 μM). Different concentrations of the MBAs were used, as indicated in the figures. Cell death was measured using the InCucyte. Each dot represents the mean, and the error bars represent the standard deviation from at least 3 independent replicates.

Next, we compared the effect of MBA-m1 with the currently available inhibitors of the pathway. These inhibitors include Necrostatin 2 racemate (Nec-1s) (specific RIPK1 inhibitor), GSK-872 (inhibitor of RIPK3), and NSA (an inhibitor that covalently binds to the C86 of human MLKL) (B. Cui et al., 2022; Hildebrand et al., 2014; Sun et al., 2012; Yan et al., 2017). The maximum cell death was observed at 8 hours, which reached approximately 100% in the absence of any added inhibitors. Notably, upon the addition of MBA-m1 and Nec-1s, we noticed comparable results where the percentage of cell death was reduced to approximately 20%. On the contrary, GSK-872 completely inhibited cell death over 8 hours. As expected, NSA did not inhibit cell death because it binds covalently to C86 of human MLKL, which is absent in mouse MLKL (Figure 3.2A, B). These findings highlight the diverse inhibitory capabilities of different inhibitors of the necroptotic pathway and show the potential of the MBA-m1 as the first known inhibitor of mouse MLKL. As the effect of MBA-h1 was observed at high concentrations, we did not perform this comparison for the human inhibitor.

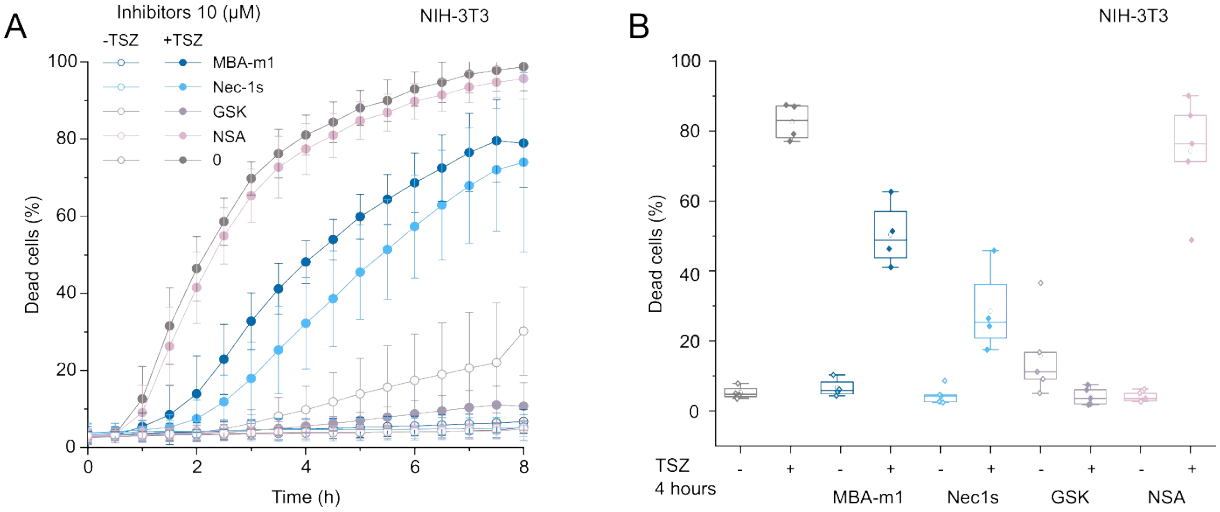

Figure 3. 3 Comparison between MBA-m1 and other inhibitors of the pathway.

(A) Kinetics of cell death in the presence and the absence of inhibitors. Nec-1s (inhibitor of RIPK1), GSK-872 (inhibitor of RIPK3), NSA (covalent inhibitor of human MLKL).

(B) Comparison between the inhibitors in the presence and the absence of TSZ at the indicated time point.

Necroptosis was induced by using a mixture of TNF (30 ng/mL), Smac mimetic (20 µM), and zVAD (20 µM). Inhibitors were tested at 10 µM. Cell death was measured using the InCucyte. Each dot represents the mean, and the error bars represent the standard deviation from at least 3 independent replicates.

Unveiling the toxic truth: MBA-m1's non-toxic threshold is 10 µM

As a next step, we evaluated the potential toxicity of the MBAs across different human and mouse cell lines to shed light on their broad applicability and safety profiles. We found that MBA-h1 was not toxic at the highest concentration used (100 µM) in both HeLa-hRIPK3 and HT-29 cell lines (Figure 3.4A). On the other hand, MBA-m1 was toxic at concentrations higher than 10 µM in wt and MLKL ko NIH-3T3, as well as in primary Bone Marrow-Derived Macrophages (BMDMs) (Figure 3.4A). In order to assess the cause of the toxicity observed with MBA-m1 in concentrations exceeding 10 µM, we exposed MLKL ko NIH-3T3 (Figure 3.4B) cells with MBA-m1 with different concentrations (20 µM and 10 µM). MBA-m1 was still toxic in these concentrations, and it was even more toxic in the MLKL ko cells compared to the wt, indicating that the toxicity is not necroptosis-mediated. In addition, we evaluated the effect of Nec-1s (10 µM) (Figure 3.4C), GSK-872 (10 µM) (Figure 3.4D), the pan-caspase inhibitor z-VAD (10 µM) (Figure 3.4E), and the ferroptosis inhibitor Fer-1 (2 µM) (Figure3.4F) on the MBA-m1 induced toxicity, and the results indicated that it is not mediated by necroptosis, apoptosis, pyroptosis or ferroptosis.

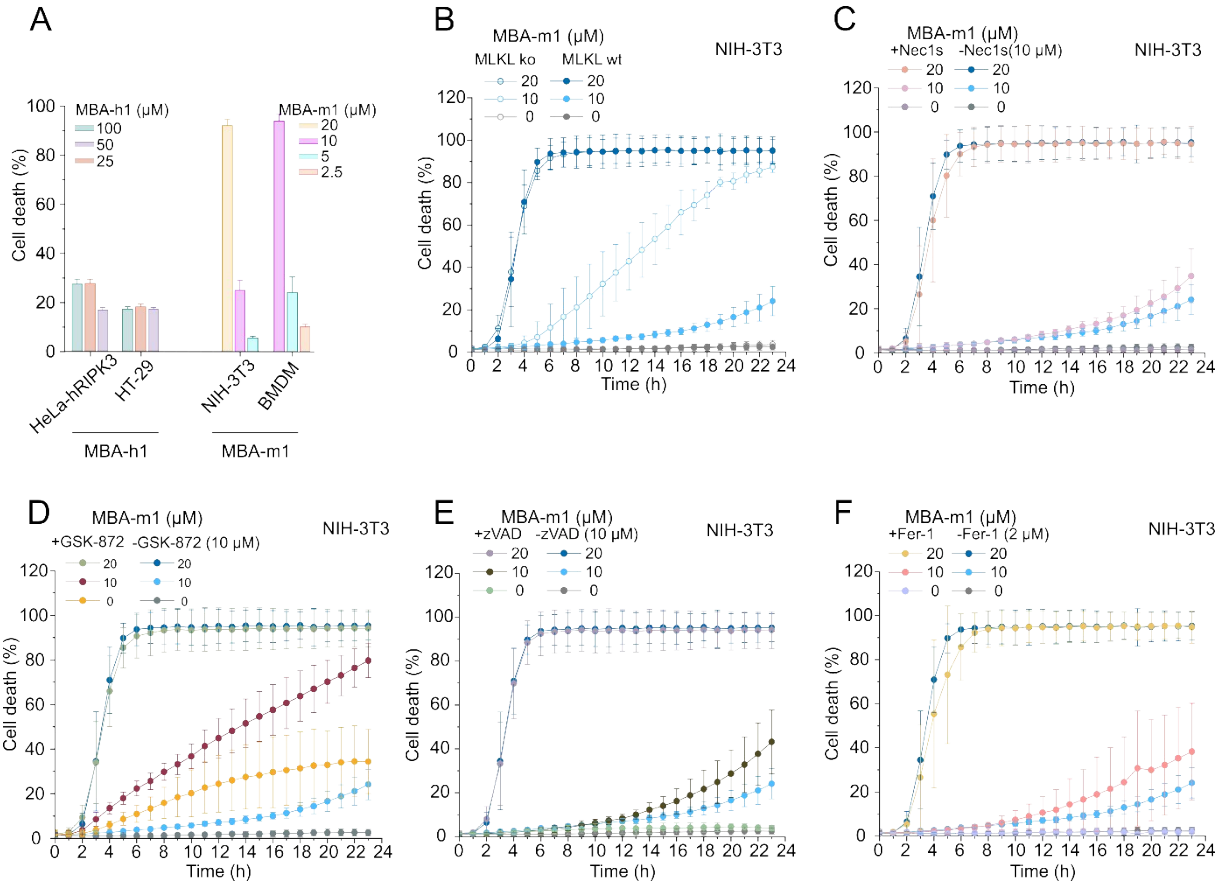

Figure 3. 4 Characterization of the toxicity of MBAs in cells.

(A) Toxicity of MBA-h1 in HeLa-hRIPK3 and HT-29 cells, and MBA-m1 in NIH-3T3 and BMDM. Cells were treated with different concentrations of MBAs, as indicated in the figure.

(B) Toxicity of MBA-m1 in wt and MLKL ko NIH-3T3 cells.

(C-F) Effect of Nec-1s (RIPK1 inhibitor) (C), GSK-872 (RIPK3 inhibitor) (D), zVAD (pan-caspase inhibitor) (E), Fer-1 (ferroptosis inhibitor) (F) on the toxicity induced by MBA-m1 in NIH-3T3 cells. Different concentrations of MBA-m1 were used, and fixed concentration of Nec-1s, GSK-872, Z-VAD, and Fer-1 was used, as indicated in the figure.

Cell death was measured using the InCucyte. Each dot represents the mean, and the error bars represent the standard deviation from at least 3 independent replicates.

Catching the MBAs in action: unveiling the effect of MBAs on hallmarks of MLKL activation and their interaction with MLKL

We then assessed the impact of MBAs on the hallmarks of MLKL activation during necroptosis, including MLKL phosphorylation, oligomerization, and membrane translocation. To conduct this, we performed WB experiments using antibodies against phosphorylated MLKL. Results demonstrated that MBA-h1 did not inhibit the phosphorylation of MLKL in human cell lines, HeLa-hRIPK3 and HT-29, respectively (Figure 3.5A). On the other hand, MBA-m1 delayed MLKL phosphorylation in NIH-3T3 cells (Figure 3.5B). The phosphorylated MLKL band became evident 90 minutes after TSZ treatment, a time point where inhibition of cell death was observed. Furthermore, both inhibitors interfered with MLKL oligomerization and membrane translocation to membranes (Figure 3.5C-F). These findings collectively indicate that MBAs can inhibit MLKL-mediated necroptosis downstream of its phosphorylation without affecting the activity of upstream RIPK1 and RIPK3 (Figure 3.5G).

To test the ability of the MBAs to target MLKL, we conducted further investigations into their binding characteristics, where we employed SPR in the *in-vitro* evaluation (Figure 3.6A). The underlying principle of SPR involves the interaction of polarized light with two surfaces having different refractive indices, causing the light to refract and trigger the formation of free plasmons that lead to the reduction in the intensity of the reflected light at a specific angle. SPR allows the real-time monitoring of the binding kinetics, including the association and dissociation rates, as well as the binding affinity of the interaction between the MBAs and the recombinant human or mouse MLKL. In these experiments, either the recombinant human MLKL (hMLKL1) or mouse MLKL (mMLKL2) were immobilized to a CM5 biosensor chip, and the binding kinetics of each compound were assessed at increasing concentrations (Figure 3.6B, C). We observed a positive dose-response curve whereby the binding response increased with increasing the inhibitor concentrations (Figure 3.6D). Subsequently, we determined the

binding affinity of both MBA-h1 (5 µM) and MBA-m1 (6 µM), which was in the low µM range (Figure 3.6E). Altogether, this assay suggested that MBAs can interact with both human and mouse MLKL.

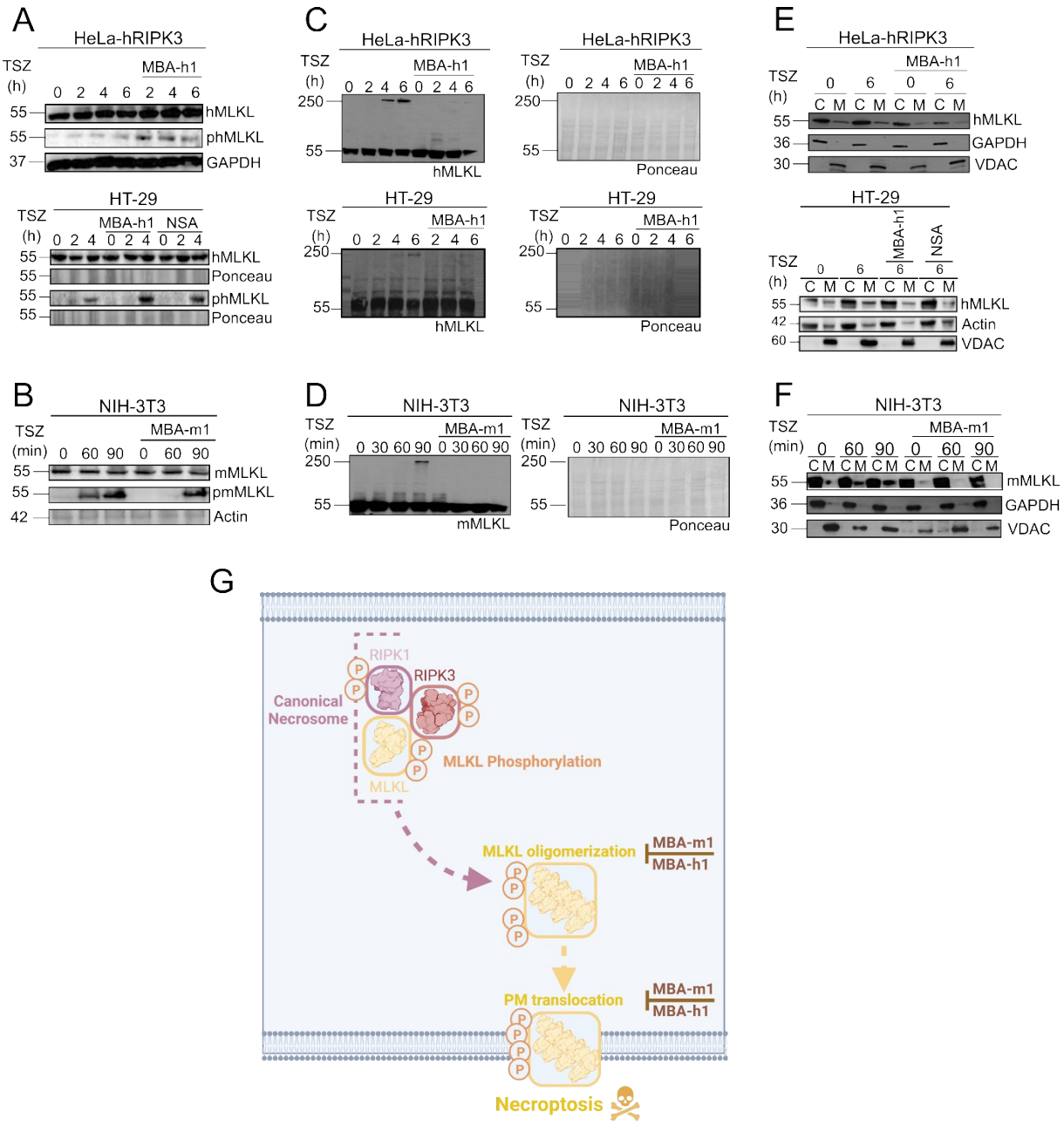

Figure 3. 5 Effect of MBA-h1 and MBA-m1 on the hallmarks of MLKL activation.

(A-F) Effect of MBA-h1 and MBA-m1 on the phosphorylation (A, B), oligomerization (C, D), and membrane translocation (E, F) of MLKL in HeLa-hRIPK3, HT-29 (Top), and NIH-3T3 (Bottom).

(G) Schematic representation showing the effect of the MBAs on the hallmarks of MLKL activation. The scheme was prepared by using BioRender.com.

Necroptosis was induced by using a mixture of TNF (30 ng/mL), Smac mimetic (20 µM), and zVAD (20 µM) in the presence or the absence of the MBAs. Samples were prepared under reducing conditions (A, B, E, F) and in non-reducing conditions (C, D) and analyzed with WB. Actin and Glyceraldehyde 3-phosphate dehydrogenase (GAPDH) are the loading control (A, B, E, and F), and Voltage-Dependent

Anion Channel (VDAC) is the membrane protein marker. C: cytosolic fraction, M: membrane fraction (E, F). Blots are representative of at least 3 independent replicates.

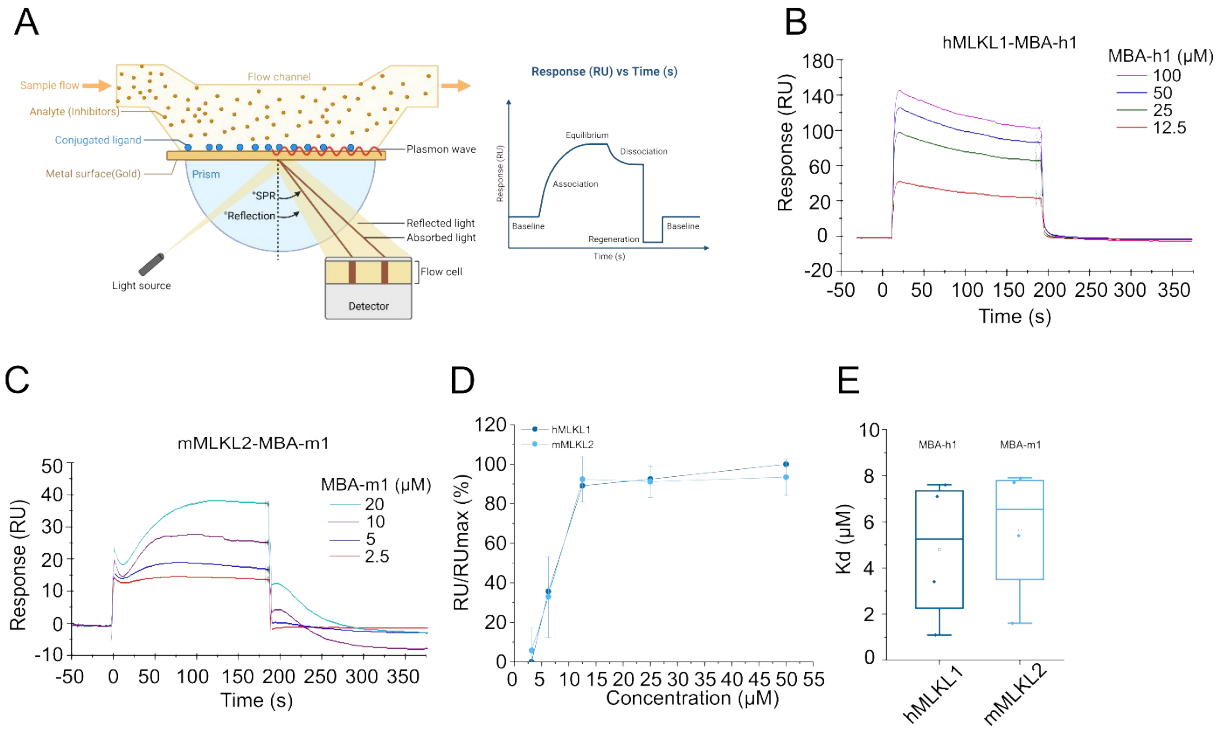

Figure 3. 6 Characterization of the interaction of MBAs and recombinant MLKL by using SPR.

(A) Schematic representation of SPR and its mechanism of action. Polarized light interacts with surfaces having different refractive indices, causing the light to refract and triggering the generation of free plasmons that lead to the reduction in the intensity of reflected light at specific angle. When ligands such as MBAs are introduced, this results in the change of the mass near the surface, which in turn alters the SPR angle. The scheme was prepared by using BioRender.com

(B, C) Representative sensograms for MBA-h1 binding to recombinant hMLKL1 (B) and MBA-m1 binding to recombinant mMLKL2 (C).

(D, E) Dose-response curves of MBA-h1 and MBA-m1 (D), and Kd values of the interaction of the MBAs (E). Each dot in the boxes corresponds to different replicates from an independent experiment.

Increasing concentrations of MBAs (12.5 μM to 100 μM for MBA-h1 and 12.5 μM to 200 μM for MBA-m1) flowed over hMLKL1 and mMLKL2 with a concentration of 1 μM immobilized on CM5 sensorchip. Data were fitted to a 1:1 binding kinetic interaction model to calculate the binding affinity Kd.

We also investigated the targeting of the MBAs to MLKL within the cellular context, employing CETSA, a technique that is suitable for investigating the thermal stability of proteins within intact cells. By subjecting the cells to a range of increasing temperature ranges, proteins undergo thermal denaturation. In this case, the addition of the ligand (MBAs) would modulate the thermal stability of the target protein (MLKL), providing insights into the interaction between the small molecule and the protein of interest (Figure 3.7A). Through WB experiments, we observed that treating HT-29 cells with MBA-h1 did not alter the thermal stability of the human MLKL (Figure 3.7B-D), which could be attributed to the high stability of the hMLKL

that is less prone to alterations upon MBA-h1 binding. However, MBA-m1 altered the thermal stability of mouse MLKL in NIH-3T3 cells (Figure 3.8) and caused a change in the temperature difference of thermal denaturation between free and ligand-bound mouse MLKL.

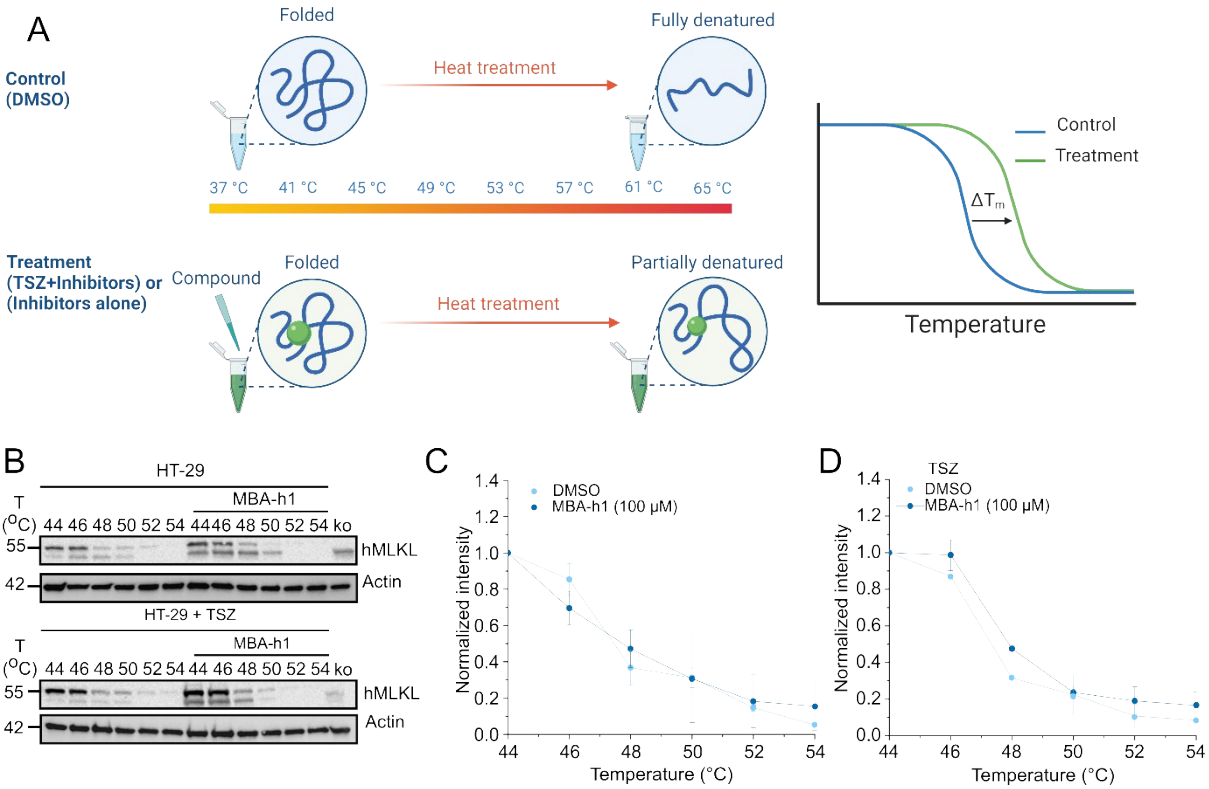

Figure 3. 7 Effect of MBA-h1 on the thermal stability of the human MLKL in HT-29 cells.

(A) Schematic representation of CETSA. The principle of CETSA assay is that the ligand binding modulates the thermal stability of the target protein by exposing it to different temperatures in the presence and the absence of the small molecule. Protein aggregates precipitate and, therefore, are removed upon centrifugation. The resulting decrease of the soluble protein fraction can be detected by WB. The scheme was prepared by using BioRender.com

(B) CETSA assay in HT-29 cells. Cells treated with MBA-h1 (100 μM) in the presence or the absence of TSZ were subjected to an increasing temperature gradient. Following the separation of soluble and insoluble proteins, MLKL was detected by WB. Actin was used as a loading control. Blots are representative of at least 3 independent replicates.

(C, D) Quantification of MLKL fraction detected from blots similar to those shown in B in the absence (C) or the presence (D) of TSZ. Blot intensities were normalized to intensity from the 44 °C sample and actin.

Necroptosis was induced by using a mixture of TNF (30 ng/mL), Smac mimetic (20 μM), and zVAD (20 μM). A fixed concentration of the MBAs was used, as indicated in the figures. Each dot represents the mean. The error bars represent the standard deviation. Graphs show results from at least 2 independent replicates.

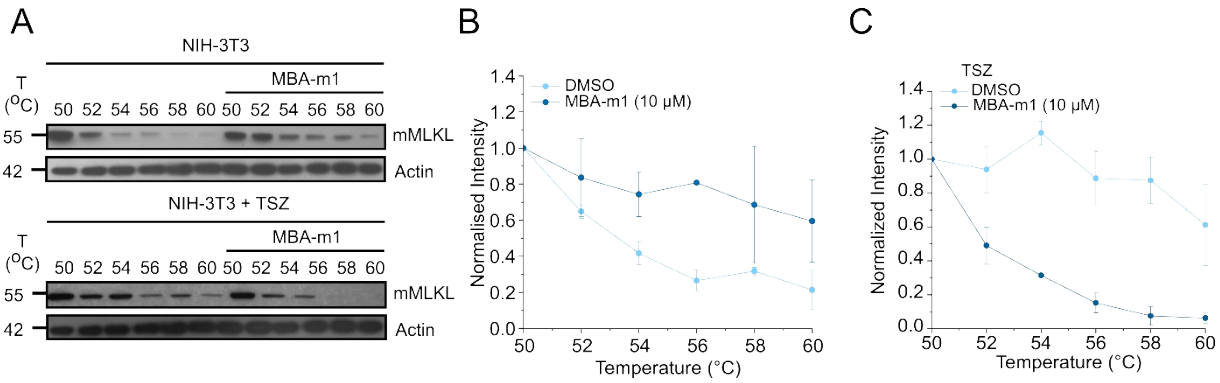

Figure 3. 8 Effect of MBA-m1 on the thermal stability of the mouse MLKL in NIH-3T3 cells.

(A) CETSA assay in NIH-3T3 cells. Cells treated with MBA-m1 (10 µM) were subjected to an increasing temperature gradient. Following the separation of soluble and insoluble proteins, MLKL was detected by WB. Actin was used as a loading control. Blots are representative of at least 3 independent replicates.

(B, C) Quantification of MLKL detected from blots similar to those shown in A in the absence (B) or the presence (C) of TSZ. Blot intensity is normalized to intensity from the 50 °C sample and actin.

Necroptosis was induced by using a mixture of TNF (30 ng/mL), Smac mimetic (20 µM), and zVAD (20 µM). A fixed concentration of the MBAs was used, as indicated in the figures. Each dot represents the mean. The error bars represent the standard deviation. Graphs show results from at least 2 independent replicates.

In light of the observed delay caused by MBA-m1 in phosphorylation of MLKL, we decided to rule out that the inhibitory effect observed on necroptosis was due to targeting the upstream effectors RIPK1 and RIPK3. For this, we conducted again CETSA-WB assay to assess the impact of MBA-m1 on the thermal denaturation of these proteins. Our findings revealed that MBA-m1 had no discernible effect on the thermal stability of RIPK1 and RIPK3 in untreated and necroptotic conditions (Figure 3.9).

To further rule out the possibility of potential off-targets for MBA-m1 and considering that RIPK1 is a common effector in both apoptosis and necroptosis, we assessed the impact of MBA-m1 on RIPK1-induced apoptosis. To achieve this, we induced apoptosis with a mixture of TNF and Smac mimetic (TS) in addition to the MBA-m1. Consistently, the results demonstrated that MBA-m1 did not exhibit any noticeable effect on the kinetics of extrinsic apoptosis in both wt and MLKL ko NIH-3T3 cells (Figure 3.10). Collectively, these results strongly support the conclusion that MBA-m1 influence on cell death is a direct consequence of its interaction with mMLKL2 and is not a result of off-target effects on upstream effectors of necroptosis.

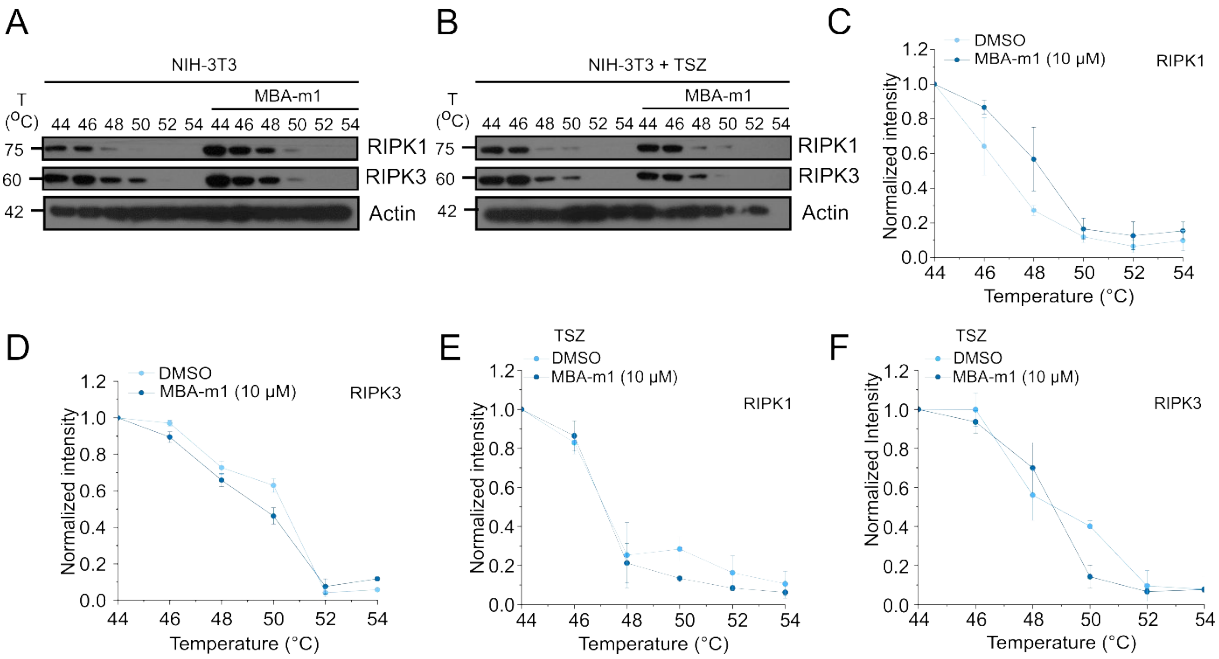

Figure 3. 9 Lack of effect of MBA-m1 on the thermal stability of the mouse RIPK1 and RIPK3 in NIH-3T3 cells.

(A, B) CETSA assay in NIH-3T3. Cells treated with MBA-m1 (10 μM) were subjected to an increasing temperature gradient in the absence (A) or the presence (B) of TSZ. Following the separation of soluble and insoluble proteins, RIPK1 and RIPK3 were detected by WB. Actin was used as a loading control. Blots are representative of at least 3 independent replicates.

(C-F) Quantification of RIPK1 (C, D) and RIPK3 (E, F) detected from blots similar to those shown in A and B. Blot intensity is normalized to intensity from the 44 °C sample and actin.

A fixed concentration of the MBA-m1 was used, as indicated in the figures. Each dot represents the mean. The error bars represent the standard deviation. Graphs show results from at least 2 independent replicates.

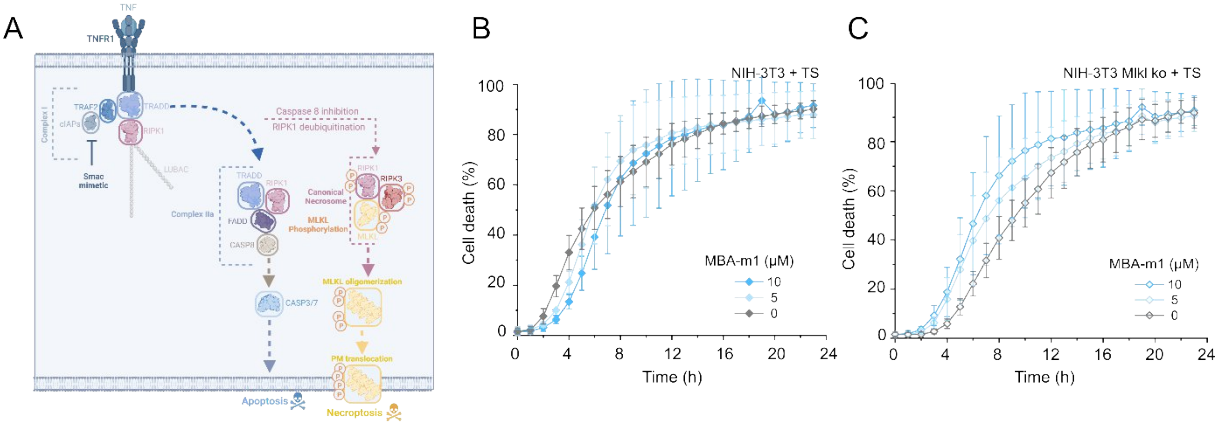

Figure 3. 10 The effect of MBA-m1 on RIPK1-mediated apoptosis.

(A) Schematic representation of the extrinsic apoptotic pathway. This is a RIPK1-dependent and MLKL-independent form of RCD.

(B, C) Effect of MBA-m1 on apoptosis induced in wt (B) and MLKL ko (C) NIH-3T3 cells.

A mixture of TNF (30 ng/mL) and Smac mimetic (20 μM) was used to induce apoptosis. Each dot represents the mean. The error bars represent the standard deviation. Graphs are representative of at least 3 independent replicates.

3.2 Extending the Novel Class of Necroptosis Inhibitors

After testing our proof-of-principle compounds, MBA-h1 and MBA-m1, and in collaboration with Prof. Dr. Antti Poso's group, molecular dynamics (MD) simulations were conducted to identify more compounds that are capable of binding to the previously discovered allosteric site of MLKL. The screening was done against a structural model of human MLKL, given its pivotal role in medical research for drug development and disease treatment. Our focus was to target the hydrophobic groove of hMLKL defined by close interactions with the Hc. Specifically, residues Arg82-Ala91 from the 4HB, Glu119-Asn115 of the brace region, and Thr468-Val456 of the Hc were found to contribute to this druggable pocket.

The screening process started with an extensive pool of 7 000 000 compounds, and a systematic refinement approach was followed. This involved pharmacophore remodeling and subsequent strict screening, which resulted in the filtering down to 3 272 989 compounds. Further iterations involving docking procedures led to the identification of 18 907 compounds and 32 209 poses. This screening led to the identification of the first list of 54 potential compounds that could potentially bind allosterically to the hydrophobic groove of hMLKL. During the compounds testing phase, we assessed their effect on both human and mouse MLKL by using recombinant MLKL in SPR screenings as well as different human and mouse cell lines to test their effect on necroptosis through cell death assays (Figure 3.11).

In our initial screening phase, the top 54 candidates of commercially available compounds were selected, and we primarily assessed their interaction with MLKL by using the SPR. Simultaneously, we examined their impact on necroptosis through cell death assays conducted on human and mouse cell lines. From the initial screening, C26 emerged as the most promising candidate, which then served as a template for a further round of optimization. In the next phase, we employed the same methodology to characterize various analogs of C26, leading to the identification of C111 as the best hit from the second round of optimization. Finally, in our last round of optimization, we thoroughly characterized the analogs of C111, resulting in the discovery of the most potent inhibitors, which are C115 and C125 (Figure 3.11).

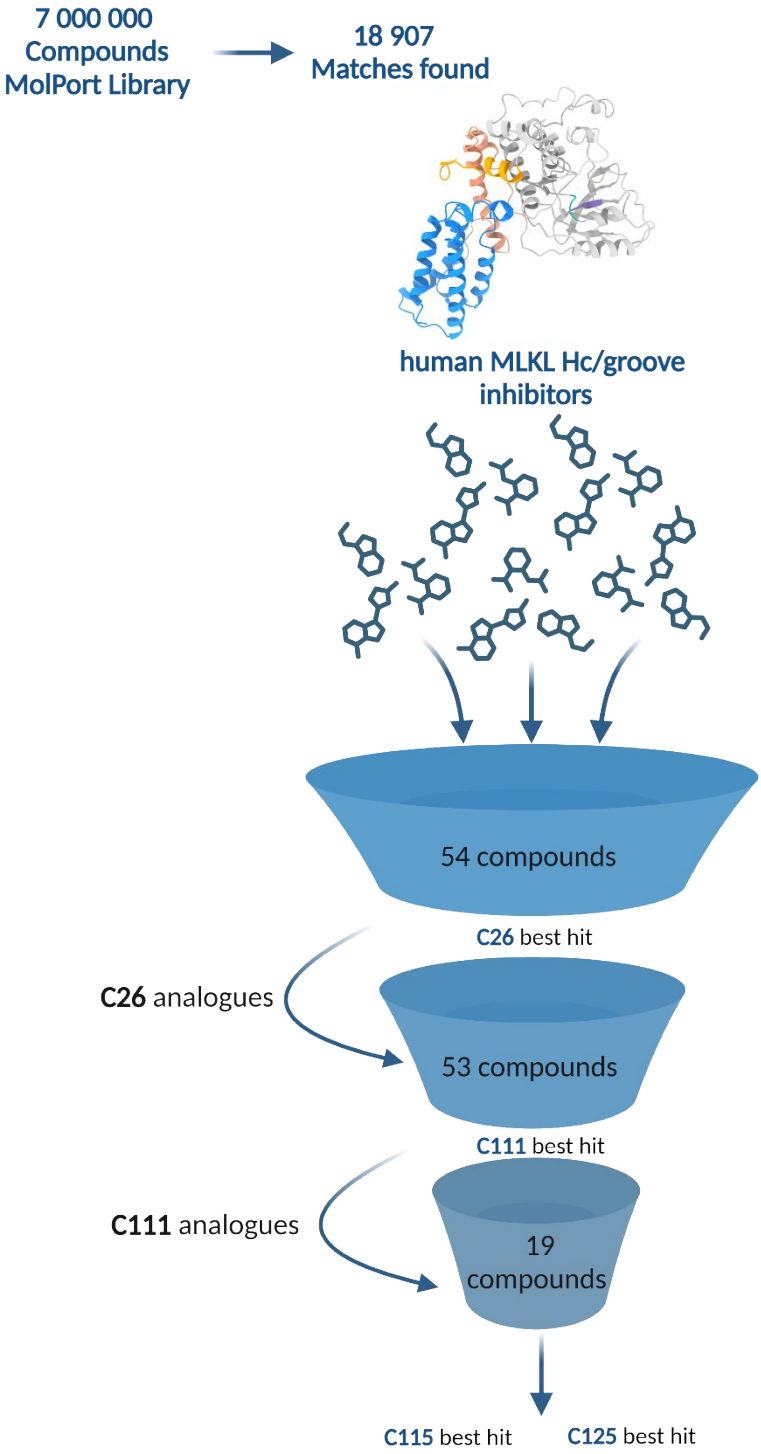

Figure 3. 11 General scheme represents the extended workflow to identify new MLKL Hc/groove inhibitors.

Screening and characterization of MLKL inhibitors started with 7 000 000 compounds that were subjected to multiple filtration steps, resulting in the identification of the most promising 54 compounds. From the initial list, C26 emerged as the best hit. The subsequent screening was done to identify analogs for C26, with C111 identified as the best candidate in the second list. In the final optimization round, screening for C111 analogs took place, resulting in the identification of C115 and C125 as the most promising candidates from the 3 lists. The scheme is prepared by BioRender.com.

C26: The top performer in the first list of potential MLKL inhibitors

During the initial phase of characterizing the top 54 small molecules derived from the extended *in-silico* screening, we assessed their solubility to determine the maximum non-soluble concentration that will be used in subsequent experiments with the inhibitors. The rationale of this assay is based on absorbance detection, which assesses the portion of light that passes through the sample and reflects the solubility of the small molecules. By comparing this with control, which is a scope medium alone, we gain an overview of the solubility of small molecules within the scope medium. Based on the results of this experiment, we selected the compounds that were soluble at a concentration of 100 µM, and these selected compounds will be used in subsequent experiments (Figure 3.12A).

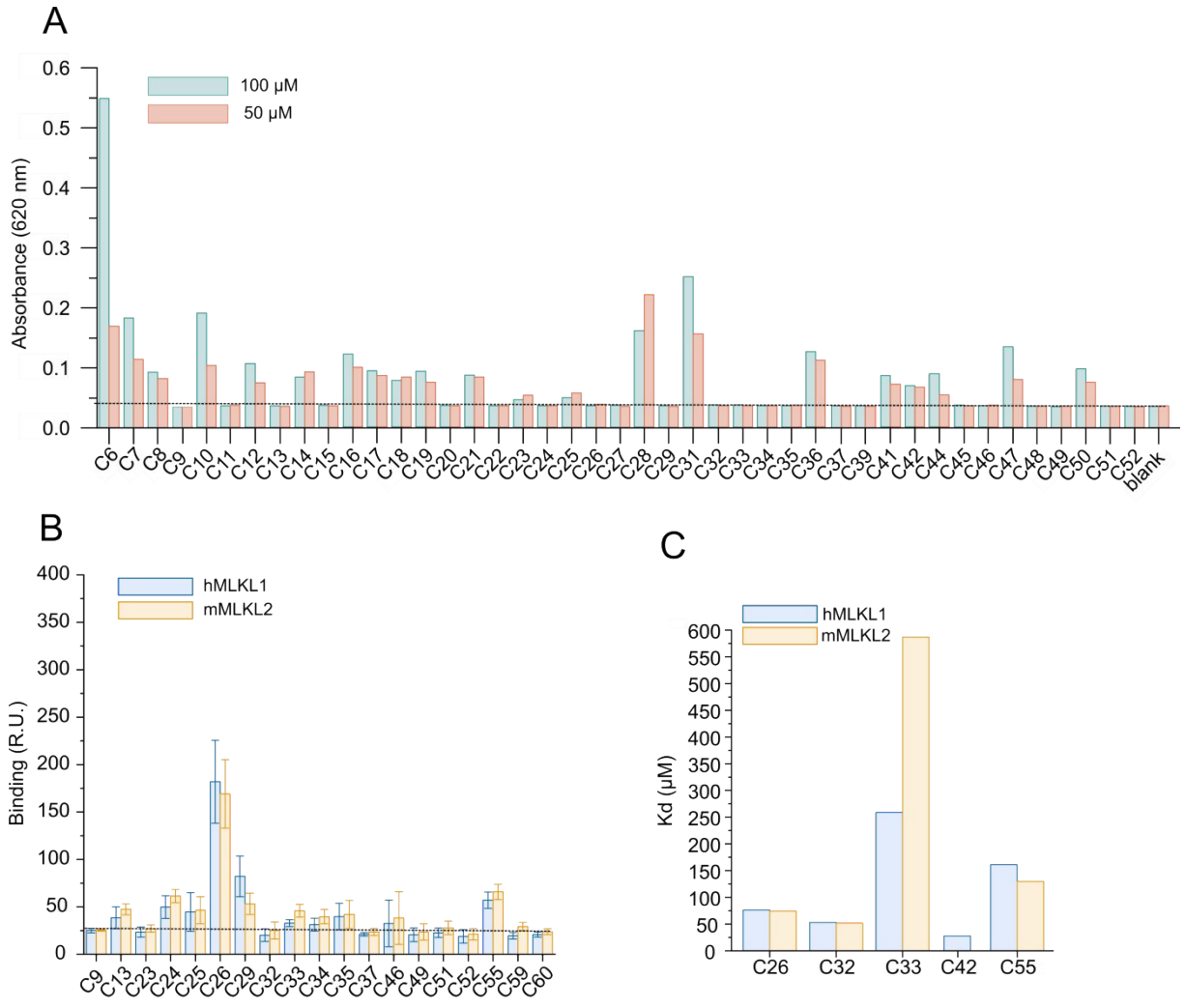

Figure 3. 12 Solubility and binding affinity characterization of the compounds from the first list obtained after the extended *in-silico* screening.

(A) Solubility measurements of the compounds. The dashed line represents the soluble threshold in comparison to the control sample.

(B) SPR primary screening of the compounds. Binding response to recombinant mouse or human MLKL was measured. A fixed concentration of the small molecules was used at 100 μM. The dashed line represents the threshold of compounds binding to MLKL.

(C) Kd values of the interaction between the inhibitors and recombinant hMLKL1 Increasing concentrations of the compounds (12.5 μM to 200 μM) were flowed over immobilized recombinant hMLKL1 or mMLKL2.

Recombinant MLKL was immobilized on a CM5 chip with a concentration of 1 μM. Data were fitted to a 1:1 binding kinetic interaction model to calculate the binding affinity Kd.

Next, we used SPR as a screening method to assess the interaction between the compounds and both the recombinant human and mouse MLKL. As a first step in this assessment, we conducted a primary screening in which we flowed a fixed concentration (100 μM) of the inhibitors over an immobilized human and mouse MLKL in a CM5 sensor chip (Figure 3.12B). This primary screening enabled us to identify 10 compounds that can interact with MLKL, which were subsequently subjected to further testing to determine their binding affinity. In the secondary screening, the binding of each compound to the recombinant MLKL was assessed at increasing concentrations, allowing us to calculate their affinity constant (Kd). The results demonstrated that the majority of these compounds targeted both the human and mouse MLKL and exhibited Kd values within the μM range. Specifically, C26, C32, and C42 that exhibited a Kd value of around 60, 55, and 45 μM, respectively (Figure 3.12 C).

Then, we evaluated the efficacy of these compounds concerning the inhibition of necroptotic cell death in human and mouse cell lines. For this, we induced necroptosis in HT-29 (Figure 3.13A) and NIH-3T3 (Figure 3.13B) cells using a combination of TSZ. At the same time of treatment, we exposed the cells to various inhibitors at a fixed concentration (100 μM). This initial screening enabled us to identify C26 with the potential to inhibit necroptosis in both HT-29 and NIH-3T3 cell lines, in addition to C13, C25, C52, C54, and C55 in NIH-3T3 cell lines only.

Following the identification of these promising candidates, we conducted a secondary screening to evaluate their impact across a range of different concentrations. Our findings indicated that these inhibitors delayed the kinetics of necroptotic cell death. Notably, the inhibitory effect demonstrated dose dependency, with increased concentrations leading to a more pronounced impact on necroptosis (Figure 3.12C). In conclusion, from this comprehensive screening, C26 emerged as the best candidate, displaying the highest inhibitory activity against necroptosis in both human and mouse cell lines. Notably, C26 exhibited a stronger inhibitory effect in human cells than MBA-h1 (Figure 3.14A, B). These are clear advantages compared to the proof-of-principle compounds. However, further enhancement is required, particularly in terms of

improving the binding affinity, the inhibitory efficacy, and the long-term effect (Figure 3.14D, E).

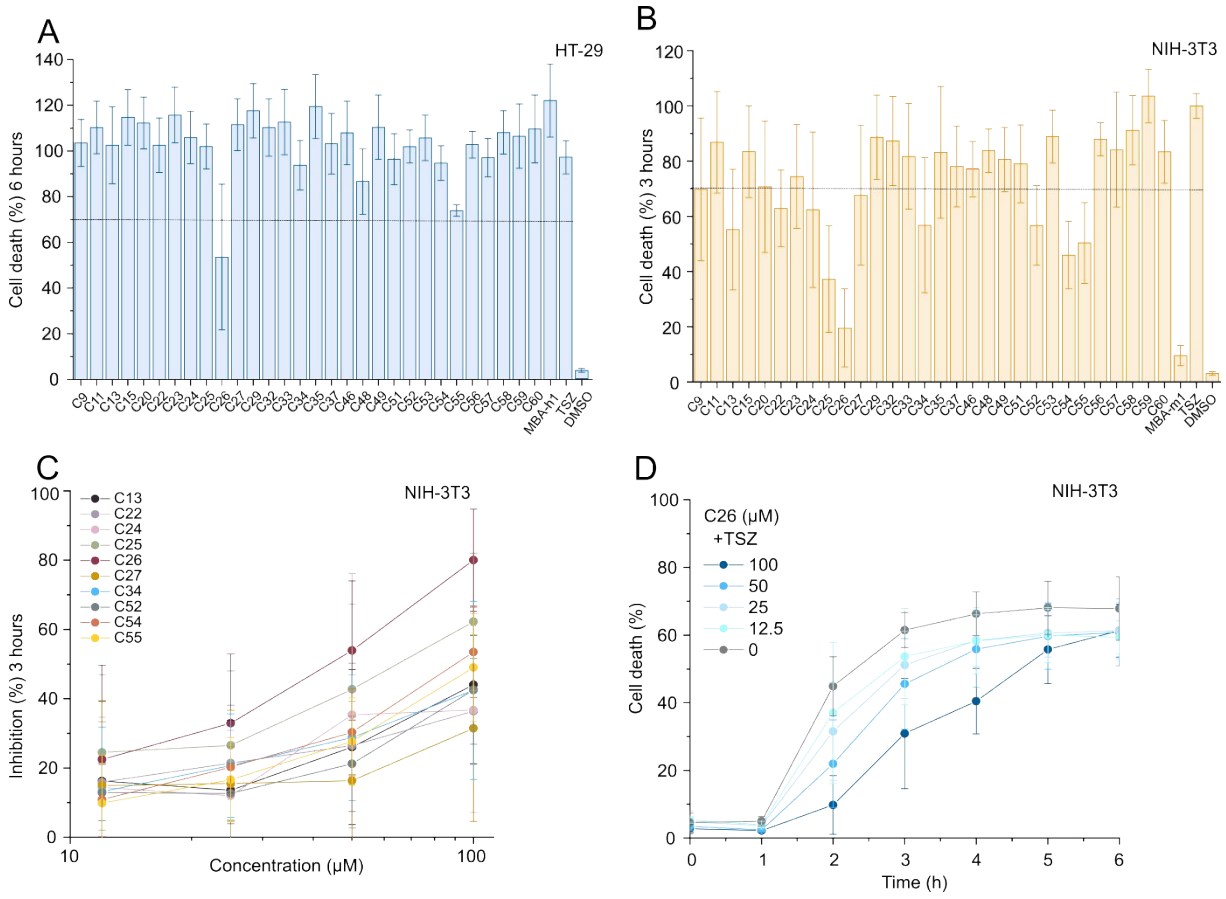

Figure 3. 13 C26 inhibits necroptosis in human and mouse cell lines.

(A, B) Inhibitory effect of compounds from the first list of potential MLKL Hc/groove inhibitors on TSZ-induced necroptotic cell death in human HT-29 (A) and mouse NIH-3T3 (B) cells. A fixed concentration (100 µM) of the molecules was used as a primary screening. The dashed line represents 70% of the TSZ activity.

(C) Dose-response curve of the different inhibitors from the first list in NIH-3T3 cell line selected after the primary screening.

(D) Effect of C26 in the kinetics of necroptosis induced in NIH-3T3 cells.

(E) Chemical structure of C26, identified as the best hit based on cellular assays and affinity measurement.

Necroptosis was induced by using a mixture of TNF (30 ng/mL), Smac mimetic (20 µM), and zVAD (20 µM). Different concentrations of the inhibitors were used, as indicated in the figures. Cell death was measured using the InCucyte. Inhibition was calculated by dividing cell death in the presence of the inhibitors by the corresponding values obtained with TSZ at the same time point and expressed as a percentage. Each dot represents the mean, and the error bars represent the standard deviation from at least 3 independent replicates.

C111: The top performer in the second list of potential MLKL inhibitors

After the identification of C26 as the best candidate from the initial extended *in-silico* screening, which demonstrated its notable efficacy in inhibiting necroptotic cell death and its ability to bind to the recombinant MLKL *in-vitro*, we performed another round of *in-silico* screening to identify new compounds with improved properties. Therefore, in this round of screening, we explore diverse chemical spaces to identify analogs for C26 from MolPort. As an initial step, we assessed the solubility of these compounds and found that the majority of them were soluble at 100 µM (Figure 3.14A). Subsequently, we performed toxicity evaluations. From this, we calculated both the soluble concentration (SC) and the non-toxic concentration (NTC) for each compound (Table 3.1). Furthermore, we proceeded with the characterization of the compounds that were soluble at 100 µM.

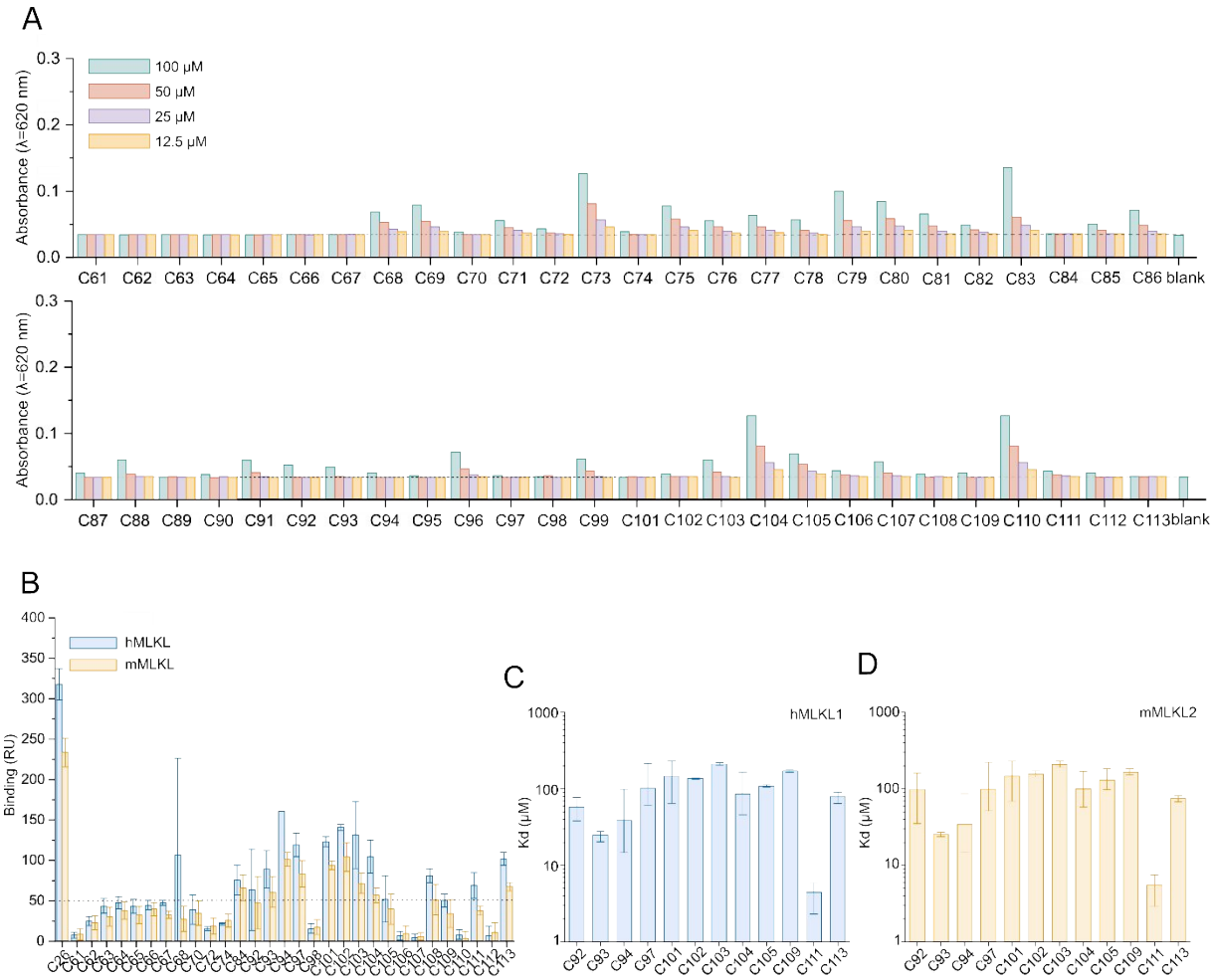

Figure 3. 14 Solubility and binding affinity characterization of the C26 analogs.

(A) Solubility measurements of the compounds. The dashed line represents the soluble threshold in comparison to the control sample.

(B) SPR primary screening of the compounds. Binding response to recombinant human or mouse MLKL was measured. A fixed concentration of the inhibitors was used at 100 µM. The dashed line represents the threshold of compounds binding to MLKL.

(C, D) Kd values of the interaction between the inhibitors and recombinant hMLKL1 (C) or mMKL2 (D). Increasing concentrations of the compounds (12.5 µM to 200 µM) were flowed over recombinant hMLKL1 and mMLKL2.

Recombinant MLKL was immobilized on a CM5 chip with a concentration of 1 µM. Data were fitted to a 1:1 binding kinetic interaction model to calculate the binding affinity Kd.

Table 3. 1 Soluble (SC) and non-toxic (NTC) concentrations of best-hits identified in the C26 analogs list

Name	SC (µM)	NTC (µM)
C92	100	50
C93	100	50
C94	100	50
C97	100	100
C101	100	100
C102	100	100
C103	50	50
C104	50	100
C105	100	100
C109	100	100
C111	100	100

First, we tested the interaction with the recombinant human and mouse MLKL by using SPR. For this, we utilized a fixed concentration of the inhibitors (100 µM) to identify potential MLKL binders (Figure 3.13B). This screening identified several candidates (C92, C93, C94, C97, C101, C102, C103, C104, C105, C109, C111, and C113) as potential binders of MLKL. In the secondary screening, we successfully calculated the Kd that characterizes their interaction with the recombinant mouse or human MLKL (Figure 3.14C, D). Our results revealed that C111 exhibited the highest binding affinity for both mouse and human MLKL, with a Kd value of approximately 6 µM.

Next, we assessed the inhibitory effects of the compounds on necroptotic cell death in both HeLa-hRIPK3 (Figure 3.15A) and NIH-3T3 (Figure 3.15B) cell lines. We conducted cell death-based assays and initiated the primary screening of these compounds at a fixed concentration as our initial approach. In this step, we identified different candidates (C92, C93, C94, C97, C101, C102, C105, and C111) that were more efficient than C26. Notably, all of them demonstrated the capability to inhibit necroptosis in both human and mouse cell lines. Subsequently, we proceeded with secondary screening that enabled us to identify their

inhibitory effect upon using different concentrations of each inhibitor (Figure 3.15C, D) and to calculate the IC50 in HeLa-hRIPK3 (Figure 3.15E) and NIH-3T3 (Figure 3.15F) cells upon the induction of necroptosis by using TSZ. Our experimental data revealed that these inhibitors exhibited a dose-response effect on the kinetics of cell death (Figure 3.15G). We identified C111 (Figure 3.15H) as the best candidate from this list, with IC50 in the low μM range (~ 5μM).

Furthermore, we aimed to evaluate whether the inhibitors that showed an effect in inhibiting necroptosis from the C26 analogs would maintain their inhibitory effect when subjected to different necroptotic cell death stimuli. To accomplish this, we conducted tests on HeLa-hRIPK3 cells inducing necroptosis using a mixture of TRAIL, Smac mimetic, and zVAD to compare with the previously used TSZ stimulus (Figure 3.16A). Remarkably, the inhibitors exhibited the same effect on cell death, underscoring their remarkable consistency in binding to MLKL and effectively preventing necroptosis. Moreover, we employed a similar approach in NIH-3T3 cells, where we induced death using TNF and zVAD (TZ) as additional necroptotic cell death stimuli with TSZ stimuli (Figure 3.16B). These inhibitors once again demonstrated the same effect in inhibiting necroptosis. Collectively, these results illustrate the success of our approach in targeting MLKL inhibition through the newly discovered hydrophobic pocket and its interaction with the Hc. This consistency across different stimuli reinforces the potential of these inhibitors as reliable candidates for the inhibition of necroptosis.

Collectively, our data point out that C111 is effective in inhibiting necroptosis when tested in necroptotic cell-based assays, as well as its ability to bind to the recombinant MLKL with high affinity. Notably, both the IC50 and Kd values showed a significant reduction compared to C26 from the previous list. Despite these promising results, further enhancements are still needed to improve the effect of the inhibitors on the kinetics of cell death. However, we observed a noticeable delay in necroptosis. Our goal was to improve this effect to achieve more significant inhibition over an extended time.

C115 and C125: The top performers in the third list of potential MLKL inhibitors

After identifying C111 as the most promising candidate from the second list of inhibitors, our research venture led us to explore additional compounds with the goal of discovering better candidates from another optimization round. We performed another round of *in-silico* screening by using the MolPort library to find analogs of C111, aiming to enhance the binding affinity to MLKL as well as the necroptotic inhibition capabilities. In this screening, the ADME of the

compounds and the partition of the compounds into membranes were taken into consideration and showed better characteristics compared to C26. Here, 18 compounds were identified, and then we proceeded to characterize them. In line with our methodology, we initiated the examination by assessing the solubility of these compounds. Notably, the majority of them exhibited solubility at concentrations starting from 50 µM. However, it is worth noting that several inhibitors were insoluble even at concentrations as low as 12 µM (Figure 3.17A). Following the determination of the SC, we also evaluated the NTC of these inhibitors (Table 3.2).

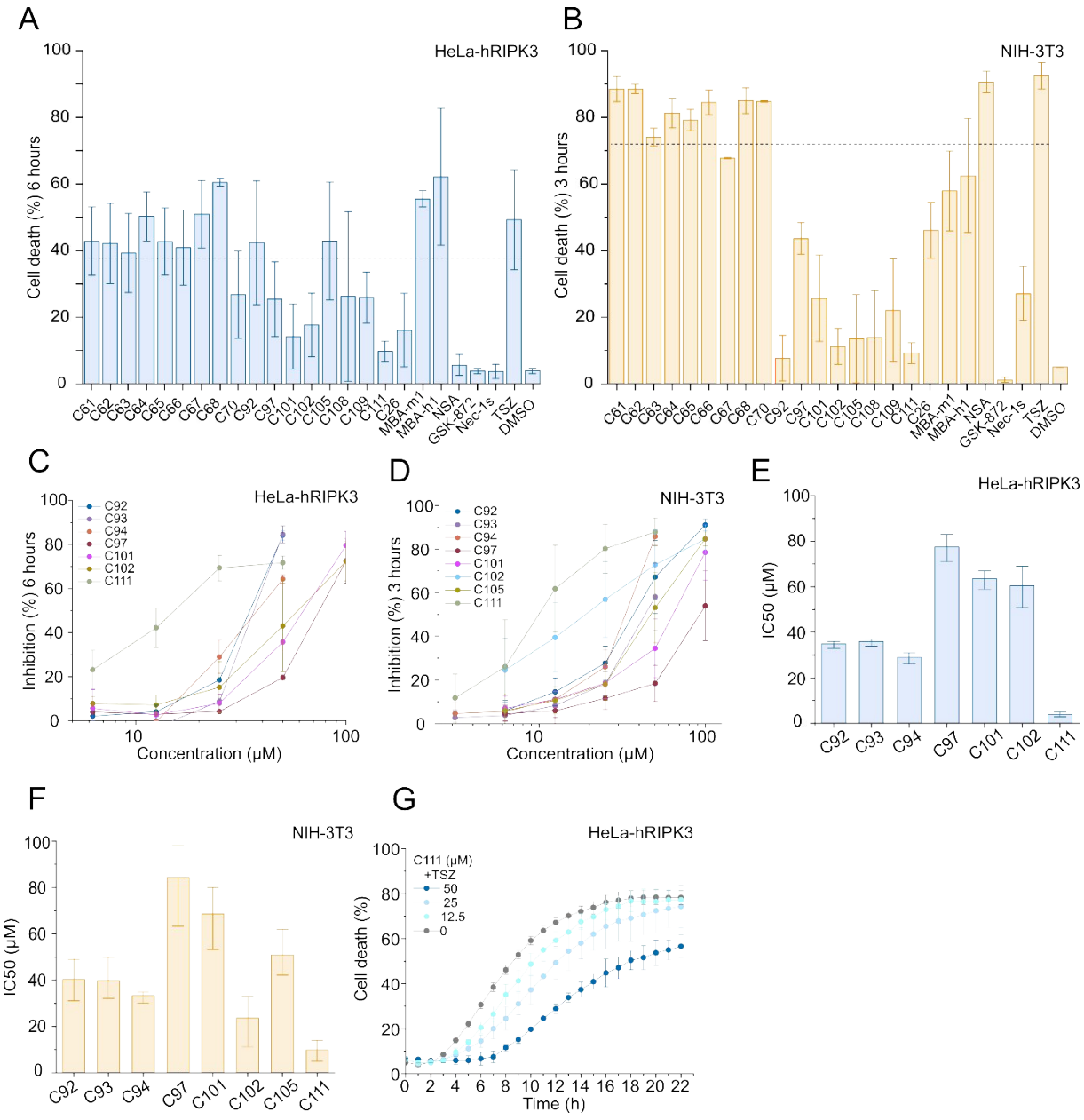

Figure 3. 15 Characterization of the inhibitory effect in cells of the C26 analogs.

(A, B) Inhibitory effect of compounds in HeLa-hRIPK3 (A) and NIH-3T3 (B) cell lines. A fixed concentration of the compounds was used (100 µM) in this primary screening. 10 µM of Nec-1s, GSK-872, and NSA were tested as a positive control. The dashed line represents 70% of the TSZ activity.

(C, D) Dose-response curves of the inhibitory effect in HeLa-hRIPK3 (C) and NIH-3T3 (D) cells.

(E, F) IC50 for the inhibitors in HeLa-hRIPK3 (E) and NIH-3T3 (F) cell lines.

(G) Effect of C111 in the kinetics of necroptosis induced in HeLa-hRIPK3 cells.

(H) Chemical structure of C111.

Necroptosis was induced by using a mixture of TNF (30 ng/mL), Smac mimetic (20 µM), and zVAD (20 µM). Different concentrations of the inhibitors were used, as indicated in the figures. Cell death was measured using the InCucyte. Inhibition was calculated by dividing cell death in the presence of the inhibitors by the corresponding values obtained with TSZ at the same time point and expressed as a percentage. Each dot represents the mean, and the error bars represent the standard deviation from at least 3 independent replicates.

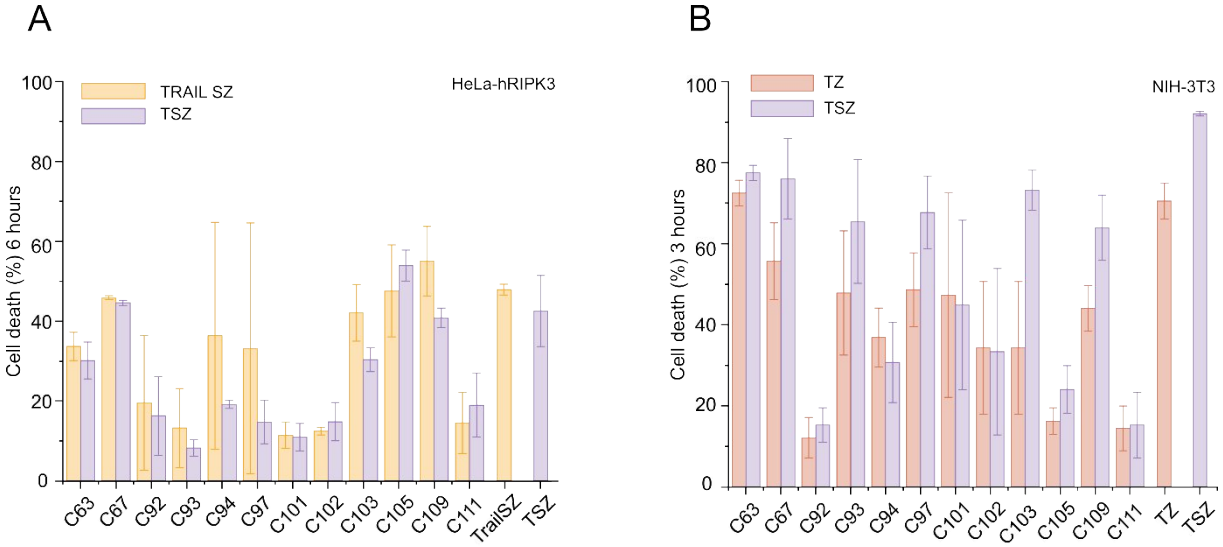

Figure 3. 16 Inhibitory effects of the C26 analogs on cells treated with different necroptotic stimuli compared to TSZ.

(A) Inhibitory effect of the compounds on necroptosis induced by TRAILSZ and TSZ in HeLa-hRIPK3 cells.

(B) Inhibitory effect of the compounds on necroptosis induced by TZ and TSZ in NIH-3T3 cells.

Necroptosis was induced by using a mixture of TNF (30 ng/mL) or TRAIL (100 ng/mL), Smac mimetic (20 µM), and zVAD (20 µM). Different concentrations of the inhibitors were used, as indicated in the figures. Cell death was measured using the InCucyte. Each dot represents the mean. The error bars represent the standard deviation. Graphs are representative of at least 3 independent replicates.

Table 3. 2 Summary of the SC and NTC of best-hits identified in the C111 analogs list

Name	MSC (µM)	MnTC (µM)
C111	100	50
C114	100	40
C115	100	50
C123	50	50
C125	50	50

Consequently, we evaluated the soluble compounds using SPR to assess their interaction with the recombinant human or mouse MLKL. Our primary screening was conducted at a fixed concentration of 50 µM. This initial screening allowed us to identify potential compounds that exhibited primary interaction with recombinant MLKL (Figure 3.17B). Following these results, we delved deeper into the characterization of these inhibitors by assessing their binding affinity to MLKL. Different concentrations of the inhibitors were flowed over the immobilized MLKL, where we managed to calculate the Kd values that were in the low µM range (Figure 3.17C). As we could not calculate the Kd of C115 by using the SPR, we employed MST as an orthogonal method. We used the recombinant mouse MLKL labeled with Atto-655 NHS ester dye. This method enabled us to calculate the Kd for the inhibitors, where C115 and C125 emerged as the most effective binders, exhibiting Kd values of approximately 25 µM and 35 µM, respectively (Figure 3.17D).

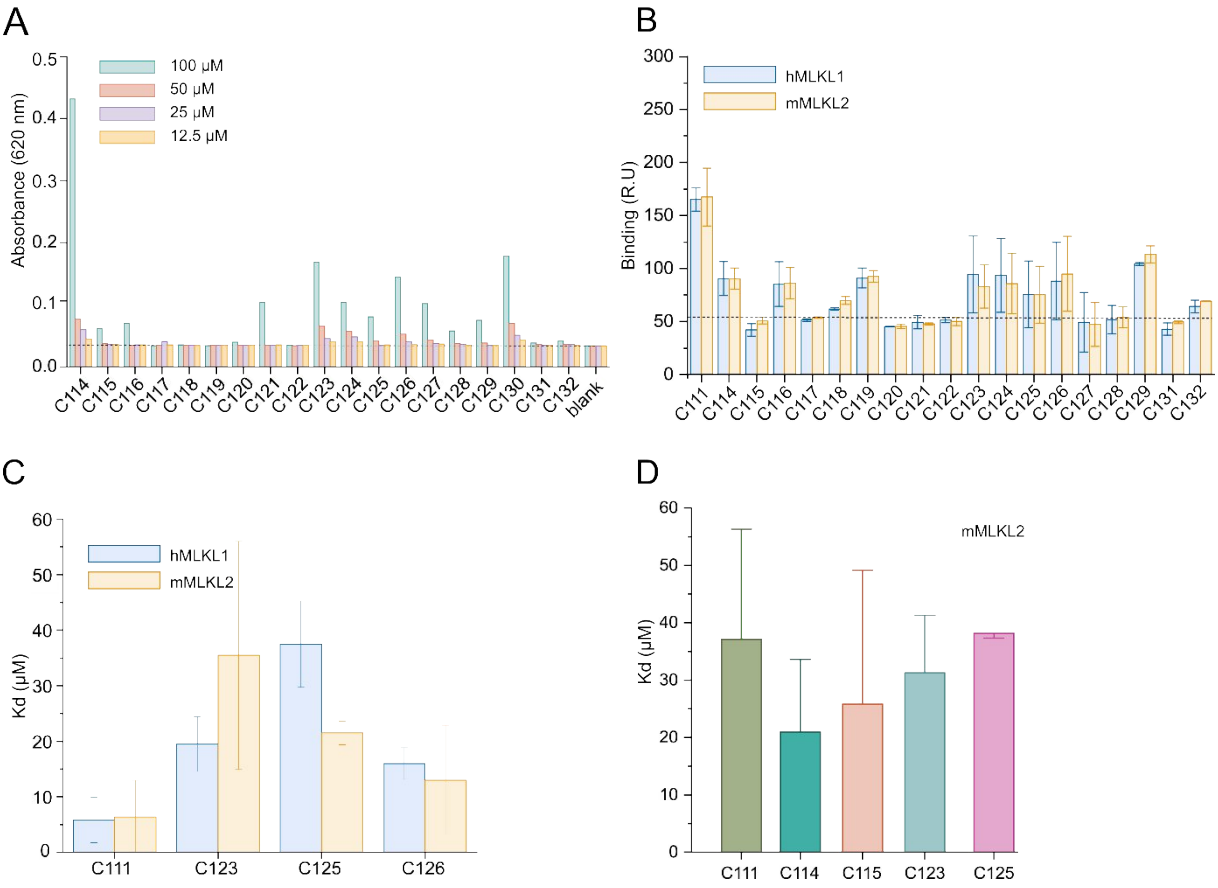

Figure 3. 17 Solubility and binding affinity characterization of the C111 analogs list.

(A) Solubility measurements of the compounds. The compounds were tested for their solubility in different concentrations, as indicated in the figure. Scope medium was used to avoid the interference of phenol red on the measurement. The dashed line represents the soluble threshold in comparison to the control sample.

(B) SPR primary screening of the compounds. Binding response to human or mouse MLKL was measured, a fixed concentration of the inhibitors was used at 100 μM, and recombinant MLKL was immobilized on a CM5 chip. The dashed line represents the threshold of compounds binding to MLKL.

(C) Kd values of the interaction between the inhibitors and recombinant hMLKL1 and mMKL2. Increasing concentrations of the compounds (12.5 μM to 200 μM) were flowed over hMLKL1 and mMLKL2 with a concentration of 1 μM immobilized on CM5 sensorchip. Data were fitted to a 1:1 binding kinetic interaction model to calculate the binding affinity Kd.

(D) Kd values of the interaction between the inhibitors and the recombinant mMLKL2 labeled with Atto-655 NHS ester dye by using MST. Increasing the concentration range of the inhibitors was used (7.6 nM to 125 μM). Data were fitted to a 1:1 binding kinetic interaction model to calculate the binding affinity Kd.

Next, we conducted necroptotic cell-based assays to investigate the inhibitory potential of these compounds upon necroptosis induction with TSZ treatment in HeLa-hRIPK3 (Figure 3.18A, B) and NIH-3T3 cells (Figure 3.18C, D). We initially performed primary screening where we used fixed concentrations (either 100 or 50 μM) of the inhibitors selected based on SC and NTC (Table 3.2). From this screening, we identified some potential inhibitors (C111, C115, C116, C123, C125, and C129) that were assessed further in the secondary screening.

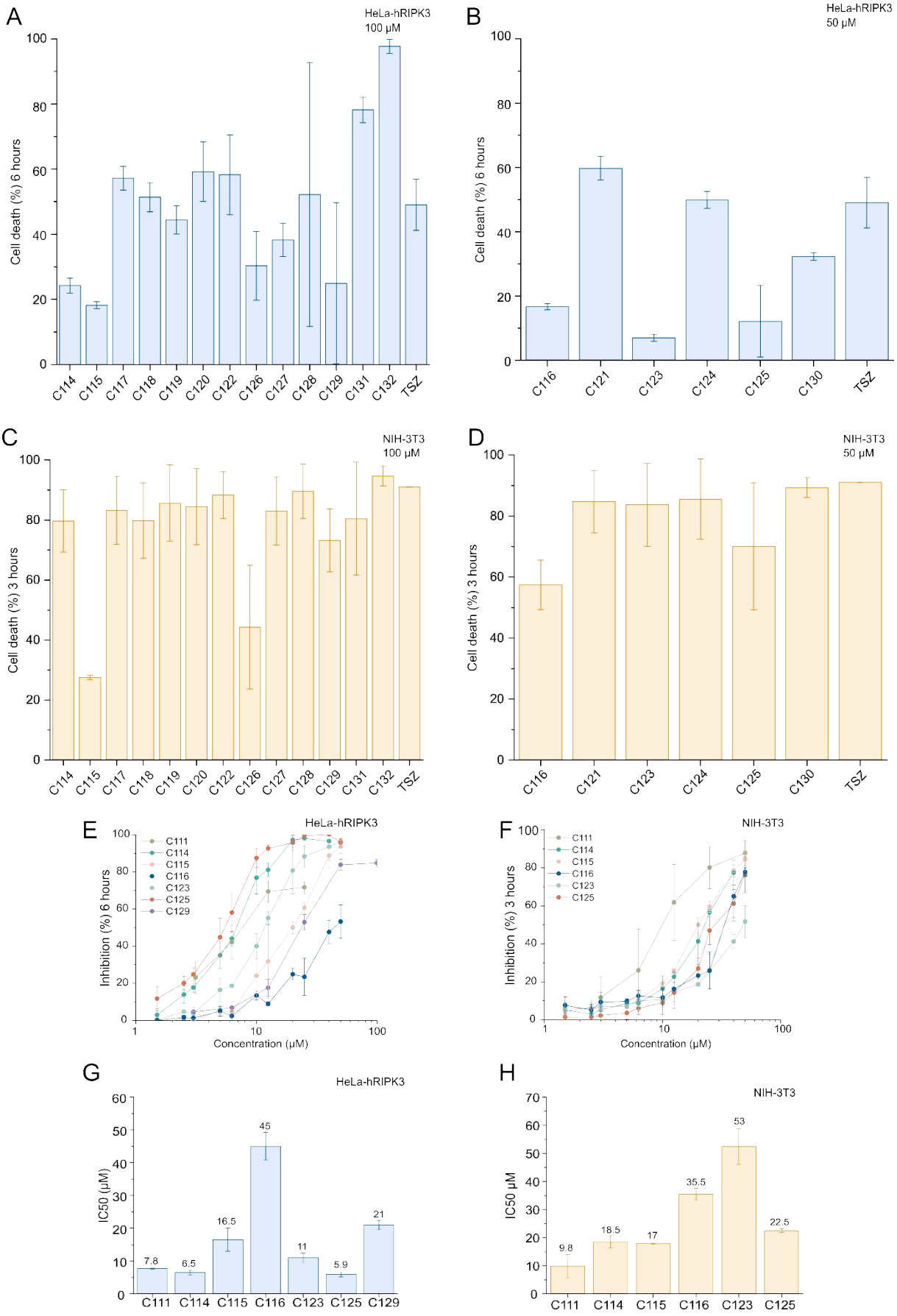
A
HeLa-hRIPK3
100 μM
Cell death (%) 6 hours
C114 C115 C117 C118 C119 C120 C122 C126 C127 C128 C129 C131 C132 TSZ
B
HeLa-hRIPK3
50 μM
Cell death (%) 6 hours
C116 C121 C123 C124 C125 C130 TSZ
C
NIH-3T3
100 μM
Cell death (%) 3 hours
C114 C115 C117 C118 C119 C120 C122 C126 C127 C128 C129 C131 C132 TSZ
D
NIH-3T3
50 μM
Cell death (%) 3 hours
C116 C121 C123 C124 C125 C130 TSZ
E
HeLa-hRIPK3
Inhibition (%) 6 hours
C111 C114 C115 C116 C123 C125 C129
Concentration (μM)
F
NIH-3T3
Inhibition (%) 3 hours
C111 C114 C115 C116 C123 C125
Concentration (μM)
G
HeLa-hRIPK3
IC50 (μM)
7.8 6.5 16.5 45 11 5.9 21
C111 C114 C115 C116 C123 C125 C129
H
NIH-3T3
IC50 μM
9.8 18.5 17 35.5 53 22.5
C111 C114 C115 C116 C123 C125

Figure 3. 18 Characterization of the inhibitory effect in cells of the C111 analogs.

(A-D) Inhibitory effect of compounds in HeLa-hRIPK3 (A, B) or NIH-3T3 (C, D) cells. A fixed concentration of the inhibitors was used (either 100 μM or 50 μM) in this primary screening.

(E, F) Dose-response curves of the inhibitory effect of the compounds in HeLa-hRIPK3 (E) and NIH-3T3 (F) cells.

(G, H) IC50 for the inhibitors in HeLa-hRIPK3 (G) and NIH-3T3 (H) cells.

Necroptosis was induced by using a mixture of TNF, Smac mimetic, and zVAD. Cell death was measured using the InCucyte. Inhibition was calculated by dividing cell death in the presence of the inhibitors by the corresponding values obtained with TSZ at the same time point and expressed as a percentage. Each dot represents the mean. The error bars represent the standard deviation; graphs are representative of at least 3 independent replicates.

In the secondary screening, we tested these inhibitors at different increasing concentrations and found that they inhibited necroptosis in a dose-dependent manner, which enabled us to calculate the IC50 (Figure 3.18E, F). Remarkably, our results from the secondary screening highlighted C125 as the best candidate in HeLa-hRIPK3 cells, with an IC50 of 5.6 μM. Meanwhile, in the NIH-3T3 cell line, C115 emerged as the top candidate with an IC50 of 17 μM (Figure 3.18G, H).

In human HeLa-RIPK3 cells, C123 and C125 demonstrated prolonged inhibition of necroptosis over an extended time (24 hours) (Figure 3.19A, B), which is an advantage in comparison to C111 from the previous list (Figure 3.15G and 3.18A, B). Notably, not only C125 but also C111 and C115 showed high efficacy of inhibition in HT-29 cells at this time point (Figure 3.19C). This effect of C115, C123, and C125 was exclusive in human cell lines and was not observed in NIH-3T3. Having witnessed the complete inhibition of necroptosis by these inhibitors for a duration of up to 24 hours, we aimed to conduct a comparative analysis of these compounds compared to the existing MLKL inhibitors that bind human MLKL covalently (e.g., NSA and the xanthine-derivative TC13172). Our findings revealed that, albeit at higher concentrations, C115 and C125 almost completely blocked necroptosis (around 70% inhibition) at 24 hours. They were characterized by an IC50 in the low μM range, while NSA and TC13172 exert their IC50 in the nM range. This comparative analysis highlights the need for further improvement of our inhibitors, which are probably less effective as they are supposed to bind in a reversible mode to MLKL.

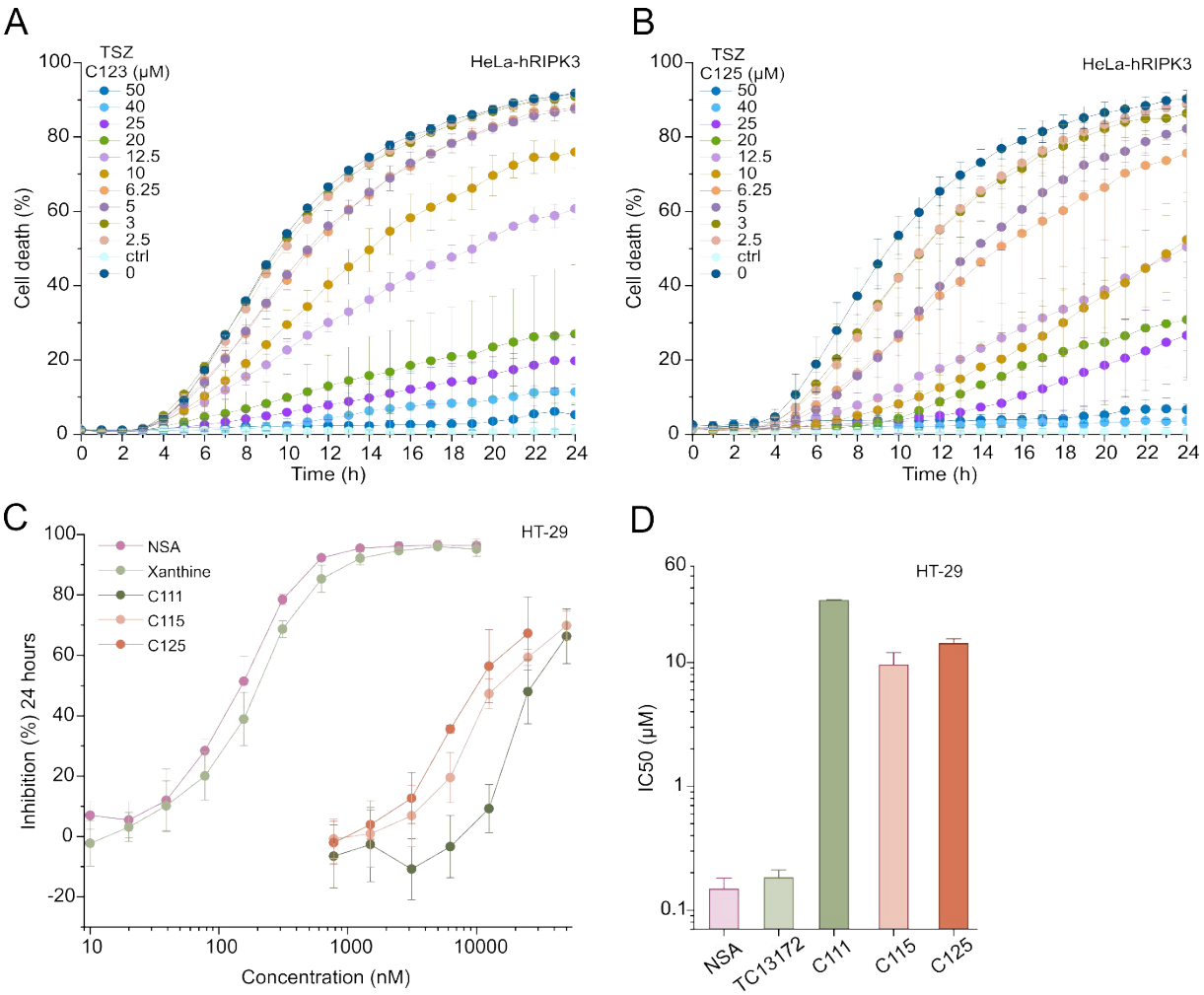

Figure 3. 19 Effect of top candidates of C111 analogs on the kinetics of necroptosis induced in HeLa-hRIPK3 cells and HT29, in comparison with existing inhibitors.

(A, B) Effect of C123 (A) and C125 (B) on the kinetics of cell death in HeLa-hRIPK3.

(C) Dose-response curves of the inhibitory effect of the compounds in HT-29. NSA and xanthine (TC13172) MLKL inhibitors were included as a control.

(D) IC50 for the inhibitors calculated in HT-29 at 24 hours. NSA and xanthine (TC13172) MLKL inhibitors were included as a control.

Necroptosis was induced by using a mixture of TNF (30 ng/mL), Smac mimetic (20 μM), and zVAD (20 μM). Cell death was measured using the InCucyte. Inhibition was calculated by dividing cell death in the presence of the inhibitors by the corresponding values obtained with TSZ at the same time point and expressed as a percentage. Each dot represents the mean. The error bars represent the standard deviation; graphs are representative of at least 3 independent replicates.

Furthermore, our screening was extended to compare the inhibitors` activity when subjected to different necroptotic stimuli, similar to our previous assessment. To achieve this, we induced necroptosis in NIH-3T3 cells by using both TSZ (Figure 3.20A) and TZ (Figure 3.20B) as necroptotic triggers. The results showed that the inhibitors consistently demonstrated the same inhibitory effects across distinct necroptosis stimuli. This uniformity in their inhibitory

performance highlights the reliability of these compounds in inhibiting necroptosis, regardless of the employed stimulus. To further rule out the possibility of potential off-targets of the inhibitors and considering that RIPK1 is a common effector in both apoptosis and necroptosis, we assessed the impact of the inhibitors on RIPK1-induced apoptosis. To achieve this, we induced apoptosis with a mixture of TNF and Smac mimetic (TS) in addition to the inhibitors. Consistently, the results demonstrated that they did not exhibit any noticeable effect on the kinetics of extrinsic apoptosis in wt NIH-3T3 cells (Figure 3.20C).

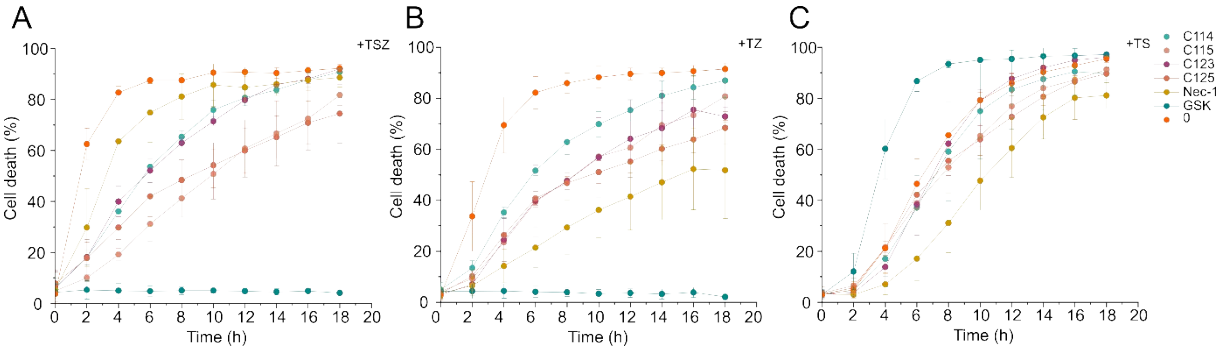

Figure 3. 20 Effect of the top candidates from the C111 analogs list on necroptosis triggered via different necroptotic stimuli compared to TSZ or during intrinsic apoptosis stimuli TS.

(A, C) Effect of compounds on cell death kinetics induced by TSZ(A), TZ (B), or TS (C) compared to other inhibitors of the pathway: Nec-1s (inhibitor of RIPK1), GSK-872 (inhibitor of RIPK3).

4. Discussion and Conclusions

Necroptosis is a form of regulated cell death that occurs when apoptosis and caspases, the conventional mechanisms of programmed cell death, are inhibited and unable to proceed (Vanlangenakker et al., 2012). Necroptosis serves as an alternative pathway for eliminating pathogens when the primary apoptotic route is compromised (Vandenabeele et al., 2010). In recent decades, necroptosis has gained increasing attention within the scientific community. Researchers are increasingly driven to explore the molecular regulators of necroptosis and elucidate their underlying mechanisms.

Emerging evidence in the cell death pathways has shed light on the critical mediators of necroptosis. The first two of these mediators are RIPK1 and RIPK3 (Cho et al., 2009c; Declercq et al., 2009; Degterev et al., 2013; Duprez et al., 2011), which have been identified as essential effectors in the initiation and execution of necroptosis. Moreover, recent research has unveiled an additional mediator that further refines our understanding of necroptosis. The MLKL pseudokinase protein has emerged as a key player in this pathway, working downstream of the RIPK3 (Sun et al., 2012; Zhao et al., 2012). It has been implicated as a crucial executor of necroptosis, capable of propagating the necroptotic signal generated by RIPK3 and driving the cell toward its programmed cell death (Samson et al., 2020).

MLKL serves as a critical component in the execution of necroptosis. It has distinct functional domains that comprise a C-terminal regulatory domain and an N-terminal executioner domain, and a brace domain intricately interconnects them. Activation of MLKL is initiated through the RIPK3-mediated phosphorylation at specific residues located within its psK domain (Murphy, 2020). This phosphorylation event triggers a chain of molecular events that ultimately culminate in necroptosis. One crucial consequence of its activation is the oligomerization of MLKL via its executioner domain (Wang et al., 2014b). The oligomerized MLKL then undergoes a transformation that is then translocated into the plasma membrane (Galluzzi et al., 2014). Despite the advancements in recent years in unraveling the complexities of necroptosis signaling, one crucial aspect remains elusive. The precise mechanism responsible for the final and pivotal step, the rupture of the plasma membrane, remains unknown. Researchers continue to investigate this process to gain a comprehensive understanding of necroptosis and its execution.

Unlocking the secret: Hc insertion in the hydrophobic groove in the psK is a key to MLKL activation

Transcriptome analyses have revealed the existence of different isoforms in both human and mouse MLKL. Building upon earlier investigations done on the human MLKL isoforms (Arnež et al., 2016), a study by (Ros et al. unpublished) has shed light on the variability in their capabilities to mediate necroptotic cell death. These MLKL isoforms can be categorized based on their necroptotic activity and the regulation by RIPK3. In this classification, we encounter a member known as the inactive isoform, denoted as mMLKL1 in mice and hMLKL0 for humans. This isoform does not exhibit necroptotic activity, raising questions about its specific role in cell death regulation. Conversely, another category encompasses isoforms with the capacity to be activated in response to external stimuli. These active isoforms, represented by hMLKL1 and mMLKL2, are prevalent in human MLKL and mouse MLKL, respectively. Based on the analysis of these opposite variants, our research revealed a pivotal and unexpected role for the Hc (disrupted in the inactive isoforms) in stabilizing the active conformation of MLKL. We have provided compelling evidence to demonstrate that the Hc plays an indispensable role in MLKL activation. Our investigations have further unveiled the significance of the Hc accommodation within a hydrophobic groove that connects the 4HB domain, the psK domain, and the brace region. This interplay is essential for the activation of MLKL in both human and mouse orthologues. We exploited this knowledge for the development of a new strategy for the pharmacological inhibition of MLKL.

4.1 Revolutionizing MLKL Inhibitors: A Novel Strategy for Targeting MLKL

Necroptosis, mediated by MLKL, is linked to various pathophysiological processes, spanning disorders of the nervous system (Picon et al., 2021), cardiovascular system (Karunakaran et al., 2016), respiratory system (Lee et al., 2018; Lu et al., 2021), and numerous types of cancer (Ando et al., 2020; X. Li et al., 2021; Martens et al., 2021; Seifert et al., 2016; Stoll et al., 2017). Consequently, there has been a growing interest in the development of potent and selective necroptosis inhibitors, with a primary focus on targeting MLKL. Another compelling factor that renders MLKL an attractive candidate for drug development is that in certain pathological conditions, necroptosis can be initiated not only via the canonical necrosome involving the RIPK1-RIPK3-MLKL pathway (Ju et al., 2022; Mocarski et al., 2012) but also via the non-canonical necrosome (D. Yang et al., 2020), as exemplified in the case of TRIF/ZBP1-RIPK3-MLKL- mediated cell death (Yuan et al., 2022).

Existing MLKL inhibitors suffer from several drawbacks, including moderate potency, a restricted structure-activity relationship, and, notably, undesirable off-target effects that hinder their progression to more advanced stages in clinical trials, thus impeding their development into effective drugs (B. Cui et al., 2022; Hildebrand et al., 2014; Sun et al., 2012; Yan et al., 2017). A prominent example of such inhibitors includes those that form covalent bonds with human MLKL, such as NSA and its derivatives. The covalent binding to C86 residue in human MLKL is a double-edged weapon. While it enhances the specificity for human MLKL, it poses a significant hindering factor to be utilized in mouse studies, where the target residue is absent in mouse MLKL. Furthermore, the covalent binding to Cys opens the door to potential off-target interactions with other reactive Cys in the system, thereby limiting their applicability in drug development due to the risk of unintended off-target effects. In fact, it has been found that NSA also binds and inhibits mouse and human GSDMD during pyroptosis, rendering it non-specific in the context of studying necroptosis (Rathkey et al., 2018). Furthermore, efforts have been made to explore the development of new inhibitors that target nucleotide binding sites within the psK domain (Hildebrand et al., 2014). However, this approach faces certain limitations, primarily concerning its potential to bind not only to the intended target but also to other kinases and pseudokinases, introducing challenges in achieving the required specificity.

Until very recently, no reversible or allosteric inhibitors for MLKL have been discovered, but in the study of (Rübbelke et al., 2021b), they have identified non-covalent binders of the executioner domain (4HB) of MLKL with an affinity of approximately 50 μM. Regrettably, their activity in cells remained untested, primarily due to issues concerning their low membrane permeability. Additionally, these binders did not exhibit activity in an *in-vitro* liposome leakage assay. Consequently, further rounds of optimization are warranted to establish their efficacy as potential MLKL inhibitors. Altogether, these challenges highlight the need for novel, more versatile, and highly specific MLKL inhibitors with improved therapeutic potential.

Here, we present a novel approach aimed at the specific targeting of MLKL and the design of small molecule regulators focusing on the Hc/groove interactions. Building upon our earlier discoveries emphasizing the pivotal role of the Hc in MLKL activity, our objective is to produce novel compounds capable of disrupting the interaction between the Hc and its integration into the recently identified hydrophobic groove within MLKL. This innovative class of inhibitors will signify a novel category of MLKL modulators, promising to provide precise control for MLKL activity.

4.2 The MBAs: Unveiling Proof-of-Principle Compounds of a new class of MLKL Inhibitors

Here, we introduce two pivotal proof of principle compounds known as MBAs. These agents are thought to work through allosteric binding to the Hc/groove of MLKL. They are commercially available compounds that were identified through the combination of MD simulations and *in-silico* screening. MBA-h1 and MBA-m1 are tailored for human MLKL and mouse MLKL, respectively.

Our research indicates that these compounds can effectively inhibit necroptosis as they exhibited a dose-dependent delay in the kinetics of cell death, with an IC50 in the µM range. It is speculated that this kinetic effect is a consequence of the inhibitors targeting MLKL via non-covalent interactions, therefore acting as reversible inhibitors. Although the exact mechanism of action is still unknown, it could be that due to its reversible mode of binding to MLKL, a fraction of free MLKL coexists with MLKL-inhibitor complexes in cells. This fraction of free MLKL could remain available for activation and subsequent irreversible binding to mediate cell death, which would, over time, shift the balance from the complex with the inhibitor towards the accumulation of active MLKL at the membrane, which explains the effect of the cell death kinetics delay in this class of inhibitors. It is noteworthy to mention that covalent inhibitors such as NSA are more potent at blocking cell death as they interact with MLKL irreversibly via covalent bonds (Sun et al., 2012). However, these types of inhibitors show specificity problems and huge potential for off-target effects because they can bind to any reactive cysteines in the cell. For instance, NSA has already been shown to bind to and inhibit GSDMD, the executor of pyroptosis, unspecifically (Rathkey et al., 2018).

Furthermore, our comprehensive characterization revealed that MBA-h1 exhibited no toxicity in HT-29 and HeLa-hRIPK3 cells, even at the highest concentrations of 100 µM. However, upon assessing the toxicity of MBA-m1, a distinct pattern emerged, with this compound demonstrating toxicity in a concentration range of 5-10 µM in primary macrophages as well as in NIH-3T3 cells. These findings suggest the potential use of MBA-m1 within the range of non-toxic concentrations in primary cells and in *in-vivo* applications.

Investigating the underlying reasons for the observed toxicity of MBA-m1, we assessed the impact of various inhibitors on MBA-m1-induced toxicity in NIH-3T3 cells. This comprehensive analysis aimed to discern the potential causes of toxicity and eliminate the likelihood of off-target effects within common cell death pathways, such as necroptosis or

apoptosis. Notably, we observed a lower toxicity threshold in BMDMs compared to NIH-3T3 cell lines. The optimal concentration for inducing toxicity in NIH-3T3 cells was determined to be 10 μM, whereas, in BMDMs, a concentration as low as 5 μM was sufficient to elicit a comparable toxic response. To evaluate the observed toxicity of MBA-m1, we primarily evaluated its effect in MLKL ko cells. As toxicity was even increased in these cells, we could conclude that it results from the interaction of this compound with other components of the cell. In addition, we employed Nec-1s and GSK-872 to ascertain that the observed toxicity is not mediated by RIPK1 or RIPK3.

Additionally, we assessed the influence of zVAD (a pan-caspase inhibitor) and Fer-1 (a ferroptosis inhibitor) to confirm that the toxicity is not attributed to the activation of apoptosis or ferroptosis. Remarkably, our data revealed that, regardless of the inhibitor applied, MBA-m1-induced toxicity persisted. This finding suggests that the toxicity is not mediated by RIPK1 or RIPK3, nor is it a consequence of apoptosis or ferroptosis activation. However, we propose several potential explanations for this persistent toxicity. Firstly, it could be attributed to the saturation of the binding site at higher concentrations of MBA-m1, which permits the establishment of nonspecific interactions with other cellular regulators, leading to toxicity via a non-regulated mechanism of cell death. Furthermore, the observed toxicity may be influenced by cell type specificity. Furthermore, our data indicated that MBA-m1 did not affect the RIPK1-mediated apoptosis in NIH-3T3 cells induced by TS. This observation argues in favor of the absence of off-target effects of the inhibitor under conditions in which it exerts its inhibitory capacity. Supporting this notion, additional evidence gathered through CETSA-WB assays strongly suggests that MBA-m1 does not bind to RIPK1 or RIPK3.

In the necroptotic pathway, MLKL serves as the final executor of this pathway, and its activation includes three major steps: RIPK3-mediated MLKL phosphorylation followed by MLKL oligomerization and the translocation to the plasma membrane and thereby executing necroptosis. We aimed to assess the mechanism of action of the MBAs by evaluating their effect on the hallmarks of MLKL activation. Similar to the covalent MLKL binders such as NSA, TC13172, and uracil derivatives, MBA-h1 displayed no discernible impact on MLKL-mediated RIPK3 phosphorylation. However, upon the treatment of mouse cells with MBA-m1, we observed a slight delay in the phosphorylation of MLKL, where the antibodies against the phosphorylated MLKL appeared in the presence of the inhibitor 90 min after TSZ treatment. Additionally, MBAs exhibited the ability to completely inhibit MLKL oligomerization and membrane translocation, similar to the effects observed with the xanthine-derivative TC13172

(Yan et al., 2017). Notably, despite the shared target residue in human MLKL and their covalent binding to human C86 (Liao et al., 2014; Rübbelke et al., 2020; Yan et al., 2017), NSA and uracil-derivatives did not exhibit a noticeable blockade of MLKL oligomerization. This observation underscores the distinctive mechanism by which MBAs influence the activation of MLKL hallmarks, primarily by impeding oligomerization and membrane translocation. Altogether, this evidence gives us an insight into the MBAs` mechanism of action on MLKL activation hallmarks. The MBAs do not block either the MLKL activation by phosphorylation or its oligomerization into higher-order oligomers. However, their interaction with MLKL immobilizes the complex in an oligomerized state, hindering its translocation to the plasma membrane and thereby inhibiting cell death.

In order to assess the specificity of the MBAs and to validate MLKL as the primary on-target effector of these compounds, we conducted a series of experiments. Firstly, we quantified the physical interaction between each inhibitor and the corresponding recombinant MLKL *in-vitro* using SPR. Our data analysis revealed that the binding affinity between hMLKL1 and MBA-h1, as well as between mMLKL2 and MBA-m1, corresponded to a Kd in the low μM range, showing improved results compared to the previously discovered allosteric non-covalent binder of MLKL with calculated Kd of 50 μM (Rübbelke et al., 2021b).

Moreover, to confirm the specificity of the MBAs within the cellular context, we employed CETSA-WB. This assay served as the first approach to validate that mouse MLKL is the target MBA-m1 in the cells. Interestingly, we noticed different effects of MBA-m1 on the thermal stability of mouse MLKL that differ according to the status of the cell death treatment. Specifically, in the absence of necroptotic stimulation, MBA-m1 reduced the thermal stability of the mouse MLKL, as WB bands were still detected at 60 degrees. Conversely, in the presence of a necroptotic stimulus, MBA-m1 enhanced the thermal stability of mouse MLKL as protein bands decreased at 56 degrees. This underscored the difference in MBA-m1's ability to affect the thermal denaturation of MLKL in the presence or absence of necroptotic stimuli. These differences might be attributed to the formation of MLKL oligomers under necroptotic conditions, which could exhibit higher thermal stability compared to the inactivated monomeric MLKL. Intriguingly, MBA-h1 did not significantly alter the thermal stability of the human MLKL in the HT-29 cell line. This might be attributed to the mode of its binding to MLKL. For instance, the binding of MBA-h1 to the allosteric site on human MLKL can alter its confirmation without directly affecting its thermal stability. This also further explains the higher stability of hMLKL which is less prone to alterations upon the binding of MBA-h1.

Of relevance, the administration of MBA-m1 exhibited a remarkable reduction in dermatitis severity and disease progression in $Tnfr1^{KO}$; $Hoip^{E\text{-}KO}$ mice model of dermatitis in which the Keratinocyte-specific absence of the LUBAC component HOIP (HoipE-KO) combined with constitutive TNFR1 deficiency (Tnfr1 ko) induces fatal dermatitis at around day 70 after birth, which is ameliorated by loss of MLKL. In addition, MBA-m1 prevents the development of aortic aneurysms in mice model that is induced by the injection of porcine pancreatic elastase (PPE) (Ros et al., unpublished). As this is the first inhibitor against mouse MLKL, this outcome underscores the promising potential of therapeutic MLKL inhibition as an effective strategy for the treatment of necroptosis-driven diseases. Collectively, these findings lay the foundation for MBAs as successful proof of principle compounds, marking a significant advancement in the development of a novel class of MLKL inhibitors.

4.3 Revealing a Promising Story: Optimized Inhibitors that Block Necroptosis in Human and Mouse Cells

After achieving success with our proof-of-principle compounds, which paved the way for a new class of MLKL inhibitors targeting MLKL allosterically by disrupting the Hc/groove interaction, we aimed to expand upon this approach. To achieve this, our collaborators conducted an extensive *in-silico* screening. From this screening, we chose the most promising commercially available compounds, which we subsequently characterized using a specific methodology. This involved identifying their soluble and non-toxic concentration, followed by assessing their interaction and binding with both human and mouse MLKL, as well as identifying their inhibitory effect on necroptotic cell death.

To evaluate the effectiveness of these compounds, we performed necroptotic cellular-based assays using various human and mouse cell lines. From the data obtained, one standout compound emerged: C26. It effectively delayed the kinetics of necroptosis in a dose-dependent manner, with an IC50 of approximately 50 µM. Additionally, it exhibited a binding affinity to human and mouse MLKL with a Kd of 60 µM. Building on the success of the initial *in-silico* screening, we embarked on a round of optimization to identify analyses for C26 that possessed improved characteristics in terms of solubility, toxicity, inhibition, and binding. This optimization round yielded 52 commercially available compounds, which we subjected to the same methodology for characterization. From this round, C111 emerged as the superior hit. Notably, it displayed a Kd of around 6 µM in binding to both human and mouse MLKL and with an IC50 of around 6 µM representing a five-fold improvement over the previous hit. Encouraged by these results, we went for a third and final round of optimization to discover

analogs for C111, yielding an additional 20 compounds. Again, following the same methodology, we identified the best hits, C115 and C125. They successfully inhibited necroptosis with an IC50 of approximately 10 μM in both human and mouse cell lines.

Our data consistently revealed substantial improvements in the physiochemical properties of the compounds during each successive optimization round compared to their predecessors. Notably, we observed a significant enhancement in the solubility and reduced toxicity as we fine-tuned the compounds throughout the optimization processes. Furthermore, we thought to confirm the capacity of these small molecules to interact with the recombinant MLKL. This was accomplished through *in-vitro* SPR, which allowed us to calculate the binding affinity of the inhibitors and the recombinant human or mouse MLKL. Throughout optimization rounds, we observed a progressive improvement in the binding affinity, starting from 60 μM for C26-mMLKL2 or hMLKL1 binding in the initial screening and decreasing to as low as 20 μM for both C115 and C125 from the final optimization. This data indicates that these molecules can successfully interact with MLKL with enhanced binding affinity than the already available allosteric non-covalent binder of MLKL (Rübbelke et al., 2021b), suggesting that the newly discovered pocket in MLKL that is not conserved among other kinases might be a good starting point for the development of more inhibitors for MLKL.

Furthermore, when assessing the inhibitory potential of these small molecules, we calculated the IC50 values over the optimization rounds. Our results consistently demonstrated a notable increase in the compound's ability to inhibit necroptosis. For instance, the IC50 of C26 in NIH-3T3 cells started at approximately 50 μM in the initial screening. It subsequently decreased to 8 μM for C111 from the first optimization round and approximately 10 μM for C115 and C125. These findings collectively indicate that the optimized small molecules can effectively and specifically target MLKL in both human and mouse cell lines.

In alignment with this concept, we have observed that the compounds within this newly discovered class of MLKL inhibitors effectively inhibit necroptosis in both human and mouse cell lines. Remarkably, this efficacy persisted despite the initial screening primarily targeting hMLKL1. This confers a significant advantage over existing inhibitors (B. Cui et al., 2022; Liao et al., 2014; Rübbelke et al., 2020; Yan et al., 2017), as it paves the way for a smoother transition to clinical trials. Here, we can leverage this insight to predict the compounds' impact on humans by assessing their effects in mice beforehand. This concept bore some resemblance to the Lck inhibitor, AMG-47a that simultaneously targets RIPK1, RIPK3, and MLKL

(Jacobsen et al., 2022), which was found to inhibit necroptosis with a more pronounced inhibition of necroptosis in human cell lines when compared to its effect in mouse cell lines.

Interestingly, as we progressed through the optimization rounds, particularly with the final hits, C115 and C125, we observed more pronounced inhibitory effects in human cell lines with almost 80 % inhibition over 24 hours compared to when they were tested in mouse cell lines. These differences could be attributed to various factors, including subtle differences in the regulation of necroptosis between different species (W. Chen et al., 2013), as well as structural differences in the hydrophobic groove between human MLKL and its mouse MLKL orthologue. These differences could offer valuable insights into the success of our optimization efforts, particularly in terms of specificity.

Throughout the successive optimization rounds applied to the compounds, we have achieved an improvement in the IC50 and better inhibition of necroptosis. This enhancement can be attributed to the enhancement of bioavailability and partitioning into membranes throughout the optimization. Indeed, the measurement of the Log Po/w of C26, a measure of its partition coefficient between octanol and water, demonstrated a substantial increase from 3.5 to 5.9 in C111. This significant enhancement might further explain the rationale behind the improvement in inhibitory efficacy. Moreover, the extended inhibitory effects observed in the compounds following the last round of optimization (C115, C123, and C125) may be attributed to slower dissociation rates. The optimization process likely led to compounds with more prolonged activity, allowing for sustained inhibitory effects on the target. This combination of enhanced Log Po/w and prolonged activity underscores the success of the optimization strategy in refining the compounds for improved pharmacological performance. These findings provide valuable insights into the potential of the optimized compounds as promising candidates for further development as necroptosis inhibitors.

To evaluate the inhibitory potential of the compounds from the latest optimization rounds, which exhibited the most promising effects, we conducted a comparative analysis against the well-established inhibitors of human MLKL. These inhibitors primarily target C86 and form covalent bonds with it (Liao et al., 2014; Yan et al., 2017). Our findings revealed that, despite the variation in the IC50 values between our compounds and the covalent binding inhibitors, our compounds exhibited somewhat similar inhibitors' effects on the kinetics of necroptotic cell death. This observation elucidates the additional advantage we have gained; even though our compounds potentially bind allosterically to MLKL, they display a comparable inhibition trend over 24 hours. These characteristics mitigate the disadvantages associated with covalent

binders, such as potential off-target effects and high reactivity toward other Cys residues (Rathkey et al., 2018).

Considering that the most well-understood pathway for inducing necroptosis involves TNFα (Z. Zhou et al., 2012a), we conducted an evaluation of our inhibitors' effects on necroptosis induction under different stimuli, all in the presence of TNF. Our findings revealed that the inhibitors effectively delayed the kinetics of necroptotic cell death, whether induced by TSZ or TZ in NIH-3T3 cells. This suggests a promising prospect that our inhibitors can effectively inhibit MLKL-mediated necroptosis regardless of the specific initial stimuli for MLKL activation. Additionally, our data revealed that the inhibitors did not inhibit RIPK1-mediated apoptosis when NIH-3T3 cells were stimulated with TS (X. Zhang et al., 2019).

While these results have provided valuable insights into the discovery of a novel class of necroptosis inhibitors that allosterically target MLKL, it is imperative to acknowledge several limitations that may have impacted our research. First and foremost, there is a need for further investigations to elucidate the precise mechanism of action of the optimized allosteric inhibitors. It is essential to understand how these inhibitors influence the hallmarks of MLKL activation and at which stage of the process they exert their function. Additionally, assessing the potential off-target effects of these inhibitors is a crucial aspect of this study to ensure that they have a high degree of specificity toward MLKL. Further optimizations can also be done in order to enhance the binding affinity to the recombinant MLKL as well as the efficacy of necroptosis inhibition to reach IC50 values within the nM range. However, increasing the specificity can cause the saturation of the allosteric site, which can yield diminishing effects and limit the ability to inhibit necroptosis. Furthermore, achieving higher selectivity can be challenging, and possible off-targets can arise, which will impact the efficacy of the inhibitors.

Moreover, a comprehensive evaluation of pharmacokinetic properties can be assessed. These parameters include absorption, distribution, metabolism, excretion, and toxicity (ADMET), which will provide valuable insights into the compounds' behavior *in-vivo*. This information will be crucial for the successful engagement of these optimized compounds in *in-vivo* studies.

4.4 Future Perspectives

In the course of this research, we have yielded significant insights into the discovery of a new druggable within the MLKL, which can be targeted by small molecules that reversibly bind to MLKL. It is crucial to acknowledge that this research represents just one step in a more extensive and prospective journey toward a deep understanding of the molecular mechanisms of necroptosis. Several promising avenues for future investigations have emerged as a result of the current study, which will be summarized in this section.

Mechanistic elucidation and specificity enhancement:

An essential avenue for this research entails delving deeper into the mechanisms of these allosteric inhibitors. Further investigations can be dedicated to unraveling the exact molecular mechanism through which these compounds modulate MLKL activity. This will expand our knowledge concerning the pathways in which these molecules influence necroptotic signaling. Furthermore, efforts can be made to improve the specificity of these compounds towards MLKL as the primary target for necroptosis inhibition. Achieving more selectivity of these allosteric molecules towards MLKL may be an outcome of further optimization rounds that aim to design more redefined and selective molecules.

Starting point for targeting MLKL by PROTACs:

The findings of this research also unveil promising potential for harnessing a PROTAC strategy to target MLKL. PROTACs represent a class of molecules designed to harness the ubiquitin-proteasome system by recruiting the protein of interest to an E3 ligase, ultimately leading to ubiquitination and proteasomal degradation. This approach gains significance as previous research has demonstrated that reducing MLKL levels through approaches like siRNA can effectively impede necroptosis in cells (Sun et al., 2012). Furthermore, the prospect of targeting a specific pocket within MLKL using reversible inhibitors or PROTACs presents advantages over the currently available covalent inhibitors of MLKL. These molecules target human MLKL only, which poses challenges when testing them in animal models. This is in contrast to reversible inhibitors or PROTACs that provide a more versatile and potentially cross-species applicable approach for modulating necroptosis through MLKL.

***In-vivo* studies:**

Last but certainly not least, following a comprehensive evaluation of pharmacokinetics and toxicity profiling are essential prerequisites for advancing these compounds toward *in-vivo*

studies. The pivotal next step lies in harnessing the potential of these compounds in animal models. The *in-vivo* studies will investigate the efficacy of the inhibitors within living organisms, paving the way for their potential application in clinical trials for human diseases associated with necroptosis.

4.5 Conclusions

The conclusions that can be derived from this thesis are as follows:

1. We introduce a novel approach to inhibit necroptosis by targeting the Hc/groove interaction, a newly discovered pocket in MLKL that is not conserved among other kinases. This approach offers a solution to the limitations associated with binders of the nucleotide-binding site, presenting a promising strategy for MLKL inhibition.
2. The two proof-of-principle compounds, MBA-h1 and MBA-m1, designed to target the allosteric site within human and mouse MLKL, respectively, served to validate this new approach. We show that they bind to recombinant MLKL and affect the kinetic of necroptosis and the activation of MLKL in cells.
3. Our extensive *in-silico* screening rounds have led to the identification of further optimized compounds. Notably, C115 and C125 have emerged as the most promising inhibitors for human and mouse MLKL, displaying stronger inhibitory profiles at long time points. They are the first generation of inhibitors that show efficacy in blocking necroptosis in mouse and human cells.

Altogether, these findings underline the success of our concept and its potential for advancing MLKL-targeted therapeutics in the context of necroptosis.

Bibliography

Adkins, I., Fucikova, J., Garg, A. D., Agostinis, P., & Špíšek, R. (2014). Physical modalities inducing immunogenic tumor cell death for cancer immunotherapy. In *Oncoimmunology* (Vol. 3, Issue 12, p. e968434). https://doi.org/10.4161/21624011.2014.968434

Alvarez-Diaz, S., Dillon, C. P., Lalaoui, N., Tanzer, M. C., Rodriguez, D. A., Lin, A., Lebois, M., Hakem, R., Josefsson, E. C., O'Reilly, L. A., Silke, J., Alexander, W. S., Green, D. R., & Strasser, A. (2016). The Pseudokinase MLKL and the Kinase RIPK3 Have Distinct Roles in Autoimmune Disease Caused by Loss of Death-Receptor-Induced Apoptosis. *Immunity*, *45*(3), 513–526. https://doi.org/10.1016/j.immuni.2016.07.016

Ando, Y., Ohuchida, K., Otsubo, Y., Kibe, S., Takesue, S., Abe, T., Iwamoto, C., Shindo, K., Moriyama, T., Nakata, K., Miyasaka, Y., Ohtsuka, T., Oda, Y., & Nakamura, M. (2020). Necroptosis in pancreatic cancer promotes cancer cell migration and invasion by release of CXCL5. *PLOS ONE*, *15*(1), e0228015. https://doi.org/10.1371/journal.pone.0228015

Annibaldi, A., & Meier, P. (2018). Checkpoints in TNF-Induced Cell Death: Implications in Inflammation and Cancer. *Trends in Molecular Medicine*, *24*(1), 49–65. https://doi.org/10.1016/j.molmed.2017.11.002

Arnež, K. H., Kindlova, M., Bokil, N. J., Murphy, J. M., Sweet, M. J., & Gunčar, G. (2016). Analysis of the N-terminal region of human MLKL, as well as two distinct MLKL isoforms, reveals new insights into necroptotic cell death. *Bioscience Reports*, *36*(1), 1–7. https://doi.org/10.1042/BSR20150246

Badimon, L., Padró, T., & Vilahur, G. (2012). Atherosclerosis, platelets and thrombosis in acute ischaemic heart disease. *European Heart Journal. Acute Cardiovascular Care*, *1*(1), 60–74. https://doi.org/10.1177/2048872612441582

Belavgeni, A., Meyer, C., Stumpf, J., Hugo, C., & Linkermann, A. (2020). Ferroptosis and Necroptosis in the Kidney. *Cell Chemical Biology*, *27*(4), 448–462. https://doi.org/10.1016/j.chembiol.2020.03.016

Bittner, S., Knoll, G., & Ehrenschwender, M. (2017). Death receptor 3 mediates necroptotic cell death. *Cellular and Molecular Life Sciences : CMLS*, *74*(3), 543–554. https://doi.org/10.1007/s00018-016-2355-2

Caccamo, A., Branca, C., Piras, I. S., Ferreira, E., Huentelman, M. J., Liang, W. S., Readhead,

B., Dudley, J. T., Spangenberg, E. E., Green, K. N., Belfiore, R., Winslow, W., & Oddo, S. (2017). Necroptosis activation in Alzheimer's disease. *Nature Neuroscience*, *20*(9), 1236–1246. https://doi.org/10.1038/nn.4608

Cai, Z., Jitkaew, S., Zhao, J., Chiang, H.-C., Choksi, S., Liu, J., Ward, Y., Wu, L.-G., & Liu, Z.-G. (2014). Plasma membrane translocation of trimerized MLKL protein is required for TNF-induced necroptosis. *Nature Cell Biology*, *16*(1), 55–65. https://doi.org/10.1038/ncb2883

Chen, H., Li, Y., Wu, J., Li, G., Tao, X., Lai, K., Yuan, Y., Zhang, X., Zou, Z., & Xu, Y. (2020). RIPK3 collaborates with GSDMD to drive tissue injury in lethal polymicrobial sepsis. *Cell Death and Differentiation*, *27*(9), 2568–2585. https://doi.org/10.1038/s41418-020-0524-1

Chen, J., & Chen, Z. J. (2013). Regulation of NF-κB by ubiquitination. *Current Opinion in Immunology*, *25*(1), 4–12. https://doi.org/10.1016/j.coi.2012.12.005

Chen, W., Zhou, Z., Li, S., Zhong, C. Q., Zheng, X., Wu, X., Zhang, Y., Ma, H., Huang, D., Li, W., Xia, Z., & Han, J. (2013). Diverse sequence determinants control human and mouse receptor interacting protein 3 (RIP3) and mixed lineage kinase domain-like (MLKL) interaction in necroptotic signaling. *Journal of Biological Chemistry*, *288*(23), 16247–16261. https://doi.org/10.1074/jbc.M112.435545

Chen, X.-Y., Dai, Y.-H., Wan, X.-X., Hu, X.-M., Zhao, W.-J., Ban, X.-X., Wan, H., Huang, K., Zhang, Q., & Xiong, K. (2022). ZBP1-Mediated Necroptosis: Mechanisms and Therapeutic Implications. *Molecules (Basel, Switzerland)*, *28*(1). https://doi.org/10.3390/molecules28010052

Chen, X., Li, W., Ren, J., Huang, D., He, W.-T., Song, Y., Yang, C., Li, W., Zheng, X., Chen, P., & Han, J. (2014). Translocation of mixed lineage kinase domain-like protein to plasma membrane leads to necrotic cell death. *Cell Research*, *24*(1), 105–121. https://doi.org/10.1038/cr.2013.171

Cho, Y. S., Challa, S., Moquin, D., Genga, R., Ray, T. D., Guildford, M., & Chan, F. K.-M. (2009a). Phosphorylation-driven assembly of the RIP1-RIP3 complex regulates programmed necrosis and virus-induced inflammation. *Cell*, *137*(6), 1112–1123. https://doi.org/10.1016/j.cell.2009.05.037

Cho, Y. S., Challa, S., Moquin, D., Genga, R., Ray, T. D., Guildford, M., & Chan, F. K. M.

(2009b). Phosphorylation-Driven Assembly of the RIP1-RIP3 Complex Regulates Programmed Necrosis and Virus-Induced Inflammation. *Cell*, *137*(6), 1112–1123. https://doi.org/10.1016/j.cell.2009.05.037

Cho, Y. S., Challa, S., Moquin, D., Genga, R., Ray, T. D., Guildford, M., & Chan, F. K. M. (2009c). Phosphorylation-Driven Assembly of the RIP1-RIP3 Complex Regulates Programmed Necrosis and Virus-Induced Inflammation. *Cell*, *137*(6), 1112–1123. https://doi.org/10.1016/j.cell.2009.05.037

Conev, N. V, Dimitrova, E. G., Bogdanova, M. K., Kashlov, Y. K., Chaushev, B. G., Radanova, M. A., Petrov, D. P., Georgiev, K. D., Bachvarov, C. H., Todorov, G. N., Kalchev, K. P., Popov, H. B., Manev, R. R., & Donev, I. S. (2019). RIPK3 expression as a potential predictive and prognostic marker in metastatic colon cancer. *Clinical and Investigative Medicine. Medecine Clinique et Experimentale*, *42*(1), E31–E38. https://doi.org/10.25011/cim.v42i1.32390

Cornillon, S., Foa, C., Davoust, J., Buonavista, N., Gross, J. D., & Golstein, P. (1994). Programmed cell death in Dictyostelium. *Journal of Cell Science*, *107 (Pt 1*, 2691–2704. https://doi.org/10.1242/jcs.107.10.2691

Crutchfield, E. C. T., Garnish, S. E., & Hildebrand, J. M. (2021). The role of the key effector of necroptotic cell death, mlkl, in mouse models of disease. *Biomolecules*, *11*(6), 1–22. https://doi.org/10.3390/biom11060803

Cui, B., Yan, B., Wang, K., Li, L., Chen, S., & Zhang, Z. (2022). Discovery of a New Class of Uracil Derivatives as Potential Mixed Lineage Kinase Domain-like Protein (MLKL) Inhibitors. *Journal of Medicinal Chemistry*, *65*(19), 12747–12780. https://doi.org/10.1021/acs.jmedchem.2c00548

Cui, J. J., Tran-Dubé, M., Shen, H., Nambu, M., Kung, P.-P., Pairish, M., Jia, L., Meng, J., Funk, L., Botrous, I., McTigue, M., Grodsky, N., Ryan, K., Padrique, E., Alton, G., Timofeevski, S., Yamazaki, S., Li, Q., Zou, H., … Edwards, M. P. (2011). Structure based drug design of crizotinib (PF-02341066), a potent and selective dual inhibitor of mesenchymal-epithelial transition factor (c-MET) kinase and anaplastic lymphoma kinase (ALK). *Journal of Medicinal Chemistry*, *54*(18), 6342–6363. https://doi.org/10.1021/jm2007613

Cui, J., Zhao, S., Li, Y., Zhang, D., Wang, B., Xie, J., & Wang, J. (2021). Regulated cell death:

discovery, features and implications for neurodegenerative diseases. *Cell Communication and Signaling : CCS*, *19*(1), 120. https://doi.org/10.1186/s12964-021-00799-8

D'Cruz, A. A., Speir, M., Bliss-Moreau, M., Dietrich, S., Wang, S., Chen, A. A., Gavillet, M., Al-Obeidi, A., Lawlor, K. E., Vince, J. E., Kelliher, M. A., Hakem, R., Pasparakis, M., Williams, D. A., Ericsson, M., & Croker, B. A. (2018). The pseudokinase MLKL activates PAD4-dependent NET formation in necroptotic neutrophils. *Science Signaling*, *11*(546). https://doi.org/10.1126/scisignal.aao1716

Dar, A. C., & Shokat, K. M. (2011). The evolution of protein kinase inhibitors from antagonists to agonists of cellular signaling. *Annual Review of Biochemistry*, *80*, 769–795. https://doi.org/10.1146/annurev-biochem-090308-173656

Dara, L., Liu, Z. X., & Kaplowitz, N. (2016a). A murder mystery in the liver: Who done it and how? *Journal of Clinical Investigation*, *126*(11), 4068–4071. https://doi.org/10.1172/JCI90830

Dara, L., Liu, Z. X., & Kaplowitz, N. (2016b). Questions and controversies: the role of necroptosis in liver disease. *Cell Death Discovery*, *2*(1), 1–10. https://doi.org/10.1038/cddiscovery.2016.89

Daskalov, A., Habenstein, B., Sabaté, R., Berbon, M., Martinez, D., Chaignepain, S., Coulary-Salin, B., Hofmann, K., Loquet, A., & Saupe, S. J. (2016). Identification of a novel cell death-inducing domain reveals that fungal amyloid-controlled programmed cell death is related to necroptosis. *Proceedings of the National Academy of Sciences of the United States of America*, *113*(10), 2720–2725. https://doi.org/10.1073/pnas.1522361113

Davies, K. A., Fitzgibbon, C., Young, S. N., Garnish, S. E., Yeung, W., Coursier, D., Birkinshaw, R. W., Sandow, J. J., Lehmann, W. I. L., Liang, L.-Y., Lucet, I. S., Chalmers, J. D., Patrick, W. M., Kannan, N., Petrie, E. J., Czabotar, P. E., & Murphy, J. M. (2020). Distinct pseudokinase domain conformations underlie divergent activation mechanisms among vertebrate MLKL orthologues. *Nature Communications*, *11*(1), 3060. https://doi.org/10.1038/s41467-020-16823-3

Davies, K. A., Tanzer, M. C., Griffin, M. D. W., Mok, Y. F., Young, S. N., Qin, R., Petrie, E. J., Czabotar, P. E., Silke, J., & Murphy, J. M. (2018). The brace helices of MLKL mediate interdomain communication and oligomerisation to regulate cell death by necroptosis. *Cell Death and Differentiation*, *25*(9), 1567–1580. https://doi.org/10.1038/s41418-018-

0061-3

de Almagro, M. C., & Vucic, D. (2015). Necroptosis: Pathway diversity and characteristics. *Seminars in Cell & Developmental Biology*, *39*, 56–62. https://doi.org/10.1016/j.semcdb.2015.02.002

Declercq, W., Vanden Berghe, T., & Vandenabeele, P. (2009). RIP Kinases at the Crossroads of Cell Death and Survival. *Cell*, *138*(2), 229–232. https://doi.org/10.1016/j.cell.2009.07.006

Degterev, A., Huang, Z., Boyce, M., Li, Y., Jagtap, P., Mizushima, N., Cuny, G. D., Mitchison, T. J., Moskowitz, M. A., & Yuan, J. (2013). Erratum: Chemical inhibitor of nonapoptotic cell death with therapeutic potential for ischemic brain injury (Nature Chemical Biology (2005) 1 (112-119)). *Nature Chemical Biology*, *9*(3), 192. https://doi.org/10.1038/nchembio0313-192a

Doerflinger, M., Deng, Y., Whitney, P., Salvamoser, R., Engel, S., Kueh, A. J., Tai, L., Bachem, A., Gressier, E., Geoghegan, N. D., Wilcox, S., Rogers, K. L., Garnham, A. L., Dengler, M. A., Bader, S. M., Ebert, G., Pearson, J. S., De Nardo, D., Wang, N., … Herold, M. J. (2020). Flexible Usage and Interconnectivity of Diverse Cell Death Pathways Protect against Intracellular Infection. *Immunity*, *53*(3), 533-547.e7. https://doi.org/10.1016/j.immuni.2020.07.004

Dondelinger, Y., Declercq, W., Montessuit, S., Roelandt, R., Goncalves, A., Bruggeman, I., Hulpiau, P., Weber, K., Sehon, C. A., Marquis, R. W., Bertin, J., Gough, P. J., Savvides, S., Martinou, J.-C., Bertrand, M. J. M., & Vandenabeele, P. (2014). MLKL compromises plasma membrane integrity by binding to phosphatidylinositol phosphates. *Cell Reports*, *7*(4), 971–981. https://doi.org/10.1016/j.celrep.2014.04.026

Dondelinger, Y., Hulpiau, P., Saeys, Y., Bertrand, M. J. M., & Vandenabeele, P. (2016). An evolutionary perspective on the necroptotic pathway. *Trends in Cell Biology*, *26*(10), 721–732. https://doi.org/10.1016/j.tcb.2016.06.004

Duprez, L., Takahashi, N., Van Hauwermeiren, F., Vandendriessche, B., Goossens, V., Vanden Berghe, T., Declercq, W., Libert, C., Cauwels, A., & Vandenabeele, P. (2011). RIP Kinase-Dependent Necrosis Drives Lethal Systemic Inflammatory Response Syndrome. *Immunity*, *35*(6), 908–918. https://doi.org/10.1016/j.immuni.2011.09.020

Ertao, Z., Jianhui, C., Kang, W., Zhijun, Y., Hui, W., Chuangqi, C., Changjiang, Q., Sile, C.,

Yulong, H., & Shirong, C. (2016). Prognostic value of mixed lineage kinase domain-like protein expression in the survival of patients with gastric caner. *Tumour Biology : The Journal of the International Society for Oncodevelopmental Biology and Medicine*, *37*(10), 13679–13685. https://doi.org/10.1007/s13277-016-5229-1

Faergeman, S. L., Evans, H., Attfield, K. E., Desel, C., Kuttikkatte, S. B., Sommerlund, M., Jensen, L. T., Frokiaer, J., Friese, M. A., Matthews, P. M., Luchtenborg, C., Brügger, B., Oturai, A. B., Dendrou, C. A., & Fugger, L. (2020). A novel neurodegenerative spectrum disorder in patients with MLKL deficiency. *Cell Death and Disease*, *11*(5). https://doi.org/10.1038/s41419-020-2494-0

Feoktistova, M., Geserick, P., Kellert, B., Dimitrova, D. P., Langlais, C., Hupe, M., Cain, K., MacFarlane, M., Häcker, G., & Leverkus, M. (2011). cIAPs block Ripoptosome formation, a RIP1/caspase-8 containing intracellular cell death complex differentially regulated by cFLIP isoforms. *Molecular Cell*, *43*(3), 449–463. https://doi.org/10.1016/j.molcel.2011.06.011

Flores-Romero, H., Ros, U., & Garcia-Saez, A. J. (2020). Pore formation in regulated cell death. *The EMBO Journal*, *39*(23), e105753. https://doi.org/10.15252/embj.2020105753

Galluzzi, L., Bravo-San Pedro, J. M., Vitale, I., Aaronson, S. A., Abrams, J. M., Adam, D., Alnemri, E. S., Altucci, L., Andrews, D., Annicchiarico-Petruzzelli, M., Baehrecke, E. H., Bazan, N. G., Bertrand, M. J., Bianchi, K., Blagosklonny, M. V, Blomgren, K., Borner, C., Bredesen, D. E., Brenner, C., … Kroemer, G. (2015). Essential versus accessory aspects of cell death: recommendations of the NCCD 2015. *Cell Death and Differentiation*, *22*(1), 58–73. https://doi.org/10.1038/cdd.2014.137

Galluzzi, L., Kepp, O., & Kroemer, G. (2014). MLKL regulates necrotic plasma membrane permeabilization. *Cell Research*, *24*(2), 139–140. https://doi.org/10.1038/cr.2014.8

Galluzzi, L., López-Soto, A., Kumar, S., & Kroemer, G. (2016). Caspases Connect Cell-Death Signaling to Organismal Homeostasis. *Immunity*, *44*(2), 221–231. https://doi.org/10.1016/j.immuni.2016.01.020

Galluzzi, L., Vitale, I., Aaronson, S. A., Abrams, J. M., Adam, D., Agostinis, P., Alnemri, E. S., Altucci, L., Amelio, I., Andrews, D. W., Annicchiarico-Petruzzelli, M., Antonov, A. V., Arama, E., Baehrecke, E. H., Barlev, N. A., Bazan, N. G., Bernassola, F., Bertrand, M. J. M., Bianchi, K., … Kroemer, G. (2018). Molecular mechanisms of cell death:

Recommendations of the Nomenclature Committee on Cell Death 2018. *Cell Death and Differentiation*, *25*(3), 486–541. https://doi.org/10.1038/s41418-017-0012-4

Garcia, L. R., Tenev, T., Newman, R., Haich, R. O., Liccardi, G., John, S. W., Annibaldi, A., Yu, L., Pardo, M., Young, S. N., Fitzgibbon, C., Fernando, W., Guppy, N., Kim, H., Liang, L.-Y., Lucet, I. S., Kueh, A., Roxanis, I., Gazinska, P., … Meier, P. (2021). Ubiquitylation of MLKL at lysine 219 positively regulates necroptosis-induced tissue injury and pathogen clearance. *Nature Communications*, *12*(1), 3364. https://doi.org/10.1038/s41467-021-23474-5

Gardner, C. R., Davies, K. A., Zhang, Y., Brzozowski, M., Czabotar, P. E., Murphy, J. M., & Lessene, G. (2022). From (Tool)Bench to Bedside: The Potential of Necroptosis Inhibitors. *Journal of Medicinal Chemistry*. https://doi.org/10.1021/acs.jmedchem.2c01621

Geserick, P., Hupe, M., Moulin, M., Wong, W. W.-L., Feoktistova, M., Kellert, B., Gollnick, H., Silke, J., & Leverkus, M. (2009). Cellular IAPs inhibit a cryptic CD95-induced cell death by limiting RIP1 kinase recruitment. *The Journal of Cell Biology*, *187*(7), 1037–1054. https://doi.org/10.1083/jcb.200904158

Gong, Y.-N., Crawford, J. C., Heckmann, B. L., & Green, D. R. (2019). To the edge of cell death and back. *The FEBS Journal*, *286*(3), 430–440. https://doi.org/10.1111/febs.14714

Gong, Y., Fan, Z., Luo, G., Yang, C., Huang, Q., Fan, K., Cheng, H., Jin, K., Ni, Q., Yu, X., & Liu, C. (2019). The role of necroptosis in cancer biology and therapy. *Molecular Cancer*, *18*(1), 100. https://doi.org/10.1186/s12943-019-1029-8

González-Juarbe, N., Gilley, R. P., Hinojosa, C. A., Bradley, K. M., Kamei, A., Gao, G., Dube, P. H., Bergman, M. A., & Orihuela, C. J. (2015). Pore-Forming Toxins Induce Macrophage Necroptosis during Acute Bacterial Pneumonia. *PLoS Pathogens*, *11*(12), e1005337. https://doi.org/10.1371/journal.ppat.1005337

Gonzalez-Juarbe, N., Riegler, A. N., Jureka, A. S., Gilley, R. P., Brand, J. D., Trombley, J. E., Scott, N. R., Platt, M. P., Dube, P. H., Petit, C. M., Harrod, K. S., & Orihuela, C. J. (2020). Influenza-Induced Oxidative Stress Sensitizes Lung Cells to Bacterial-Toxin-Mediated Necroptosis. *Cell Reports*, *32*(8), 108062. https://doi.org/10.1016/j.celrep.2020.108062

Green, D. R., & Fitzgerald, P. (2016). Just So Stories about the Evolution of Apoptosis. *Current Biology : CB*, *26*(13), R620–R627. https://doi.org/10.1016/j.cub.2016.05.023

Günther, C., He, G.-W., Kremer, A. E., Murphy, J. M., Petrie, E. J., Amann, K., Vandenabeele, P., Linkermann, A., Poremba, C., Schleicher, U., Dewitz, C., Krautwald, S., Neurath, M. F., Becker, C., & Wirtz, S. (2016). The pseudokinase MLKL mediates programmed hepatocellular necrosis independently of RIPK3 during hepatitis. *The Journal of Clinical Investigation*, *126*(11), 4346–4360. https://doi.org/10.1172/JCI87545

Hanks, S. K., Quinn, A. M., & Hunter, T. (1988). The protein kinase family: conserved features and deduced phylogeny of the catalytic domains. *Science (New York, N.Y.)*, *241*(4861), 42–52. https://doi.org/10.1126/science.3291115

Harris, P. A., Berger, S. B., Jeong, J. U., Nagilla, R., Bandyopadhyay, D., Campobasso, N., Capriotti, C. A., Cox, J. A., Dare, L., Dong, X., Eidam, P. M., Finger, J. N., Hoffman, S. J., Kang, J., Kasparcova, V., King, B. W., Lehr, R., Lan, Y., Leister, L. K., … Bertin, J. (2017). Discovery of a First-in-Class Receptor Interacting Protein 1 (RIP1) Kinase Specific Clinical Candidate (GSK2982772) for the Treatment of Inflammatory Diseases. *Journal of Medicinal Chemistry*, *60*(4), 1247–1261. https://doi.org/10.1021/acs.jmedchem.6b01751

He, L., Peng, K., Liu, Y., Xiong, J., & Zhu, F.-F. (2013). Low expression of mixed lineage kinase domain-like protein is associated with poor prognosis in ovarian cancer patients. *OncoTargets and Therapy*, *6*, 1539–1543. https://doi.org/10.2147/OTT.S52805

He, S., Liang, Y., Shao, F., & Wang, X. (2011). Toll-like receptors activate programmed necrosis in macrophages through a receptor-interacting kinase-3-mediated pathway. *Proceedings of the National Academy of Sciences of the United States of America*, *108*(50), 20054–20059. https://doi.org/10.1073/pnas.1116302108

He, S., Wang, L., Miao, L., Wang, T., Du, F., Zhao, L., & Wang, X. (2009). Receptor interacting protein kinase-3 determines cellular necrotic response to TNF-alpha. *Cell*, *137*(6), 1100–1111. https://doi.org/10.1016/j.cell.2009.05.021

He, S., & Wang, X. (2018). RIP kinases as modulators of inflammation and immunity. *Nature Immunology*, *19*(9), 912–922. https://doi.org/10.1038/s41590-018-0188-x

Hildebrand, J. M., Lo, B., Tomei, S., Mattei, V., Young, S. N., Fitzgibbon, C., Murphy, J. M., & Fadda, A. (2021). A family harboring an MLKL loss of function variant implicates impaired necroptosis in diabetes. *Cell Death and Disease*, *12*(4). https://doi.org/10.1038/s41419-021-03636-5

Hildebrand, J. M., Tanzer, M. C., Lucet, I. S., Young, S. N., Spall, S. K., Sharma, P., Pierotti, C., Garnier, J. M., Dobson, R. C. J., Webb, A. I., Tripaydonis, A., Babon, J. J., Mulcair, M. D., Scanlon, M. J., Alexander, W. S., Wilks, A. F., Czabotar, P. E., Lessene, G., Murphy, J. M., & Silke, J. (2014). Activation of the pseudokinase MLKL unleashes the four-helix bundle domain to induce membrane localization and necroptotic cell death. *Proceedings of the National Academy of Sciences of the United States of America*, *111*(42), 15072–15077. https://doi.org/10.1073/pnas.1408987111

Huang, D., Zheng, X., Wang, Z., Chen, X., He, W., Zhang, Y., Xu, J.-G., Zhao, H., Shi, W., Wang, X., Zhu, Y., & Han, J. (2017). The MLKL Channel in Necroptosis Is an Octamer Formed by Tetramers in a Dyadic Process. *Molecular and Cellular Biology*, *37*(5), e00497-16. https://doi.org/10.1128/MCB.00497-16

Iannielli, A., Bido, S., Folladori, L., Segnali, A., Cancellieri, C., Maresca, A., Massimino, L., Rubio, A., Morabito, G., Caporali, L., Tagliavini, F., Musumeci, O., Gregato, G., Bezard, E., Carelli, V., Tiranti, V., & Broccoli, V. (2018). Pharmacological Inhibition of Necroptosis Protects from Dopaminergic Neuronal Cell Death in Parkinson's Disease Models. *Cell Reports*, *22*(8), 2066–2079. https://doi.org/https://doi.org/10.1016/j.celrep.2018.01.089

Jacobsen, A. V., Pierotti, C. L., Lowes, K. N., Au, A. E., Zhang, Y., Etemadi, N., Fitzgibbon, C., Kersten, W. J. A., Samson, A. L., van Delft, M. F., Huang, D. C. S., Sabroux, H. J., Lessene, G., Silke, J., & Murphy, J. M. (2022). The Lck inhibitor, AMG-47a, blocks necroptosis and implicates RIPK1 in signalling downstream of MLKL. *Cell Death and Disease*, *13*(4), 1–13. https://doi.org/10.1038/s41419-022-04740-w

Jorgensen, I., Rayamajhi, M., & Miao, E. A. (2017). Programmed cell death as a defence against infection. *Nature Reviews. Immunology*, *17*(3), 151–164. https://doi.org/10.1038/nri.2016.147

Ju, E., Park, K. A., Shen, H. M., & Hur, G. M. (2022). The resurrection of RIP kinase 1 as an early cell death checkpoint regulator—a potential target for therapy in the necroptosis era. *Experimental and Molecular Medicine*, *54*(9), 1401–1411. https://doi.org/10.1038/s12276-022-00847-4

Jubic, L. M., Saile, S., Furzer, O. J., El Kasmi, F., & Dangl, J. L. (2019). Help wanted: helper NLRs and plant immune responses. *Current Opinion in Plant Biology*, *50*, 82–94. https://doi.org/10.1016/j.pbi.2019.03.013

Kaiser, W. J., Sridharan, H., Huang, C., Mandal, P., Upton, J. W., Gough, P. J., Sehon, C. A., Marquis, R. W., Bertin, J., & Mocarski, E. S. (2013). Toll-like receptor 3-mediated necrosis via TRIF, RIP3, and MLKL. *The Journal of Biological Chemistry*, *288*(43), 31268–31279. https://doi.org/10.1074/jbc.M113.462341

Kamal, A. M., Sebak, S. A., & Sanad, E. F. (2021). Mixed Lineage Kinase Domain-Like Pseudokinase (MLKL) Gene Expression in Human Atherosclerosis with and without Type 2 Diabetes Mellitus. *Iranian Biomedical Journal*, *25*(4), 265–274. https://doi.org/10.52547/ibj.25.4.265

Karunakaran, D., Geoffrion, M., Wei, L., Gan, W., Richards, L., Shangari, P., DeKemp, E. M., Beanlands, R. A., Perisic, L., Maegdefessel, L., Hedin, U., Sad, S., Guo, L., Kolodgie, F. D., Virmani, R., Ruddy, T., & Rayner, K. J. (2016). Targeting macrophage necroptosis for therapeutic and diagnostic interventions in atherosclerosis. *Science Advances*, *2*(7). https://doi.org/10.1126/sciadv.1600224

Kearney, C. J., Cullen, S. P., Clancy, D., & Martin, S. J. (2014). RIPK1 can function as an inhibitor rather than an initiator of RIPK3-dependent necroptosis. *The FEBS Journal*, *281*(21), 4921–4934. https://doi.org/10.1111/febs.13034

Kircheis, R., & Planz, O. (2023). The Role of Toll-like Receptors (TLRs) and Their Related Signaling Pathways in Viral Infection and Inflammation. In *International journal of molecular sciences* (Vol. 24, Issue 7). https://doi.org/10.3390/ijms24076701

Kitur, K., Wachtel, S., Brown, A., Wickersham, M., Paulino, F., Peñaloza, H. F., Soong, G., Bueno, S., Parker, D., & Prince, A. (2016). Necroptosis Promotes Staphylococcus aureus Clearance by Inhibiting Excessive Inflammatory Signaling. *Cell Reports*, *16*(8), 2219–2230. https://doi.org/10.1016/j.celrep.2016.07.039

Lee, J.-M., Yoshida, M., Kim, M.-S., Lee, J.-H., Baek, A.-R., Jang, A. S., Kim, D. J., Minagawa, S., Chin, S. S., Park, C.-S., Kuwano, K., Park, S. W., & Araya, J. (2018). Involvement of Alveolar Epithelial Cell Necroptosis in Idiopathic Pulmonary Fibrosis Pathogenesis. *American Journal of Respiratory Cell and Molecular Biology*, *59*(2), 215–224. https://doi.org/10.1165/rcmb.2017-0034OC

Li, X., Dong, G., Xiong, H., & Diao, H. (2021). A narrative review of the role of necroptosis in liver disease: a double-edged sword. *Annals of Translational Medicine*, *9*(5), 422–422. https://doi.org/10.21037/atm-20-5162

Li, Z., Hao, Y., Yang, C., Yang, Q., Wu, S., Ma, H., Tian, S., Lu, H., Wang, J., Yang, T., He, S., & Zhang, X. (2022). Design, synthesis, and evaluation of potent RIPK1 inhibitors with in vivo anti-inflammatory activity. *European Journal of Medicinal Chemistry*, *228*, 114036. https://doi.org/https://doi.org/10.1016/j.ejmech.2021.114036

Liao, D., Sun, L., Liu, W., He, S., Wang, X., & Lei, X. (2014). Necrosulfonamide inhibits necroptosis by selectively targeting the mixed lineage kinase domain-like protein. *MedChemComm*, *5*(3), 333–337. https://doi.org/10.1039/c3md00278k

Liccardi, G., & Annibaldi, A. (2023). MLKL post-translational modifications: road signs to infection, inflammation and unknown destinations. *Cell Death and Differentiation*, *30*(2), 269–278. https://doi.org/10.1038/s41418-022-01061-5

Lin, Q.-S., Chen, P., Wang, W.-X., Lin, C.-C., Zhou, Y., Yu, L.-H., Lin, Y.-X., Xu, Y.-F., & Kang, D.-Z. (2020). RIP1/RIP3/MLKL mediates dopaminergic neuron necroptosis in a mouse model of Parkinson disease. *Laboratory Investigation; a Journal of Technical Methods and Pathology*, *100*(3), 503–511. https://doi.org/10.1038/s41374-019-0319-5

Liu, S., Liu, H., Johnston, A., Hanna-Addams, S., Reynoso, E., Xiang, Y., & Wang, Z. (2017). MLKL forms disulfide bond-dependent amyloid-like polymers to induce necroptosis. *Proceedings of the National Academy of Sciences of the United States of America*, *114*(36), E7450–E7459. https://doi.org/10.1073/pnas.1707531114

Liu, X., Xie, X., Ren, Y., Shao, Z., Zhang, N., Li, L., Ding, X., & Zhang, L. (2021). The role of necroptosis in disease and treatment. *MedComm*, *2*(4), 730–755. https://doi.org/10.1002/mco2.108

Liu, Z., Dagley, L. F., Shield-Artin, K., Young, S. N., Bankovacki, A., Wang, X., Tang, M., Howitt, J., Stafford, C. A., Nachbur, U., Fitzgibbon, C., Garnish, S. E., Webb, A. I., Komander, D., Murphy, J. M., Hildebrand, J. M., & Silke, J. (2021). Oligomerization-driven MLKL ubiquitylation antagonizes necroptosis. *The EMBO Journal*, *40*(23), e103718. https://doi.org/https://doi.org/10.15252/embj.2019103718

Lu, Z., Van Eeckhoutte, H. P., Liu, G., Nair, P. M., Jones, B., Gillis, C. M., Nalkurthi, B. C., Verhamme, F., Buyle-Huybrecht, T., Vandenabeele, P., Vanden Berghe, T., Brusselle, G. G., Horvat, J. C., Murphy, J. M., Wark, P. A., Bracke, K. R., Fricker, M., & Hansbro, P. M. (2021). Necroptosis Signaling Promotes Inflammation, Airway Remodeling, and Emphysema in Chronic Obstructive Pulmonary Disease. *American Journal of Respiratory*

and Critical Care Medicine, *204*(6), 667–681. https://doi.org/10.1164/rccm.202009-3442OC

Luedde, T., Kaplowitz, N., & Schwabe, R. F. (2014). Cell death and cell death responses in liver disease: mechanisms and clinical relevance. *Gastroenterology*, *147*(4), 765-783.e4. https://doi.org/10.1053/j.gastro.2014.07.018

Ma, B., Marcotte, D., Paramasivam, M., Michelsen, K., Wang, T., Bertolotti-Ciarlet, A., Jones, J. H., Moree, B., Butko, M., Salafsky, J., Sun, X., McKee, T., & Silvian, L. F. (2016). ATP-Competitive MLKL Binders Have No Functional Impact on Necroptosis. *PLoS ONE*, *11*(11), 1–19. https://doi.org/10.1371/journal.pone.0165983

Madeo, F., Fröhlich, E., & Fröhlich, K. U. (1997). A yeast mutant showing diagnostic markers of early and late apoptosis. *The Journal of Cell Biology*, *139*(3), 729–734. https://doi.org/10.1083/jcb.139.3.729

Maelfait, J., Liverpool, L., Bridgeman, A., Ragan, K. B., Upton, J. W., & Rehwinkel, J. (2017). Sensing of viral and endogenous RNA by ZBP1/DAI induces necroptosis. *The EMBO Journal*, *36*(17), 2529–2543. https://doi.org/10.15252/embj.201796476

Mahdi, A. L., Huang, M., Zhang, X., Nakano, T., Kopp, L. B., Saur, I. M. L., Jacob, F., Kovacova, V., Lapin, D., Parker, J. E., & Murphy, J. M. (2019). *Title : Plant mixed lineage kinase domain-like proteins limit biotrophic pathogen growth One Sentence Summary : Plants have a protein family that is structurally homologous to vertebrate mixed lineage kinase domain- like protein , which induces necroptoti*.

Majdi, A., Aoudjehane, L., Ratziu, V., Islam, T., Afonso, M. B., Conti, F., Mestiri, T., Lagouge, M., Foufelle, F., Ballenghien, F., Ledent, T., Moldes, M., Cadoret, A., Fouassier, L., Delaunay, J.-L., Aït-Slimane, T., Courtois, G., Fève, B., Scatton, O., … Gautheron, J. (2020). Inhibition of receptor-interacting protein kinase 1 improves experimental non-alcoholic fatty liver disease. *Journal of Hepatology*, *72*(4), 627–635. https://doi.org/10.1016/j.jhep.2019.11.008

Martens, S., Bridelance, J., Roelandt, R., Vandenabeele, P., & Takahashi, N. (2021). MLKL in cancer: more than a necroptosis regulator. In *Cell Death and Differentiation* (Vol. 28, Issue 6, pp. 1757–1772). https://doi.org/10.1038/s41418-021-00785-0

Martens, S., Hofmans, S., Declercq, W., Augustyns, K., & Vandenabeele, P. (2020). Inhibitors Targeting RIPK1/RIPK3: Old and New Drugs. *Trends in Pharmacological Sciences*,

41(3), 209–224. https://doi.org/10.1016/j.tips.2020.01.002

Martinez-Osorio, V., Abdelwahab, Y., & Ros, U. (2023). The Many Faces of MLKL, the Executor of Necroptosis. *International Journal of Molecular Sciences*, *24*(12), 10108. https://doi.org/10.3390/ijms241210108

McCormick, K. D., Ghosh, A., Trivedi, S., Wang, L., Coyne, C. B., Ferris, R. L., & Sarkar, S. N. (2016). Innate immune signaling through differential RIPK1 expression promote tumor progression in head and neck squamous cell carcinoma. *Carcinogenesis*, *37*(5), 522–529. https://doi.org/10.1093/carcin/bgw032

Meng, Y., Garnish, S. E., Davies, K. A., Black, K. A., Leis, A. P., Horne, C. R., Hildebrand, J. M., Hoblos, H., Fitzgibbon, C., Young, S. N., Dite, T., Dagley, L. F., Venkat, A., Kannan, N., Koide, A., Koide, S., Glukhova, A., Czabotar, P. E., & Murphy, J. M. (2023). Phosphorylation-dependent pseudokinase domain dimerization drives full-length MLKL oligomerization. *Nature Communications*, *14*(1), 1–18. https://doi.org/10.1038/s41467-023-42255-w

Meng, Y., Horne, C. R., Samson, A. L., Dagley, L. F., Young, S. N., Sandow, J. J., Czabotar, P. E., & Murphy, J. M. (2022). Human RIPK3 C-lobe phosphorylation is essential for necroptotic signaling. *Cell Death & Disease*, *13*(6), 565. https://doi.org/10.1038/s41419-022-05009-y

Meng, Y., Sandow, J. J., Czabotar, P. E., & Murphy, J. M. (2021). The regulation of necroptosis by post-translational modifications. *Cell Death and Differentiation*, *28*(3), 861–883. https://doi.org/10.1038/s41418-020-00722-7

Miyata, T., Wu, X., Fan, X., Huang, E., Sanz-Garcia, C., Cajigas-Du Ross, C. K., Roychowdhury, S., Bellar, A., McMullen, M. R., Dasarathy, J., Allende, D. S., Caballeria, J., Sancho-Bru, P., McClain, C. J., Mitchell, M., McCullough, A. J., Radaeva, S., Barton, B., Szabo, G., … Nagy, L. E. (2021). Differential role of MLKL in alcohol-associated and non-alcohol-associated fatty liver diseases in mice and humans. *JCI Insight*, *6*(4). https://doi.org/10.1172/jci.insight.140180

Mocarski, E. S., Upton, J. W., & Kaiser, W. J. (2012). Viral infection and the evolution of caspase 8-regulated apoptotic and necrotic death pathways. *Nature Reviews Immunology*, *12*(2), 79–88. https://doi.org/10.1038/nri3131

Moerke, C., Bleibaum, F., Kunzendorf, U., & Krautwald, S. (2019). Combined Knockout of

RIPK3 and MLKL Reveals Unexpected Outcome in Tissue Injury and Inflammation. *Frontiers in Cell and Developmental Biology*, *7*, 19. https://doi.org/10.3389/fcell.2019.00019

Montico, B., Nigro, A., Casolaro, V., & Dal Col, J. (2018). Immunogenic Apoptosis as a Novel Tool for Anticancer Vaccine Development. *International Journal of Molecular Sciences*, *19*(2). https://doi.org/10.3390/ijms19020594

Muendlein, H. I., Connolly, W. M., Magri, Z., Jetton, D., Smirnova, I., Degterev, A., Balachandran, S., & Poltorak, A. (2022). ZBP1 promotes inflammatory responses downstream of TLR3/TLR4 via timely delivery of RIPK1 to TRIF. *Proceedings of the National Academy of Sciences of the United States of America*, *119*(24), e2113872119. https://doi.org/10.1073/pnas.2113872119

Murphy, J. M. (2020). The killer pseudokinase mixed lineage kinase domain-like protein (MLKL). *Cold Spring Harbor Perspectives in Biology*, *12*(8), 1–19. https://doi.org/10.1101/cshperspect.a036376

Murphy, J. M., Czabotar, P. E., Hildebrand, J. M., Lucet, I. S., Zhang, J. G., Alvarez-Diaz, S., Lewis, R., Lalaoui, N., Metcalf, D., Webb, A. I., Young, S. N., Varghese, L. N., Tannahill, G. M., Hatchell, E. C., Majewski, I. J., Okamoto, T., Dobson, R. C. J., Hilton, D. J., Babon, J. J., … Alexander, W. S. (2013). The pseudokinase MLKL mediates necroptosis via a molecular switch mechanism. *Immunity*, *39*(3), 443–453. https://doi.org/10.1016/j.immuni.2013.06.018

Murphy, J. M., Lucet, I. S., Hildebrand, J. M., Tanzer, M. C., Young, S. N., Sharma, P., Lessene, G., Alexander, W. S., Babon, J. J., Silke, J., & Czabotar, P. E. (2014). Insights into the evolution of divergent nucleotide-binding mechanisms among pseudokinases revealed by crystal structures of human and mouse MLKL. *Biochemical Journal*, *457*(3), 369–377. https://doi.org/10.1042/BJ20131270

Nagata, S., & Tanaka, M. (2017). Programmed cell death and the immune system. *Nature Reviews. Immunology*, *17*(5), 333–340. https://doi.org/10.1038/nri.2016.153

Newton, K. (2015). RIPK1 and RIPK3: Critical regulators of inflammation and cell death. *Trends in Cell Biology*, *25*(6), 347–353. https://doi.org/10.1016/j.tcb.2015.01.001

Newton, K., Dugger, D. L., Maltzman, A., Greve, J. M., Hedehus, M., Martin-Mcnulty, B., Carano, R. A. D., Cao, T. C., Van Bruggen, N., Bernstein, L., Lee, W. P., Wu, X., Devoss,

J., Zhang, J., Jeet, S., Peng, I., McKenzie, B. S., Roose-Girma, M., Caplazi, P., … Vucic, D. (2016). RIPK3 deficiency or catalytically inactive RIPK1 provides greater benefit than MLKL deficiency in mouse models of inflammation and tissue injury. *Cell Death and Differentiation*, *23*(9), 1565–1576. https://doi.org/10.1038/cdd.2016.46

Ni, H. M., Chao, X., Kaseff, J., Deng, F., Wang, S., Shi, Y. H., Li, T., Ding, W. X., & Jaeschke, H. (2019). Receptor-Interacting Serine/Threonine-Protein Kinase 3 (RIPK3)–Mixed Lineage Kinase Domain-Like Protein (MLKL)–Mediated Necroptosis Contributes to Ischemia-Reperfusion Injury of Steatotic Livers. *American Journal of Pathology*, *189*(7), 1363–1374. https://doi.org/10.1016/j.ajpath.2019.03.010

Nugues, A.-L., El Bouazzati, H., Hétuin, D., Berthon, C., Loyens, A., Bertrand, E., Jouy, N., Idziorek, T., & Quesnel, B. (2014). RIP3 is downregulated in human myeloid leukemia cells and modulates apoptosis and caspase-mediated p65/RelA cleavage. *Cell Death & Disease*, *5*(8), e1384–e1384. https://doi.org/10.1038/cddis.2014.347

Obeid, M., Tesniere, A., Ghiringhelli, F., Fimia, G. M., Apetoh, L., Perfettini, J.-L., Castedo, M., Mignot, G., Panaretakis, T., Casares, N., Métivier, D., Larochette, N., van Endert, P., Ciccosanti, F., Piacentini, M., Zitvogel, L., & Kroemer, G. (2007). Calreticulin exposure dictates the immunogenicity of cancer cell death. *Nature Medicine*, *13*(1), 54–61. https://doi.org/10.1038/nm1523

Ofengeim, D., Ito, Y., Najafov, A., Zhang, Y., Shan, B., DeWitt, J. P., Ye, J., Zhang, X., Chang, A., Vakifahmetoglu-Norberg, H., Geng, J., Py, B., Zhou, W., Amin, P., Lima, J. B., Qi, C., Yu, Q., Trapp, B., & Yuan, J. (2015). Activation of necroptosis in multiple sclerosis. *Cell Reports*, *10*(11), 1836–1849. https://doi.org/10.1016/j.celrep.2015.02.051

Oh, J. H., Park, S., Hong, E., Choi, M. A., Kwon, Y. M., Park, J. W., Lee, A. H., Park, G. R., Kim, H. Y., Lee, S. M., Lee, J. Y., Bae, S. H., Lee, J. H., Lee, J. Y., & Jun, D. W. (2023). Novel Inhibitor of Mixed-Lineage Kinase Domain-Like Protein: The Antifibrotic Effects of a Necroptosis Antagonist. *ACS Pharmacology and Translational Science*. https://doi.org/10.1021/acsptsci.3c00131

Patton, T., Zhao, Z., Lim, X. Y., Eddy, E., Wang, H., Nelson, A. G., Ennis, B., Eckle, S. B. G., Souter, M. N. T., Pediongco, T. J., Koay, H.-F., Zhang, J.-G., Djajawi, T. M., Louis, C., Lalaoui, N., Jacquelot, N., Lew, A. M., Pellicci, D. G., McCluskey, J., … Corbett, A. J. (2023). RIPK3 controls MAIT cell accumulation during development but not during infection. *Cell Death & Disease*, *14*(2), 111. https://doi.org/10.1038/s41419-023-05619-

0

Petrie, E. J., Birkinshaw, R. W., Koide, A., Denbaum, E., Hildebrand, J. M., Garnish, S. E., Davies, K. A., Sandow, J. J., Samson, A. L., Gavin, X., Fitzgibbon, C., Young, S. N., Hennessy, P. J., Smith, P. P. C., Webb, A. I., Czabotar, P. E., Koide, S., & Murphy, J. M. (2020). Identification of MLKL membrane translocation as a checkpoint in necroptotic cell death using Monobodies. *Proceedings of the National Academy of Sciences of the United States of America*, *117*(15), 8468–8475. https://doi.org/10.1073/pnas.1919960117

Petrie, E. J., Czabotar, P. E., & Murphy, J. M. (2019). The Structural Basis of Necroptotic Cell Death Signaling. *Trends in Biochemical Sciences*, *44*(1), 53–63. https://doi.org/10.1016/j.tibs.2018.11.002

Petrie, E. J., Hildebrand, J. M., & Murphy, J. M. (2017a). Insane in the membrane: A structural perspective of MLKL function in necroptosis. *Immunology and Cell Biology*, *95*(2), 152–159. https://doi.org/10.1038/icb.2016.125

Petrie, E. J., Hildebrand, J. M., & Murphy, J. M. (2017b). Insane in the membrane: a structural perspective of MLKL function in necroptosis. *Immunology and Cell Biology*, *95*(2), 152–159. https://doi.org/10.1038/icb.2016.125

Petrie, E. J., Sandow, J. J., Jacobsen, A. V, Smith, B. J., Griffin, M. D. W., Lucet, I. S., Dai, W., Young, S. N., Tanzer, M. C., Wardak, A., Liang, L.-Y., Cowan, A. D., Hildebrand, J. M., Kersten, W. J. A., Lessene, G., Silke, J., Czabotar, P. E., Webb, A. I., & Murphy, J. M. (2018). Conformational switching of the pseudokinase domain promotes human MLKL tetramerization and cell death by necroptosis. *Nature Communications*, *9*(1), 2422. https://doi.org/10.1038/s41467-018-04714-7

Picon, C., Jayaraman, A., James, R., Beck, C., Gallego, P., Witte, M. E., van Horssen, J., Mazarakis, N. D., & Reynolds, R. (2021). Neuron-specific activation of necroptosis signaling in multiple sclerosis cortical grey matter. *Acta Neuropathologica*, *141*(4), 585–604. https://doi.org/10.1007/s00401-021-02274-7

Pierotti, C. L., Tanzer, M. C., Jacobsen, A. V., Hildebrand, J. M., Garnier, J. M., Sharma, P., Lucet, I. S., Cowan, A. D., Kersten, W. J. A., Luo, M. X., Liang, L. Y., Fitzgibbon, C., Garnish, S. E., Hempel, A., Nachbur, U., Huang, D. C. S., Czabotar, P. E., Silke, J., Van Delft, M. F., … Lessene, G. (2020). Potent Inhibition of Necroptosis by Simultaneously Targeting Multiple Effectors of the Pathway. *ACS Chemical Biology*, *15*(10), 2702–2713.

https://doi.org/10.1021/acschembio.0c00482

Quarato, G., Guy, C. S., Grace, C. R., Llambi, F., Nourse, A., Rodriguez, D. A., Wakefield, R., Frase, S., Moldoveanu, T., & Green, D. R. (2016). Sequential Engagement of Distinct MLKL Phosphatidylinositol-Binding Sites Executes Necroptosis. *Molecular Cell*, *61*(4), 589–601. https://doi.org/10.1016/j.molcel.2016.01.011

Rasheed, A., Robichaud, S., Nguyen, M. A., Geoffrion, M., Wyatt, H., Cottee, M. L., Dennison, T., Pietrangelo, A., Lee, R., Lagace, T. A., Ouimet, M., & Rayner, K. J. (2020). Loss of MLKL (Mixed Lineage Kinase Domain-Like Protein) Decreases Necrotic Core but Increases Macrophage Lipid Accumulation in Atherosclerosis. *Arteriosclerosis, Thrombosis, and Vascular Biology*, *May*, 1155–1167. https://doi.org/10.1161/ATVBAHA.119.313640

Rashidi, M., Simpson, D. S., Hempel, A., Frank, D., Petrie, E., Vince, A., Feltham, R., Murphy, J., Chatfield, S. M., Salvesen, G. S., Murphy, J. M., Wicks, I. P., & Vince, J. E. (2019). The Pyroptotic Cell Death Effector Gasdermin D Is Activated by Gout-Associated Uric Acid Crystals but Is Dispensable for Cell Death and IL-1β Release. *Journal of Immunology (Baltimore, Md. : 1950)*, *203*(3), 736–748. https://doi.org/10.4049/jimmunol.1900228

Rathje, O. H., Perryman, L., Payne, R. J., & Hamprecht, D. W. (2023a). PROTACs Targeting MLKL Protect Cells from Necroptosis. *Journal of Medicinal Chemistry*, *66*(16), 11216–11236. https://doi.org/10.1021/acs.jmedchem.3c00665

Rathje, O. H., Perryman, L., Payne, R. J., & Hamprecht, D. W. (2023b). PROTACs Targeting MLKL Protect Cells from Necroptosis. *Journal of Medicinal Chemistry*. https://doi.org/10.1021/acs.jmedchem.3c00665

Rathkey, J. K., Zhao, J., Liu, Z., Chen, Y., Yang, J., Kondolf, H. C., Benson, B. L., Chirieleison, S. M., Huang, A. Y., Dubyak, G. R., Xiao, T. S., Li, X., & Abbott, D. W. (2018). Chemical disruption of the pyroptotic pore-forming protein gasdermin D inhibits inflammatory cell death and sepsis. *Science Immunology*, *3*(26). https://doi.org/10.1126/sciimmunol.aat2738

Ren, Y., Su, Y., Sun, L., He, S., Meng, L., Liao, D., Liu, X., Ma, Y., Liu, C., Li, S., Ruan, H., Lei, X., Wang, X., & Zhang, Z. (2017). Discovery of a Highly Potent, Selective, and Metabolically Stable Inhibitor of Receptor-Interacting Protein 1 (RIP1) for the Treatment of Systemic Inflammatory Response Syndrome. *Journal of Medicinal Chemistry*, *60*(3), 972–986. https://doi.org/10.1021/acs.jmedchem.6b01196

Ruan, J., Mei, L., Zhu, Q., Shi, G., & Wang, H. (2015). Mixed lineage kinase domain-like protein is a prognostic biomarker for cervical squamous cell cancer. *International Journal of Clinical and Experimental Pathology*, *8*(11), 15035–15038.

Rübbelke, M., Fiegen, D., Bauer, M., Binder, F., Hamilton, J., King, J., Thamm, S., Nar, H., & Zeeb, M. (2020). Locking mixed-lineage kinase domain-like protein in its auto-inhibited state prevents necroptosis. *Proceedings of the National Academy of Sciences of the United States of America*, *117*(52), 33272–33281. https://doi.org/10.1073/PNAS.2017406117

Rübbelke, M., Hamilton, J., Binder, F., Bauer, M., King, J., Nar, H., & Zeeb, M. (2021a). Discovery and Structure-Based Optimization of Fragments Binding the Mixed Lineage Kinase Domain-like Protein Executioner Domain. *Journal of Medicinal Chemistry*, *64*(21), 15629–15638. https://doi.org/10.1021/acs.jmedchem.1c00686

Rübbelke, M., Hamilton, J., Binder, F., Bauer, M., King, J., Nar, H., & Zeeb, M. (2021b). Discovery and Structure-Based Optimization of Fragments Binding the Mixed Lineage Kinase Domain-like Protein Executioner Domain. *Journal of Medicinal Chemistry*, *64*(21), 15629–15638. https://doi.org/10.1021/acs.jmedchem.1c00686

Saeed, W. K., Jun, D. W., Jang, K., Oh, J. H., Chae, Y. J., Lee, J. S., Koh, D. H., & Kang, H. T. (2019). Decrease in fat de novo synthesis and chemokine ligand expression in non-alcoholic fatty liver disease caused by inhibition of mixed lineage kinase domain-like pseudokinase. *Journal of Gastroenterology and Hepatology*, *34*(12), 2206–2218. https://doi.org/10.1111/jgh.14740

Sammond, D. M., Nailor, K. E., Veal, J. M., Nolte, R. T., Wang, L., Knick, V. B., Rudolph, S. K., Truesdale, A. T., Nartey, E. N., Stafford, J. A., Kumar, R., & Cheung, M. (2005). Discovery of a novel and potent series of dianilinopyrimidineurea and urea isostere inhibitors of VEGFR2 tyrosine kinase. *Bioorganic & Medicinal Chemistry Letters*, *15*(15), 3519–3523. https://doi.org/https://doi.org/10.1016/j.bmcl.2005.05.096

Samson, A. L., Zhang, Y., Geoghegan, N. D., Gavin, X. J., Davies, K. A., Mlodzianoski, M. J., Whitehead, L. W., Frank, D., Garnish, S. E., Fitzgibbon, C., Hempel, A., Young, S. N., Jacobsen, A. V., Cawthorne, W., Petrie, E. J., Faux, M. C., Shield-Artin, K., Lalaoui, N., Hildebrand, J. M., … Murphy, J. M. (2020). MLKL trafficking and accumulation at the plasma membrane control the kinetics and threshold for necroptosis. In *Nature Communications* (Vol. 11, Issue 1). https://doi.org/10.1038/s41467-020-16887-1

Seifert, L., Werba, G., Tiwari, S., Giao Ly, N. N., Alothman, S., Alqunaibit, D., Avanzi, A., Barilla, R., Daley, D., Greco, S. H., Torres-Hernandez, A., Pergamo, M., Ochi, A., Zambirinis, C. P., Pansari, M., Rendon, M., Tippens, D., Hundeyin, M., Mani, V. R., … Miller, G. (2016). The necrosome promotes pancreatic oncogenesis via CXCL1 and Mincle-induced immune suppression. *Nature*, *532*(7598), 245–249. https://doi.org/10.1038/nature17403

Sender, R., & Milo, R. (2021). The distribution of cellular turnover in the human body. *Nature Medicine*, *27*(1), 45–48. https://doi.org/10.1038/s41591-020-01182-9

Seo, J., Nam, Y. W., Kim, S., Oh, D. B., & Song, J. (2021). Necroptosis molecular mechanisms: Recent findings regarding novel necroptosis regulators. *Experimental and Molecular Medicine*, *53*(6), 1007–1017. https://doi.org/10.1038/s12276-021-00634-7

Shi, C., Kim, T., Steiger, S., Mulay, S. R., Klinkhammer, B. M., Bäuerle, T., Melica, M. E., Romagnani, P., Möckel, D., Baues, M., Yang, L., Brouns, S. L. N., Heemskerk, J. W. M., Braun, A., Lammers, T., Boor, P., & Anders, H.-J. (2020). Crystal Clots as Therapeutic Target in Cholesterol Crystal Embolism. *Circulation Research*, *126*(8), e37–e52. https://doi.org/10.1161/CIRCRESAHA.119.315625

Stoll, G., Ma, Y., Yang, H., Kepp, O., Zitvogel, L., & Kroemer, G. (2017). Pro-necrotic molecules impact local immunosurveillance in human breast cancer. *OncoImmunology*, *6*(4), e1299302. https://doi.org/10.1080/2162402X.2017.1299302

Strilic, B., Yang, L., Albarrán-Juárez, J., Wachsmuth, L., Han, K., Müller, U. C., Pasparakis, M., & Offermanns, S. (2016). Tumour-cell-induced endothelial cell necroptosis via death receptor 6 promotes metastasis. *Nature*, *536*(7615), 215–218. https://doi.org/10.1038/nature19076

Su, L., Quade, B., Wang, H., Sun, L., Wang, X., & Rizo, J. (2014). A plug release mechanism for membrane permeation by MLKL. *Structure (London, England : 1993)*, *22*(10), 1489–1500. https://doi.org/10.1016/j.str.2014.07.014

Sun, L., Wang, H., Wang, Z., He, S., Chen, S., Liao, D., Wang, L., Yan, J., Liu, W., Lei, X., & Wang, X. (2012). Mixed lineage kinase domain-like protein mediates necrosis signaling downstream of RIP3 kinase. *Cell*, *148*(1–2), 213–227. https://doi.org/10.1016/j.cell.2011.11.031

Tanzer, M. C., Matti, I., Hildebrand, J. M., Young, S. N., Wardak, A., Tripaydonis, A., Petrie,

E. J., Mildenhall, A. L., Vaux, D. L., Vince, J. E., Czabotar, P. E., Silke, J., & Murphy, J. M. (2016). Evolutionary divergence of the necroptosis effector MLKL. *Cell Death & Differentiation*, *23*(7), 1185–1197. https://doi.org/10.1038/cdd.2015.169

Tanzer, M. C., Tripaydonis, A., Webb, A. I., Young, S. N., Varghese, L. N., Hall, C., Alexander, W. S., Hildebrand, J. M., Silke, J., & Murphy, J. M. (2015). Necroptosis signalling is tuned by phosphorylation of MLKL residues outside the pseudokinase domain activation loop. *The Biochemical Journal*, *471*(2), 255–265. https://doi.org/10.1042/BJ20150678

Taraborrelli, L., Peltzer, N., Montinaro, A., Kupka, S., Rieser, E., Hartwig, T., Sarr, A., Darding, M., Draber, P., Haas, T. L., Akarca, A., Marafioti, T., Pasparakis, M., Bertin, J., Gough, P. J., Bouillet, P., Strasser, A., Leverkus, M., Silke, J., & Walczak, H. (2018). LUBAC prevents lethal dermatitis by inhibiting cell death induced by TNF, TRAIL and CD95L. *Nature Communications*, *9*(1), 3910. https://doi.org/10.1038/s41467-018-06155-8

Taylor, R. C., Cullen, S. P., & Martin, S. J. (2008). Apoptosis: controlled demolition at the cellular level. *Nature Reviews. Molecular Cell Biology*, *9*(3), 231–241. https://doi.org/10.1038/nrm2312

Tenev, T., Bianchi, K., Darding, M., Broemer, M., Langlais, C., Wallberg, F., Zachariou, A., Lopez, J., MacFarlane, M., Cain, K., & Meier, P. (2011). The Ripoptosome, a signaling platform that assembles in response to genotoxic stress and loss of IAPs. *Molecular Cell*, *43*(3), 432–448. https://doi.org/10.1016/j.molcel.2011.06.006

Thapa, R. J., Ingram, J. P., Ragan, K. B., Nogusa, S., Boyd, D. F., Benitez, A. A., Sridharan, H., Kosoff, R., Shubina, M., Landsteiner, V. J., Andrake, M., Vogel, P., Sigal, L. J., tenOever, B. R., Thomas, P. G., Upton, J. W., & Balachandran, S. (2016). DAI Senses Influenza A Virus Genomic RNA and Activates RIPK3-Dependent Cell Death. *Cell Host & Microbe*, *20*(5), 674–681. https://doi.org/10.1016/j.chom.2016.09.014

Upton, J. W., Kaiser, W. J., & Mocarski, E. S. (2012). DAI/ZBP1/DLM-1 complexes with RIP3 to mediate virus-induced programmed necrosis that is targeted by murine cytomegalovirus vIRA. *Cell Host & Microbe*, *11*(3), 290–297. https://doi.org/10.1016/j.chom.2012.01.016

Vanden Berghe, T., Linkermann, A., Jouan-Lanhouet, S., Walczak, H., & Vandenabeele, P. (2014). Regulated necrosis: the expanding network of non-apoptotic cell death pathways.

Nature Reviews. Molecular Cell Biology, *15*(2), 135–147. https://doi.org/10.1038/nrm3737

Vandenabeele, P., Galluzzi, L., Vanden Berghe, T., & Kroemer, G. (2010). Molecular mechanisms of necroptosis: An ordered cellular explosion. *Nature Reviews Molecular Cell Biology*, *11*(10), 700–714. https://doi.org/10.1038/nrm2970

Vanlangenakker, N., Vanden Berghe, T., & Vandenabeele, P. (2012). Many stimuli pull the necrotic trigger, an overview. *Cell Death and Differentiation*, *19*(1), 75–86. https://doi.org/10.1038/cdd.2011.164

Wang, H., Sun, L., Su, L., Rizo, J., Liu, L., Wang, L.-F., Wang, F.-S., & Wang, X. (2014a). Mixed lineage kinase domain-like protein MLKL causes necrotic membrane disruption upon phosphorylation by RIP3. *Molecular Cell*, *54*(1), 133–146. https://doi.org/10.1016/j.molcel.2014.03.003

Wang, H., Sun, L., Su, L., Rizo, J., Liu, L., Wang, L. F., Wang, F. S., & Wang, X. (2014b). Mixed Lineage Kinase Domain-like Protein MLKL Causes Necrotic Membrane Disruption upon Phosphorylation by RIP3. *Molecular Cell*, *54*(1), 133–146. https://doi.org/10.1016/j.molcel.2014.03.003

Weinlich, R., Oberst, A., Beere, H. M., & Green, D. R. (2017). Necroptosis in development, inflammation and disease. *Nature Reviews. Molecular Cell Biology*, *18*(2), 127–136. https://doi.org/10.1038/nrm.2016.149

Weisel, K., Berger, S., Thorn, K., Taylor, P. C., Peterfy, C., Siddall, H., Tompson, D., Wang, S., Quattrocchi, E., Burriss, S. W., Walter, J., & Tak, P. P. (2021). A randomized, placebo-controlled experimental medicine study of RIPK1 inhibitor GSK2982772 in patients with moderate to severe rheumatoid arthritis. *Arthritis Research & Therapy*, *23*(1), 85. https://doi.org/10.1186/s13075-021-02468-0

Won, K. Y., Min, S. Y., Song, J. Y., Lim, S. J., & Han, S. A. (2021). Clinical Significance of Receptor-Interacting Protein 3 and Parkin, Essential Molecules for Necroptosis, in Breast Cancer. *Journal of Breast Cancer*, *24*(1), 34–48. https://doi.org/10.4048/jbc.2021.24.e12

Wong, R. S. Y. (2011). Apoptosis in cancer: from pathogenesis to treatment. *Journal of Experimental & Clinical Cancer Research : CR*, *30*(1), 87. https://doi.org/10.1186/1756-9966-30-87

Wu, J., Huang, Z., Ren, J., Zhang, Z., He, P., Li, Y., Ma, J., Chen, W., Zhang, Y., Zhou, X., Yang, Z., Wu, S. Q., Chen, L., & Han, J. (2013). Mlkl knockout mice demonstrate the indispensable role of Mlkl in necroptosis. *Cell Research*, *23*(8), 994–1006. https://doi.org/10.1038/cr.2013.91

Wu, S., Xu, C., Xia, K., Lin, Y., Tian, S., Ma, H., Ji, Y., Zhu, F., He, S., & Zhang, X. (2021). Ring closure strategy leads to potent RIPK3 inhibitors. *European Journal of Medicinal Chemistry*, *217*, 113327. https://doi.org/10.1016/j.ejmech.2021.113327

Xia, X., Lei, L., Wang, S., Hu, J., & Zhang, G. (2020). Necroptosis and its role in infectious diseases. *Apoptosis*, *25*(3–4), 169–178. https://doi.org/10.1007/s10495-019-01589-x

Xie, T., Peng, W., Yan, C., Wu, J., Gong, X., & Shi, Y. (2013). Structural insights into RIP3-mediated necroptotic signaling. *Cell Reports*, *5*(1), 70–78. https://doi.org/10.1016/j.celrep.2013.08.044

Xu, H., Du, X., Liu, G., Huang, S., Du, W., Zou, S., Tang, D., Fan, C., Xie, Y., Wei, Y., Tian, Y., & Fu, X. (2019). The pseudokinase MLKL regulates hepatic insulin sensitivity independently of inflammation. *Molecular Metabolism*, *23*, 14–23. https://doi.org/10.1016/j.molmet.2019.02.003

Xu, Y., Ma, H., Shao, J., Wu, J., Zhou, L., Zhang, Z., Wang, Y., Huang, Z., Ren, J., Liu, S., Chen, X., & Han, J. (2015). A role for tubular necroptosis in cisplatin-induced AKI. *Journal of the American Society of Nephrology*, *26*(11), 2647–2658. https://doi.org/10.1681/ASN.2014080741

Yan, B., Liu, L., Huang, S., Ren, Y., Wang, H., Yao, Z., Li, L., Chen, S., Wang, X., & Zhang, Z. (2017). Discovery of a new class of highly potent necroptosis inhibitors targeting the mixed lineage kinase domain-like protein. *Chemical Communications*, *53*(26), 3637–3640. https://doi.org/10.1039/c7cc00667e

Yang, D., Liang, Y., Zhao, S., Ding, Y., Zhuang, Q., Shi, Q., Ai, T., Wu, S. Q., & Han, J. (2020). ZBP1 mediates interferon-induced necroptosis. *Cellular and Molecular Immunology*, *17*(4), 356–368. https://doi.org/10.1038/s41423-019-0237-x

Yang, J., Zhao, Y., Zhang, L., Fan, H., Qi, C., Zhang, K., Liu, X., Fei, L., Chen, S., Wang, M., Kuang, F., Wang, Y., & Wu, S. (2018). RIPK3/MLKL-mediated neuronal necroptosis modulates the M1/M2 polarization of microglia/macrophages in the ischemic cortex. *Cerebral Cortex*, *28*(7), 2622–2635. https://doi.org/10.1093/cercor/bhy089

Ying, Z., Pan, C., Shao, T., Liu, L., Li, L., Guo, D., Zhang, S., Yuan, T., Cao, R., Jiang, Z., Chen, S., Wang, F., & Wang, X. (2018). Mixed Lineage Kinase Domain-like Protein MLKL Breaks Down Myelin following Nerve Injury. *Molecular Cell*, *72*(3), 457-468.e5. https://doi.org/10.1016/j.molcel.2018.09.011

Yoon, S., Bogdanov, K., & Wallach, D. (2022). Site-specific ubiquitination of MLKL targets it to endosomes and targets Listeria and Yersinia to the lysosomes. *Cell Death & Differentiation*, *29*(2), 306–322. https://doi.org/10.1038/s41418-021-00924-7

Yuan, F., Cai, J., Wu, J., Tang, Y., Zhao, K., Liang, F., Li, F., Yang, X., He, Z., Billiar, T. R., Wang, H., Su, L., & Lu, B. (2022). Z-DNA binding protein 1 promotes heatstroke-induced cell death. *Science*, *376*(6593), 609–615. https://doi.org/10.1126/science.abg5251

Zhang, D.-W., Shao, J., Lin, J., Zhang, N., Lu, B.-J., Lin, S.-C., Dong, M.-Q., & Han, J. (2009). RIP3, an energy metabolism regulator that switches TNF-induced cell death from apoptosis to necrosis. *Science (New York, N.Y.)*, *325*(5938), 332–336. https://doi.org/10.1126/science.1172308

Zhang, H., Xu, L., Qin, X., Chen, X., Cong, H., Hu, L., Chen, L., Miao, Z., Zhang, W., Cai, Z., & Zhuang, C. (2019). N-(7-Cyano-6-(4-fluoro-3-(2-(3-(trifluoromethyl)phenyl)acetamido)phenoxy)benzo[d]thiazol-2-yl)cyclopropanecarboxamide (TAK-632) Analogues as Novel Necroptosis Inhibitors by Targeting Receptor-Interacting Protein Kinase 3 (RIPK3): Synthesis, Structure-Act. *Journal of Medicinal Chemistry*, *62*(14), 6665–6681. https://doi.org/10.1021/acs.jmedchem.9b00611

Zhang, T., Yin, C., Boyd, D. F., Quarato, G., Ingram, J. P., Shubina, M., Ragan, K. B., Ishizuka, T., Crawford, J. C., Tummers, B., Rodriguez, D. A., Xue, J., Peri, S., Kaiser, W. J., López, C. B., Xu, Y., Upton, J. W., Thomas, P. G., Green, D. R., & Balachandran, S. (2020). Influenza Virus Z-RNAs Induce ZBP1-Mediated Necroptosis. *Cell*, *180*(6), 1115-1129.e13. https://doi.org/10.1016/j.cell.2020.02.050

Zhang, X., Dowling, J. P., & Zhang, J. (2019). RIPK1 can mediate apoptosis in addition to necroptosis during embryonic development. *Cell Death and Disease*, *10*(3). https://doi.org/10.1038/s41419-019-1490-8

Zhao, J., Jitkaew, S., Cai, Z., Choksi, S., Li, Q., Luo, J., & Liu, Z. G. (2012). Mixed lineage kinase domain-like is a key receptor interacting protein 3 downstream component of TNF-

induced necrosis. *Proceedings of the National Academy of Sciences of the United States of America*, *109*(14), 5322–5327. https://doi.org/10.1073/pnas.1200012109

Zhe-Wei, S., Li-Sha, G., & Yue-Chun, L. (2018). The role of necroptosis in cardiovascular disease. *Frontiers in Pharmacology*, *9*(JUL), 1–9. https://doi.org/10.3389/fphar.2018.00721

Zhou, W., & Yuan, J. (2014). Necroptosis in health and diseases. *Seminars in Cell & Developmental Biology*, *35*, 14–23. https://doi.org/10.1016/j.semcdb.2014.07.013

Zhou, Y., Zhou, B., Tu, H., Tang, Y., Xu, C., Chen, Y., Zhao, Z., & Miao, Z. (2017). The degradation of mixed lineage kinase domain-like protein promotes neuroprotection after ischemic brain injury. *Oncotarget*, *8*(40), 68393–68401. https://doi.org/10.18632/oncotarget.19416

Zhou, Z., Han, V., & Han, J. (2012a). New components of the necroptotic pathway. *Protein and Cell*, *3*(11), 811–817. https://doi.org/10.1007/s13238-012-2083-9

Zhou, Z., Han, V., & Han, J. (2012b). New components of the necroptotic pathway. *Protein & Cell*, *3*(11), 811–817. https://doi.org/10.1007/s13238-012-2083-9

Cui, B., Yan, B., Wang, K., Li, L., Chen, S., & Zhang, Z. (2022). Discovery of a New Class of Uracil Derivatives as Potential Mixed Lineage Kinase Domain-like Protein (MLKL) Inhibitors. *Journal of Medicinal Chemistry*, *65*(19), 12747–12780. https://doi.org/10.1021/acs.jmedchem.2c00548

Rathkey, J. K., Zhao, J., Liu, Z., Chen, Y., Yang, J., Kondolf, H. C., Benson, B. L., Chirieleison, S. M., Huang, A. Y., Dubyak, G. R., Xiao, T. S., Li, X., & Abbott, D. W. (2018). Chemical disruption of the pyroptotic pore-forming protein gasdermin D inhibits inflammatory cell death and sepsis. *Science Immunology*, *3*(26). https://doi.org/10.1126/sciimmunol.aat2738

Samson, A. L., Zhang, Y., Geoghegan, N. D., Gavin, X. J., Davies, K. A., Mlodzianoski, M. J., Whitehead, L. W., Frank, D., Garnish, S. E., Fitzgibbon, C., Hempel, A., Young, S. N., Jacobsen, A. V, Cawthorne, W., Petrie, E. J., Faux, M. C., Shield-Artin, K., Lalaoui, N., Hildebrand, J. M., … Murphy, J. M. (2020). MLKL trafficking and accumulation at the plasma membrane control the kinetics and threshold for necroptosis. *Nature Communications*, *11*(1), 3151. https://doi.org/10.1038/s41467-020-16887-1

Sun, L., Wang, H., Wang, Z., He, S., Chen, S., Liao, D., Wang, L., Yan, J., Liu, W., Lei, X.,

& Wang, X. (2012). Mixed lineage kinase domain-like protein mediates necrosis signaling downstream of RIP3 kinase. *Cell*, *148*(1–2), 213–227. https://doi.org/10.1016/j.cell.2011.11.031

Weinlich, R., Oberst, A., Beere, H. M., & Green, D. R. (2017). Necroptosis in development, inflammation and disease. *Nature Reviews. Molecular Cell Biology*, *18*(2), 127–136. https://doi.org/10.1038/nrm.2016.149

García Sáez, A., Ros Quincoces, U., Valiente Flores, P., Wong, W.-L., Walczak, H., & de las Vieves Peltzer, M. (2021). *germany/europe Patent No. EP 3 906 924 A1*.